UPAS / GDOAS 4.0 Upgrade of the GOME Data Processor for Improved Total Ozone Columns

Delta validation report for ERS-2 GOME Data Processor upgrade to version 4.0

Prepared by: Jean-Christopher Lambert and Dimitris S. Balis

Contributors: Dimitris Balis, Pierre Gerard, José Granville, Jean-Christopher Lambert, Yakov Livschitz, Diego Loyola, Robert Spurr, Pieter Valks, and Michel Van Roozendael

Document: ERSE-CLVL-EOPG-TN-04-0001
Issue: Version 1.0, 15 December 2004
Authorised: Claus Zehner – ESA/ESRIN, Frascati, Italy

Belgian Institute for Space Aeronomy

Aristotle University of Thessaloniki

German Aerospace Centre

UPAS / GDOAS 4.0 Upgrade
of the GOME Data Processor
for Improved Total Ozone Columns

Delta validation report for ERS-2 GOME Data Processor upgrade to version 4.0

CONTENTS

ACRONYMS AND ABBREVIATIONS

AMF	Air Mass Factor, or optical enhancement factor
AUTH	Aristotle University of Thessaloniki
BIRA	Belgisch Instituut voor Ruimte-Aëronomie
BUV	Backscatter Ultra Violet
DLR	German Aerospace Centre
DOAS	Differential Optical Absorption Spectroscopy
D-PAF	German Processing and Archiving Facility
DU	Dobson Unit
EP	Earth Probe satellite
ERS-2	European Remote Sensing Satellite -2
ESA/ESRIN	European Space Agency/European Space Research Institute
F&K	Fortuin and Kelder climatology
GAW	WMO's Global Atmospheric Watch programme
GDOAS	GODFIT-DOAS
GDP	GOME Data Processor
GODFIT	GOME Direct Fitting algorithm
GOME	Global Ozone Monitoring Experiment
GVC	Ghost Vertical Column
IASB	Institut d'Aéronomie Spatiale de Belgique
ICFA	Initial Cloud Fitting Algorithm
IMF	Remote Sensing Technology Institute
LIDORT	Linearized Discrete Ordinate Radiative Transfer model
LOS	Line Of Sight
LUT	Look Up Table
NDSC	Network for the Detection of Stratospheric Change
NLLS	Non Linear Least Squares fitting
NO_2	Nitrogen Dioxide
O_3	Ozone
OCRA	Optical Cloud Recognition Algorithm
ROCINN	Retrieval of Cloud Information using Neural Networks
RRS	Rotational Raman Scattering
SAO	Smithsonian Astrophysical Observatory
SAOZ	Système d'Analyse par Observation Zénithale
SCD	Slant Column Density
SHADOZ	Southern Hemisphere Additional Ozonesonde programme
SZA	Solar Zenith Angle
TOA	Top Of Atmosphere
TOMS	Total Ozone Mapping Spectrometer
UPAS	Universal Processor for UV/VIS Atmospheric Spectrometers
UV	ultraviolet
VCD	Vertical Column Density
VIS	visible
WMO	World Meteorological Organization
WOUDC	World Ozone and Ultraviolet radiation Data Center

I INTRODUCTION

I.1 GOME OPERATION AND DATA PROCESSOR

The Global Ozone Monitoring Experiment (GOME) on board ERS-2 (launched in April 1995) is the successful predecessor of a series of new generation sensors (SCIAMACHY, OMI, GOME-2) aiming at the needed global measurement of key ozone-related species to assess current and future changes of the atmosphere [1-3]. Providing the global picture of atmospheric ozone (O_3), GOME is also the first orbiting instrument having the capability to measure the vertical column amount of nitrogen dioxide (NO_2), a trace species playing a crucial role in the ozone photochemistry. Since August 1996, GOME total O_3 and NO_2 column data are routinely processed at the German Processing and Archiving Facility (D-PAF) established at the German Aerospace Centre (DLR) on behalf of ESA with the GOME Data Processor (GDP) [4-6]. Since the release in summer 1995 of its first developmental version, GDP was upgraded on many occasions and the quality of both ozone and NO_2 products has improved significantly (e.g., [7,8]).

GOME has now been producing global distributions of total ozone for nine years. The length of this data record makes it desirable for use in long-term ozone trend monitoring, for which a crucial requirement is the ability to measure 1-% changes in total ozone concentrations globally and over a period of 10 years. Such a level of accuracy had not been met yet with GDP version 3.0 [9]. To this end, ESA-ESRIN issued an Invitation to Tender (ITT) in June 2002 to develop improved GOME total ozone column retrieval algorithms capable of producing trend-quality data. Three consortia were awarded contracts to perform this work in competition. The Final Review Board met in December 2003, and a further delta validation was finished in January 2004 [10]. Following the Board's recommendations, the GDOAS algorithm (developed jointly by the Belgian Institute for Space Aeronomy, BIRA-IASB, and the Smithsonian Astrophysical Observatory, SAO) was selected for operational implementation in the D-PAF at DLR as part of the ESA ERS Ground Segment. On the operational side, the GDP environment at D-PAF, designed in the early 1990s, was replaced recently by a more flexible environment called Universal Processor for UV/VIS Atmospheric Spectrometers (UPAS). GDP 4.0 replaces version 3.0 of GDP since November 2004 and the reprocessed GOME data record, including historical data, is already available to the public via the ERS Help & Order Desk (see GOME Data Disclaimer 2004 in Annexe).

I.2 OBJECTIVES OF UPAS/GDOAS PROJECT

The UPAS/GDOAS project covers the necessary requirements to implement, verify and validate the UPAS/GDOAS 4.0 system in a new version 4.0 of the operational GOME Data Processor, and to perform a complete reprocessing of the entire GOME total ozone record by the end of 2004.

Like previous versions of the GDP algorithms, GDOAS and GDP 4.0 are classical DOAS-style inversion packages, comprising a least-squares Beer-Lambert fitting for the total slant column of ozone followed by an Air Mass Factor computation to derive a vertical column amount. GDP 4.0 is similar in scope to its previous version 3.0, the major differences being:

(1) the inclusion of a new Ring effect treatment with proper account for both Fraunhoffer and telluric line filling-in by rotational Raman scattering (RRS);

(2) the use of on-the-fly radiative transfer AMF simulations with the LIDORT code, at the modified wavelength of 325.5 nm;

(3) the use of cloud property information derived from GOME data using state-of-the-art algorithms (OCRA and ROCCIN);

(4) the use of improved surface data bases;

(5) the use of the UPAS system: a completely new processing environment based on a C++ architecture.

These differences and other aspects of the GDP 4.0 implementation are discussed in more detail in the Interim SRD/SUM Document [11] and the GDP 4.0 Algorithm Theoretical Basis Document ATBD [12].

I.3 DELTA VALIDATION OF GDP 4.0

Prior to the implementation of any major change in the operational GDP processing chain, it is essential to verify the accuracy and effectiveness of the modification and to assess the quality of the new data product. Such 'delta' validations of the expected product improvements have been executed after every major GDP upgrade by a sub-group of the GOME Validation Group responsible for the investigation of GOME data product quality throughout the mission lifetime.

In the context of the present GDP upgrade to version 4.0, a delta validation campaign was set up in 2004 with the main emphasis on the quality assessment of new ozone column amounts on the global scale and in the long term. Improving the nitrogen dioxide column product was not the focus of this new GDP upgrade, nevertheless, possible changes due to its processing in the new UPAS environment system were checked as well.

The campaign involved the Belgian Institute for Space Aeronomy (IASB-BIRA, Brussels, Belgium), the Laboratory of Atmospheric Physics (AUTH, Aristotle University of Thessaloniki, Greece), and DLR's Remote Sensing Technology Institute (DLR-IMF, Oberpfaffenhofen, Germany). The composition of the team was defined according to the following objectives:

- To ensure the availability of correlative data sets suitable for global-scale and long-term investigation of the new GOME ozone column product;
- To ensure the availability of correlative data sets suitable for global-scale and long-term verification of the GOME nitrogen dioxide column product processed in the new UPAS environment;
- To ensure the GDP 4.0 processing of needed GOME delta validation orbits;
- To combine complementary expertise;
- To get independent studies and data quality assessments;
- To foster feedback between validation teams and operational processing team.

Intermediate results were exchanged and discussed among the group by email, during two project meetings held at DLR in May 2004 and at ESA/HQ in August 2004, and during an

informal working meeting held in Helsinki in September 2004. Final results were presented and discussed at a dedicated workshop organised at ESA/ESRIN on November 9, 2004.

The present document outlines main results of the UPAS/GDOAS GDP 4.0 Delta Validation Campaign 2004. Results consist of:

- A summary of the main algorithmic improvements in the new GDP version, including a description of some of the key aspects of the verification performed as part of validation activities.
- Characterisation of the new version 4.0 of GOME total ozone level-2 data product by comparison with correlative measurements from extensive ground-based networks archived in the World Ozone and UV Data Center (WOUDC) operated at Toronto (Canada), and in the database of the Network for the Detection of Stratospheric Change (NDSC) operated at NOAA (USA) and mirrored at NILU (Norway).
- Similar characterisation of the new version 8 of Earth Probe TOMS total ozone gridded data product as available from NASA/GSFC (USA);
- Verification of the new version 4.0 of GOME total nitrogen dioxide level-2 data product by comparison with correlative measurements from the ground-based Network for the Detection of Stratospheric Change;
- Update of the documentation on GDP data products, including the validation summary in the GDP Algorithm Theoretical Basis Document (ATBD) version 4.0 and the GOME Data Disclaimer (see Annexe).

A summary of GOME Data Processor upgrades to version 4.0 is given in Chapter II of the present report. Details can be found in the GDP 4.0 ATBD [12]. The selection of reference data sets for the aimed delta validation is addressed in Chapter III. Chapter IV deals with ground-based data uncertainties that might impact the validation of satellite ozone columns. A summary of the TOMS ozone algorithm upgrade to version 8 is given in Chapter V. Ground-based comparison results are reported in Chapter VI for ozone columns and Chapter VII for nitrogen dioxide columns, respectively. After the concluding remarks of Chapter VIII, the updated ‘GOME Data Disclaimer’ document resulting from the campaign is provided in the Annexe.

REFERENCES

[1] GOME Interim Science Report, ESA SP-1151, 59 pp., 1993.

[2] GOME Users Manual, ESA SP-1182, 200 pp., 1995.

[3] Burrows, J.P., M. Weber, M. Buchwitz, V. Rozanov, V. Ladstätter-Weißenmayer, A. Richter, A. De Beek, R. Hoogen, K. Bramstedt, K.U. Eichmann, and M. Eisinger, The Global Ozone Monitoring Experiment (GOME): Mission concept and first Scientific Results, *J. Atmos. Sci.*, 56, pp. 151-175, 1999.

[4] GOME Level 0 to 1 Algorithms Description, Technical Note, ER–TN–DLR–GO–0022, Iss./Rev. 5/B, July 31, 2002.

[5] GOME Level 1 to 2 Algorithms Description, Technical Note, ER–TN–DLR–GO–0025, Iss./Rev. 3/A, July 31, 2002.

[6] Product Specification Document of the GOME Data Processor, ER-PS-DLR-GO-0016, Iss./Rev. 4/B, December 2004.

[7] GOME Data Improvement Validation Report, B. Greco (Ed.), ESA/ESRIN APP/AEF/17/GB, 58 pp. 1998.

[8] ERS-2 GOME Data Products Delta Characterisation Report 1999, J.-C. Lambert and P. Skarlas (Eds.), IASB, issue 1, November 1999.

[9] ERS-2 GOME GDP3.0 Implementation and Validation, ESA Technical Note ERSE-DTEX-EOAD-TN-02-0006, 138 pp., Ed. by J.-C. Lambert (IASB), November 2002.

[10] GDOAS Delta-validation report, ESA contract AO/1-4235/02/I-LG, 28 January 2004.

[11] Interim SRD/SUM for GDOAS Implementation at DLR, ESA contract AO/1-4235/02/I-LG, R.J.D. Spurr and M. van Roozendael, March 2004.

[12] Algorithm Theoretical Basis Document for GOME Total Column Densities of Ozone and Nitrogen Dioxide, UPAS/GDOAS: GDP 4.0, ESA Technical Note ERSE-DTEX-EOPG-TN-04-0007, DLR/UPAS/GOME/ATBD/01, Iss./Rev. 1/A, 15 December 2004.

II SUMMARY OF GOME DATA PROCESSOR UPGRADES

The upgrade from GDP 3.0 to the present GDP 4.0 version essentially concerns the level 1-to-2 processing environment, with main emphasis on the total ozone determination. A detailed description of the new system is given in the GDP 4.0 Algorithm Theoretical Basis Document [1] and, therefore, will not be repeated here. Instead, this section concentrates on a short overview of main algorithmic improvements and some aspects of the verification work carried out as part of the total ozone product validation.

II.1 MAIN ALGORITHMIC IMPROVEMENTS IN GDP 4.0

As will be shown in the following sections, the present validation report concludes to significant improvements in the accuracy of the new GDP 4.0 total ozone product in comparison to GDP 3.0. The overall better agreement with ground-based instruments strongly suggests that several key issues regarding the accuracy of total ozone retrieval from GOME have been properly identified and handled in the new algorithms. Major improvements can be summarized as follows:

a. Appropriate handling of both Fraunhoffer and telluric filling-in of spectral features, due to rotational Raman scattering (Ring effect).

b. Optimized wavelength alignment schemes, minimizing bias due to spectral mis-registration.

c. Use of improved cloud data products as well as surface property databases.

d. Implementation of flexible, fast and accurate linearized scattering code LIDORT v.2.5 with exclusive capability for "on-the-fly" spectral RT simulations.

e. Use of optimized column-resolved climatology of O_3 profiles inherited from TOMS algorithmic developments.

II.2 RING

It is fair to say that the new Ring effect treatment implemented in GDP 4.0 is one of the key improvements from GDP 3.0. In contrast to that used in previous GDP versions, the new Ring correction method explicitly accounts for both Fraunhoffer and telluric filling-in due to rotational Raman scattering (RRS). The approach adopted is based on a simplified representation of the atmospheric scattering in presence of RRS, as described in the GDP 4.0 ATBD [1]. The reliability of this approach has been investigated in two ways as part of verification activities.

(1) Closed-loop testing

First closed-loop exercises were performed based on realistic simulations of the earthshine backscattered radiances using the SCIATRAN v.2.1 radiative transfer code [6]. The SCIATRAN model has a build-in capability to simulate radiances with or without the inelastic contribution due to RRS by molecular nitrogen and oxygen [7]. Here the model was

used to synthesize Top-of-Atmosphere (TOA) radiance spectra in the spectral range from 320 to 340 nm which includes the GOME ozone fitting window (325-335 nm). The atmosphere was set up using realistic ozone profiles from the season and latitude-resolved Fortuin and Kelder climatology [8], while temperatures were prescribed according to the Trenberth climatology [9]. Simulations were performed at solar zenith angles representative of GOME observations at latitudes and seasons sampled by the climatology. Close-loop retrievals were performed using same settings and methodology as used for real GOME retrievals.

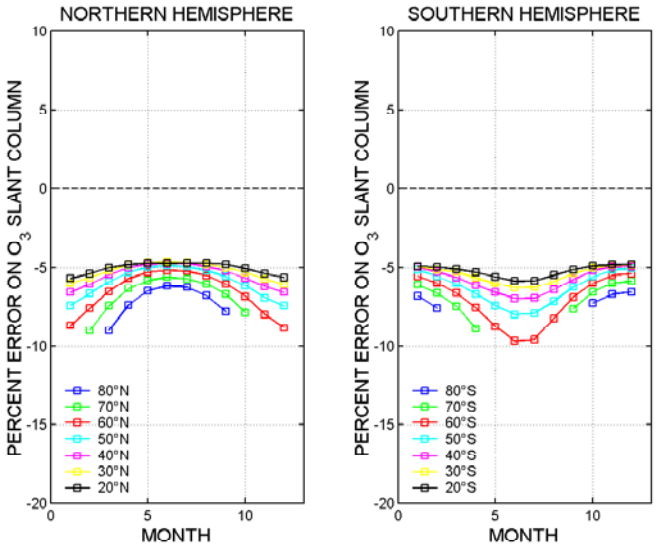

Figure 1 - Ring effect close-loop tests: error on retrieved ozone slant column when not accounting for molecular filling-in (GDP 3.0 baseline).

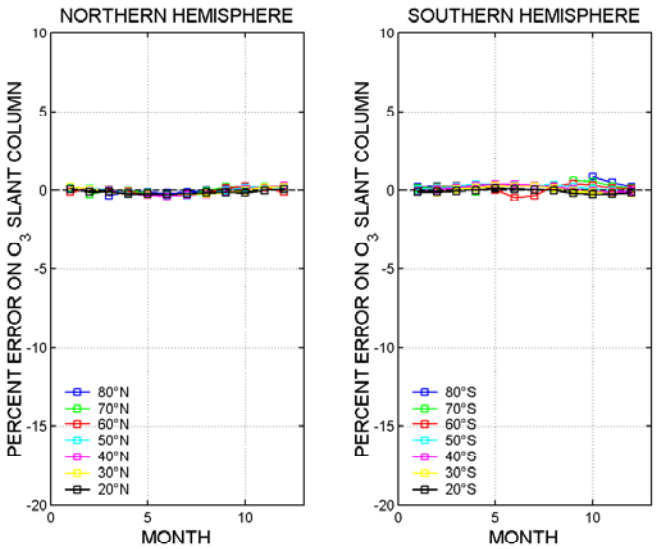

Figure 2 - Ring effect close-loop tests: error on retrieved ozone slant column after application of the new Ring effect treatment (GDP 4.0 baseline).

In **Figure 1** and **Figure 2**, the error on the retrieved ozone slant columns is evaluated in the case of retrievals performed with a basic "Fraunhoffer-only" Ring correction (as used in GDP 3.0 and earlier versions), and using the new correction method developed for GDP 4.0. One can see that the significant and systematic underestimation of the ozone columns already discussed in [2] is largely compensated by the new correction, in all conditions of seasons and latitudes.

(2) Consistency of DOAS and Direct-Fitting retrievals on actual GOME data sets

Another test of our understanding of the Ring effect was performed using actual GOME measurements. As described in [1] and [2], the ozone bias due to the use of an oversimplified "Fraunhoffer-only" Ring correction takes a different form depending on the formulation used for the retrieval. For logarithm-based DOAS-type retrievals, an underestimation of the ozone column is expected (cf. **Figure 1**), while in the case of direct-fitting of GOME reflectivities, an overestimation of the column should be observed. This behaviour was tested on actual GOME retrievals through parallel analysis of the same GOME data set, using either DOAS or direct-fitting (GODFIT). Results obtained using a "Fraunhoffer-only" Ring correction are displayed in **Figure 3**, for the Hohenpeisenberg overpass data set. Monthly-averaged differences between GOME retrievals and ground-based total ozone measurements clearly show the expected behaviour: overestimation in the direct-fitting case, underestimation in the DOAS case.

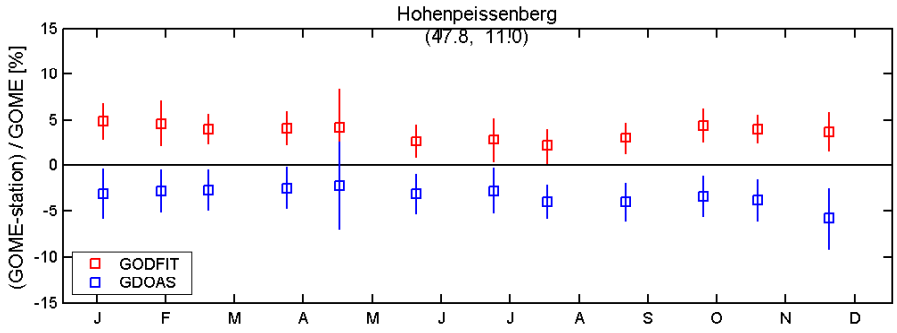

Figure 3 - Monthly averaged percent difference between GOME and ground-based total ozone values at the Hohenpeissenberg station. Both direct-fitting (GODFIT) and DOAS GOME retrievals have been performed using a simple "Frauhnoffer-only" Ring correction.

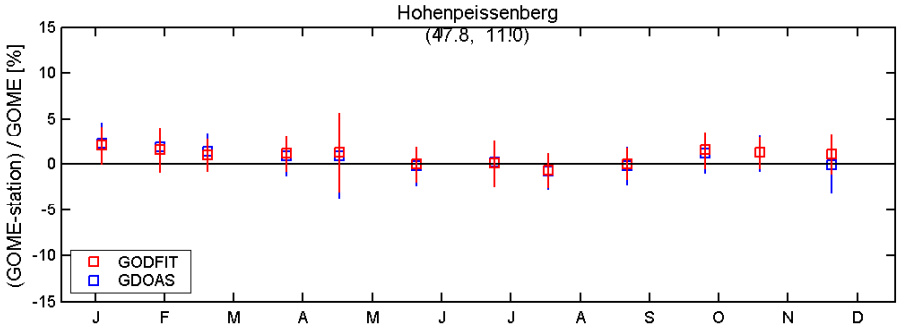

Figure 4 - Same as **Figure 3**, except that GOME evaluations have been performed using the new Ring correction scheme developed for GDP 4.0.

Figure 4 shows the resulting comparisons, after application of the new Ring correction scheme. It is striking to note the excellent agreement between the two GOME evaluations, despite the use of completely different fitting techniques in different wavelength intervals (GODFIT retrievals are performed in the 331.6-336.6 nm wavelength range). Besides confirming our understanding of the role of Ring effect on GOME retrievals, these results also strongly reinforce our confidence in the reliability of the DOAS approach adopted for GDP 4.0.

II.3 TEMPERATURE DEPENDENCE OF O_3 ABSORPTION CROSS-SECTIONS

In the two-step DOAS approach still used for GDP 4.0, the largest impact of atmospheric temperature is through the temperature-dependence of the ozone absorption cross-sections. This dependence is accounted for in the DOAS algorithm by fitting two ozone spectra at two different temperatures. This procedure, which was first suggested by Andreas Richter (Uni. Bremen), allows for linear adjustment of the slant column retrieval to the actual O_3 profile weighted mean atmospheric temperature [2]. The accuracy of this approach is possibly limited (1) towards large SZA due to the breakdown of the optically thin approximation, (2) for extreme stratospheric temperatures (due to non-linearities in the temperature dependence of the ozone cross-sections), and (3) by the accuracy of the laboratory cross-sections themselves.

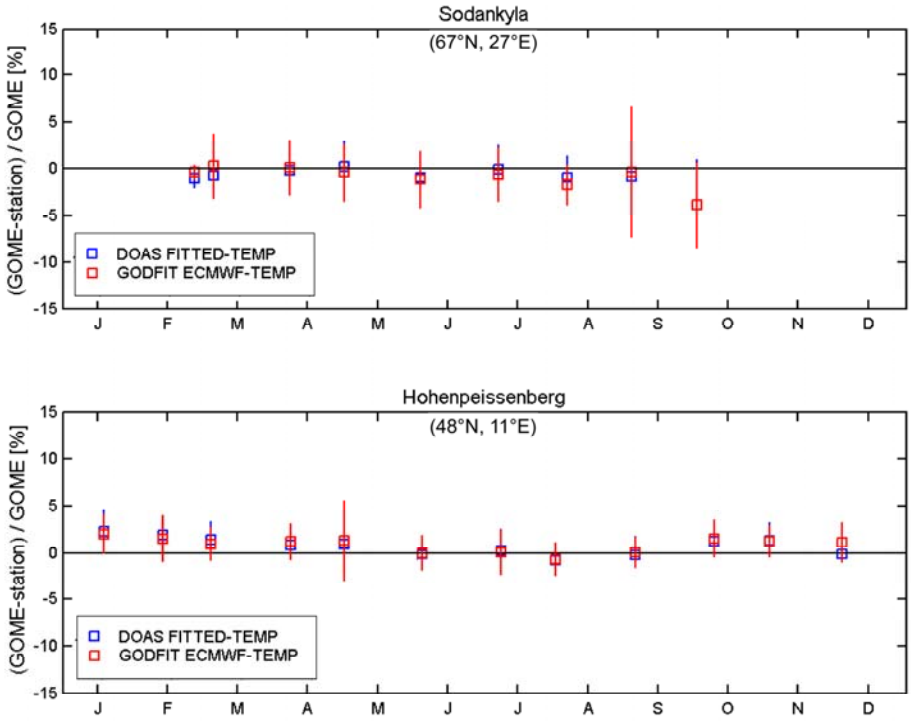

Figure 5 - Monthly averaged percent difference between GOME and ground-based total ozone values for the Sodankyla and Hohenpeissenberg stations. In the DOAS case (blue symbols), the temperature is adjusted as part of the fitting process (GDP 4.0 baseline) while in the direct-fitting case (red symbols), the temperature vertical profiles have been prescribed using ECMWF analysis.

Although results from close-loop tests (see Figure 7 at the end of this chapter) indicate that the linear temperature fitting approach (based on use of two cross-sections) provides stable retrievals even for elevated solar zenith angle values, another internal verification was performed here, once again based on a comparison between DOAS and direct fitting retrievals. Results of parallel GOME retrievals are displayed in **Figure 5**, for two stations representative of Northern mid- and high latitudes. In this way, a large variety of temperatures and solar zenith angle conditions are sampled. The excellent agreement found between DOAS and GODFIT ozone results in all seasons at both latitudes is a confirmation of the stability of the temperature fitting process (in addition to other aspects of the retrieval).

II.4 CLOUDS

In contrast to GDP 3.0 where cloud fractions were still inferred from the initial cloud fitting algorithm (ICFA) [3], the UPAS/GDOAS GDP 4.0 system uses an advanced combination of the cloud processing algorithms OCRA and ROCINN both developed in-house at DLR. OCRA [4] is a data-fusion algorithm using GOME sub-pixel PMD measurements to deliver cloud fraction; ROCINN [5] is a O_2 *A* band reflectivity algorithm delivering cloud-top height and cloud albedo by means of neural-network inversion from a look-up table of transmittance reflectivities. For concise descriptions and validation results, see [1].

II.5 AIRMASS FACTORS

As in GDP 3.0, GDP 4.0 uses a traditional DOAS retrieval approach, where slant column fitting and AMF calculation steps are performed sequentially. The ozone column dependency of the ozone profile and associated AMF is accounted for using an iterative scheme. In contrast to GDP 3.0, GDP 4.0 has been given a capability for on-the-fly AMFs calculations using LIDORT v. 2.5. This means that cumbersome calculations of multi-dimensional look-up tables of AMFs are no longer required to operate GDP 4.0, allowing for full flexibility in terms of climatology updates, etc.

In GDP 3.0 and earlier versions, AMFs for total ozone column were calculated at 325 nm at the lower end of the DOAS fitting window (325-335 nm). However closed-loop tests [2] have shown that with this choice of AMF wavelength, total column errors of up to 5% are possible for solar zenith angles in excess of 80°; and generally, errors at the 0.5-1% level are found for sun angles < 80°. It was recently found that these errors are reduced (to the 1-2% level for SZA> 80°) when 325.5 nm is used as the representative AMF wavelength. This value was now adopted for GDP 3.4 as the current baseline.

The impact of the change in wavelength for the computation of the ozone AMFs is illustrated in **Figure 6** and **Figure 7**, based on close-loop test results. The ozone vertical column error displayed in **Figure 7** includes all basic aspects of the DOAS retrieval approach adopted for GDP 4.0 (except for cloud effects). It can be seen as the “theoretical” best accuracy that can be expected from actual GOME retrievals. Errors below one percent are obtained in all typical GOME observation conditions, which is compliant with requirements on GOME total ozone accuracy given the size of error sources in actual measuring conditions (GDP 4.0 ATBD) [1].

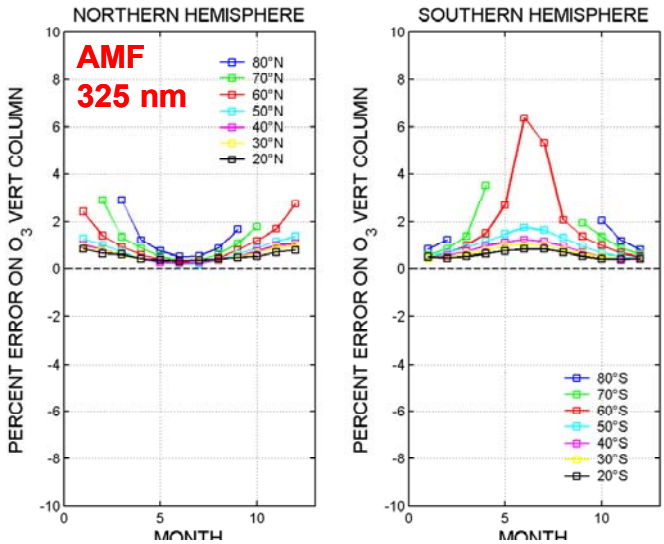

Figure 6 - Close-loop test of DOAS total ozone retrievals including RRS: ozone AMFs calculated at 325 nm, other settings as per baseline.

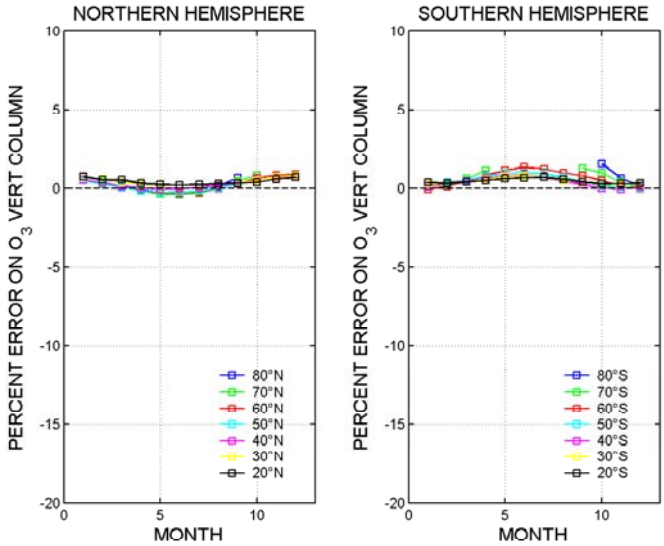

Figure 7 - Close-loop test of DOAS total ozone retrievals including RRS: ozone AMFs calculated at 325.5 nm, other settings as per baseline.

REFERENCES

[1] Algorithm Theoretical Basis Document for GOME Total Column Densities of Ozone and Nitrogen Dioxide, UPAS/GDOAS: GDP 4.0, DLR/UPAS/GOME/ATBD/01, Issue 1A, 15 December 2004.

[2] Van Roozendael, M., V. Soebijanta, C. Fayt, and J-C. Lambert, Investigation of DOAS issues affecting the accuracy of the GDP Version 3.0 total ozone product, in "ERS-2 GOME GDP3.0 Implementation and Validation", ESA Technical Note ERSE-DTEX-EOAD-TN-02-0006, 138 pp., Ed. By J.-C. Lambert (IASB), November 2002, p. 99-130.

[3] GOME Level 1 to 2 Algorithms Description, Technical Note, ER–TN–DLR–GO–0025, Iss./Rev. 3/A, July 31, 2002.

[4] Loyola, D., Cloud Retrieval for SCIAMACHY, ERS-ENVISAT Symposium, Gothenburg, 2000.

[5] Loyola, D., Automatic Cloud Analysis from Polar-Orbiting Satellites using Neural Network and Data Fusion Techniques, IEEE International Geoscience and Remote Sensing Symposium, Alaska, Vol. 4, 2530-2534, 2004.

[6] Buchwitz, M., et al., User's Guide for the Radiative Transfer Program SCIATRAN, Version 1.2, Institute of Remote Sensing, University of Bremen, FB1, Germany, May 2000.

[7] Vountas, M., V.V. Rozanov, and J.P. Burrows, Ring effect : Impact of rotational Raman scattering on radiative transfer in earth's atmosphere, J. Quant. Spectrosc. Rad. Transfer, 60, 943-961, 1998.

[8] Fortuin, J.P.F., and H. Kelder, An ozone climatology based on ozonesonde and satellite measurements, J. Geophys. Res., 103, 31709-31734, 1998.

[9] Trenberth, NCAR/TN-373+STR, 191pp., 1992.

III DELTA VALIDATION ORBITS

In 2002, a list of 2257 validation orbits was selected for the delta validation of GDP upgrade to version 3.0 [ESA, 2002]. Owing to the new needs of the GDP upgrade to version 4.0, we have selected here a set of about 5000 validation orbits that meet the following objectives:

- To optimise validation studies relying on ground-based ozone column data records available from the NDSC, WOUDC and ENVISAT Cal/Val databases;
- To allow the detection of changes in cyclic errors, i.e. dependence on the season, the latitude, the ozone column value and the solar zenith angle;
- To allow delta validation of GOME ozone column data from 1995 till 2004;
- To allow delta validation of EP-TOMS ozone column data from 1996 till 2004;
- To allow verification of GOME NO_2 column data from 1995 till 2004;
- To make sure that GDP 3 validation results obtained with this new set of validation orbits are consistent with GDP 3 results based on the previous set of 2257 validation orbits;
- To find the best compromise between minimum processing time and maximum representativeness of GDP 3 characteristics and expected changes.

The current selection of orbits is based on histograms of GOME/ground comparisons at a list of 40 stations from pole to pole: among them, 30 WMO/GAW stations equipped with Dobson and/or Brewer spectrophotometers, including the Canadian and NOAA/CMDL sub-networks and a few NDSC sites; and 20 NDSC sites operating UV-visible DOAS spectrometers. Orbits have been selected when leading to the closest value to the median value of the relative difference in total ozone. The selection has been constrained for both ozone and NO_2 in such a way that the sampling of the column range and of its cyclic variations - with season, latitude and solar zenith angle - complies with both Nyquist and Central Limit theorems. Another constraint is to yield sufficient sampling of seasonal and meridian variations of the effective temperature as derived from the DOAS spectral analysis.

Figure 8 displays the meridian sampling offered by the GOME/ground coincidences based on the Dobson and Brewer WOUDC stations used for the selection. Selected orbits yield a total amount of about 3000 coincidences by station on an average. **Figure 9** shows the coincidences dedicated to polar day studies (see Chapter VI for details) at a Siberian station located on the Arctic Polar Circle, where the SZA dependence of about 6% observed between GDP 3.0 ozone columns recorded in the mid-morning (moderate SZA) and during midnight sun conditions (large SZA) is supposed to vanish with GDP 4.0. **Figure 10** displays time-series of the coincidences obtained at typical stations of the Arctic, Northern mid-latitudes, the Equator, and the Antarctic. This figure illustrates how well selected coincidences capture geophysical variations of the ozone column (left panel), as well as major GDP 3.0 features (right panel) that are expected to attenuate with GDP 4.0, such as errors varying with the season. The set of selected orbits also offer adequate sampling of the Antarctic springtime when the extreme ozone column range facilitates the detection of changes in the ozone column dependence. It must be noted that due to the selection objectives the sampling at single stations can vary with time.

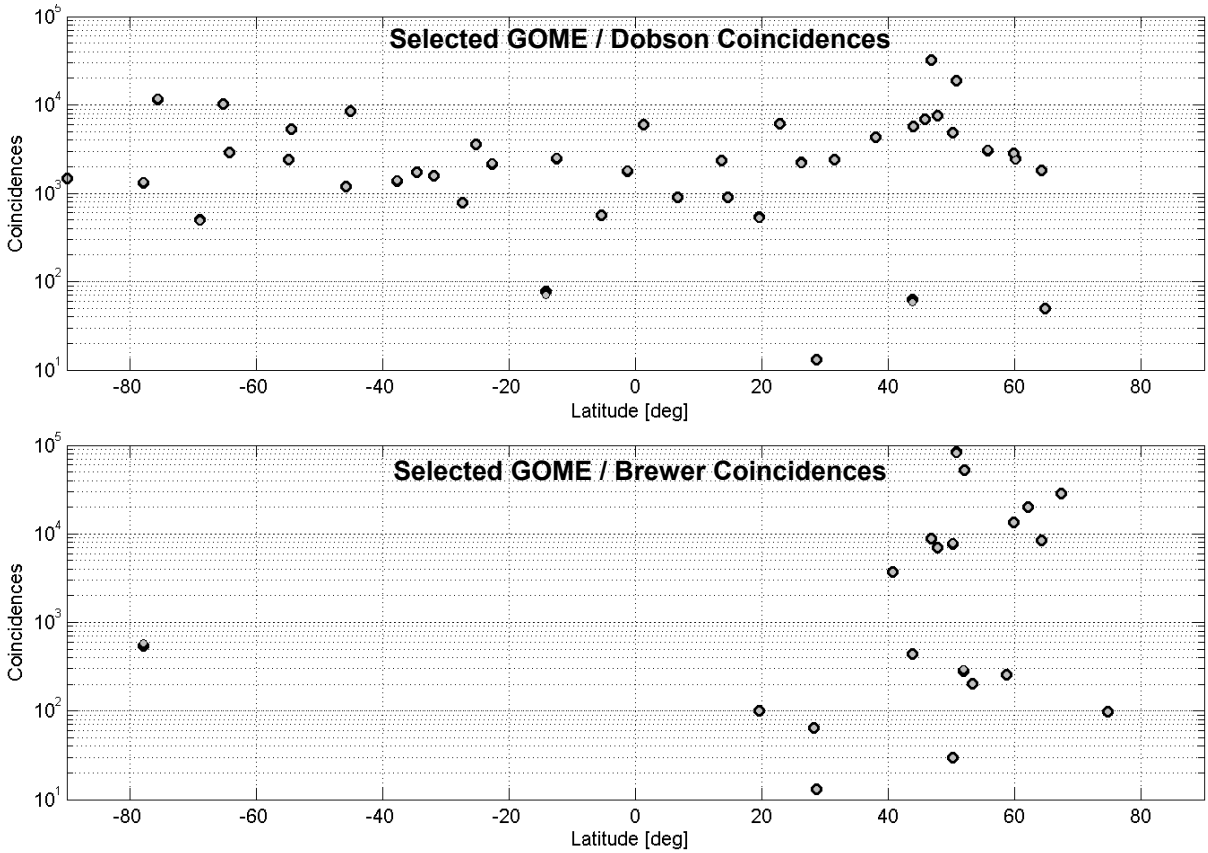

Figure 8 – Total amount (station by station) of selected coincidences between GOME GDP 3.0 and the ground-based ozone column measurements used for the selection, plotted as a function of latitude. Top: coincidences with selected Dobson data; bottom: coincidences with selected Brewer data.

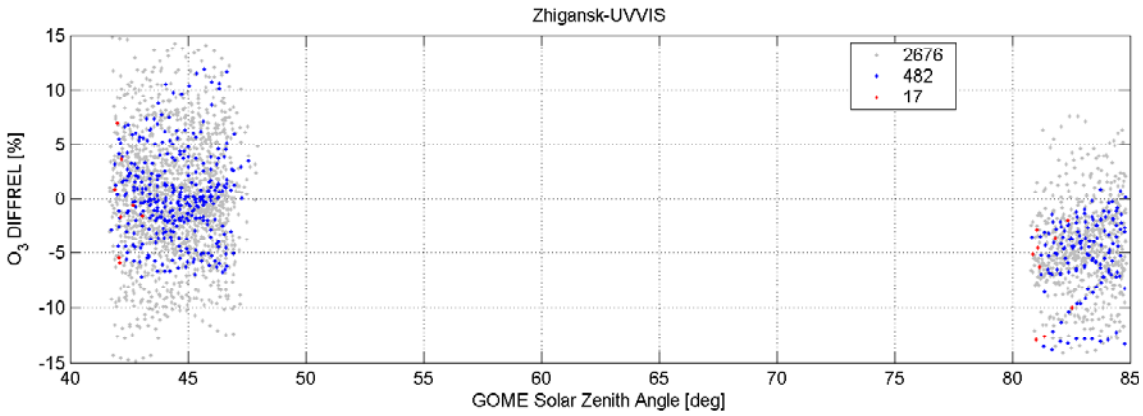

Figure 9 – Selected GOME/ground coincidences for polar day studies at the Arctic Polar Circle station of Zhigansk (67°N). The percent relative difference between GOME GDP 3.0 and ground-based SAOZ ozone column data exhibits a solar zenith angle dependence of 5% to 6% appearing between mid-morning (moderate SZA) and midnight sun (large SZA) GOME measurements. Grey dots show all coincidences between the available GOME and ground-based data records; the subset of coincidences plotted as red dots satisfies minimal sampling requirements; blue dots show coincidences actually yielded with the selected set of delta validation orbits. The total amount of coincidences for each subset of orbits is indicated in the legend.

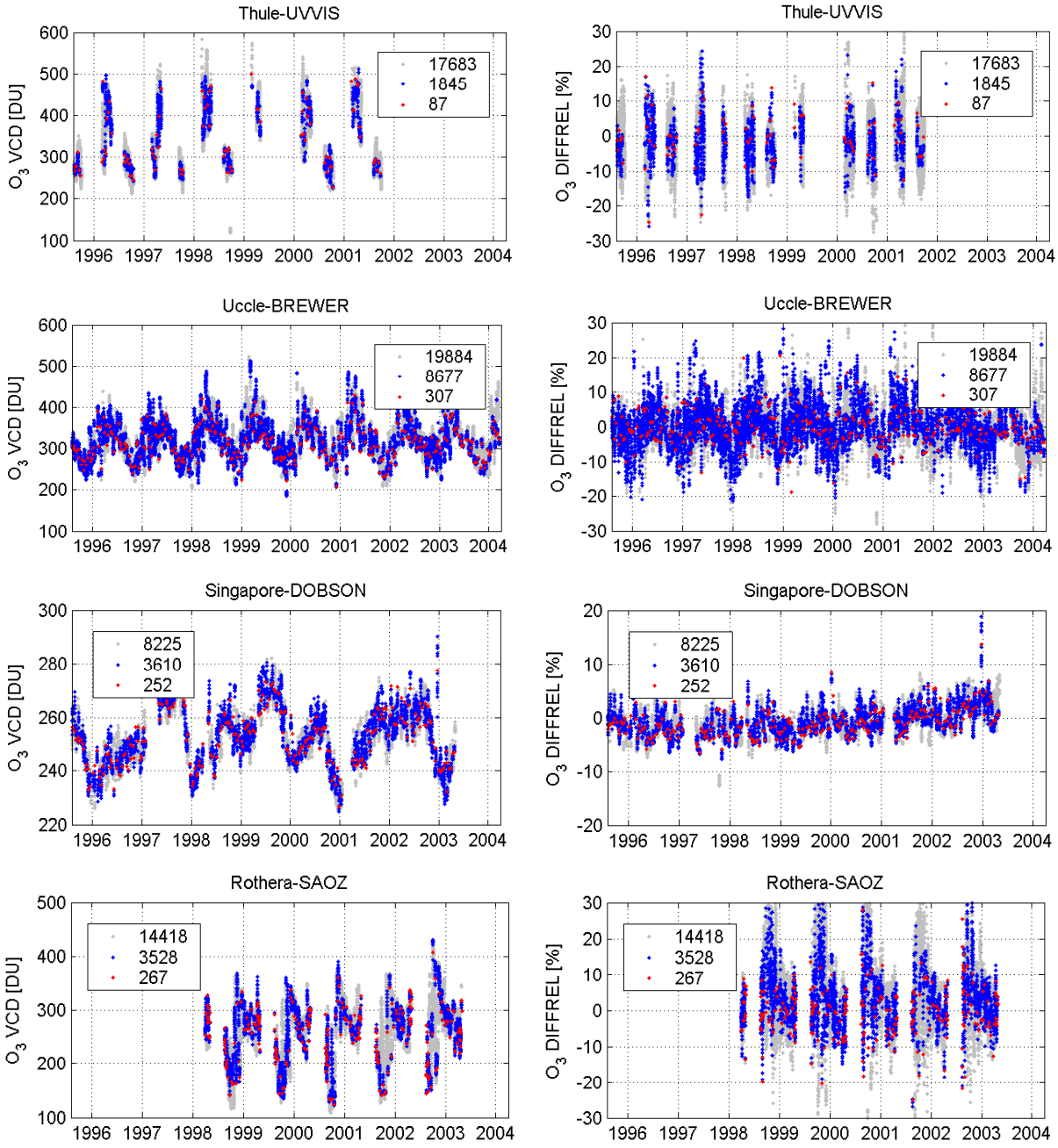

Figure 10 – Time-series of selected coincidences between GOME and ground-based ozone column observations at (from top to bottom): the Arctic station of Thule (77°N), the Northern mid-latitude station of Uccle (50°N), the equatorial station of Singapore (1°N), and the Antarctic station of Rothera (68°S). Left: coincident ozone column measurements; right: percent relative difference of GOME GDP 3 vs. ground-based ozone column data. Note that the vertical scale differs from one station to another. Colour code and legend as in **Figure 9**.

Finally, **Figure 11** displays the amount of TOMS overpass data corresponding to the selected GOME/ground coincidences. As overpass data files provided by NASA/GSFC report only one value a day, corresponding to the closest ground pixel to the station, the total amount of coincidences by station is closer to 1000 than to 3000 on an average. This should be however sufficient for reliable statistics. There is also a little difference between the TOMS V7 and TOMS V8 data sets: due to severe calibration problems with the TOMS instrument after 2001, TOMS data sets processed with version 7 of the algorithm become sparse. As version 8 corrects for some calibration problems, it yields overpass data sets slightly more extended in time, explaining the larger amount of coincidences noticed in **Figure 11**.

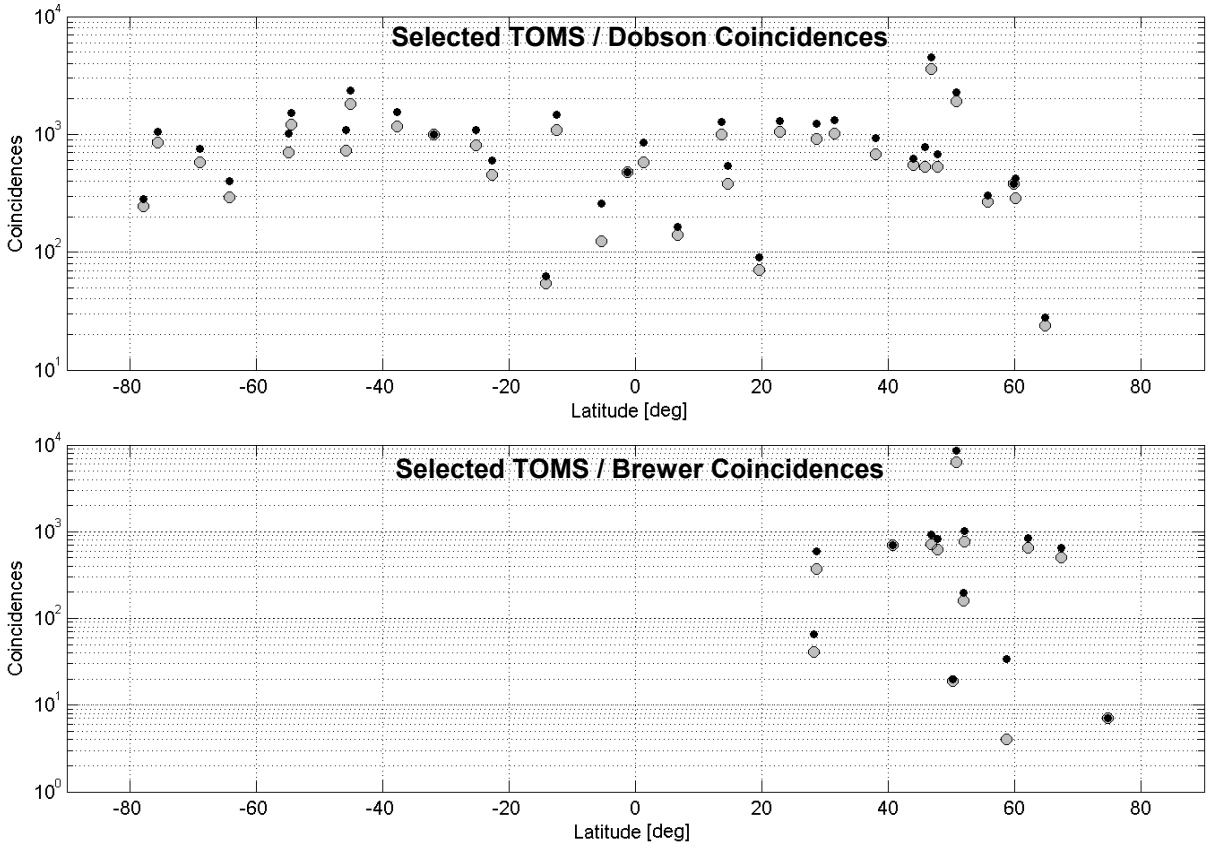

Figure 11 - Total amount (station by station) of selected coincidences between TOMS and the ground-based ozone column measurements used for the selection, plotted as a function of latitude. Top: coincidences with selected Dobson data; bottom: coincidences with selected Brewer data. Grey circles and black dots show coincidences with available TOMS V7 and TOMS V8 overpass data sets, respectively.

Reference

ESA, 2002: ERS-2 GOME GDP3.0 Implementation and Validation, ESA Technical Note ERSE-DTEX-EOAD-TN-02-0006, 138 pp., Ed. By J.-C. Lambert (IASB), November 2002.

IV ERROR BUDGET OF GROUND-BASED VALIDATION

IV.1 INTRODUCTION

Three main objectives of this delta validation exercise are:

- To assess the improvement of GDP 4.0 ozone columns with respect to GDP 3.0;
- To establish whether GDP 4.0 quality meets requirements of most demanding geophysical research applications like long term trend monitoring on the global scale and polar process studies;
- To investigate the consistency between GOME GDP 4.0 and the new TOMS v8 ozone data records, both on the global scale and in the long term.

To fulfil these objectives, it is essential to detect and quantify long-term instrumental degradation effects, and errors reflecting the sensitivity of the satellite algorithms to variations of the solar zenith angle, the atmospheric profile of temperature, the ozone column amount, the fractional cloud cover etc.

In principle, ground-based monitoring networks contributing to World Meteorological Organization's Global Atmospheric Watch programme (WMO/GAW) are natural candidates for the aimed studies. Indeed, ground-based stations delivering ozone column data regularly to the World Ozone and UV Data Center (WOUDC) and/or the international Network for the Detection of Stratospheric Change (NDSC) are expected to provide well-controlled, long-term time-series. Furthermore, the variety of stations from pole to pole covers most of relevant atmospheric states. Nevertheless, due to the high level of quality requirement, it is of prime importance to quantify in a first stage the actual capabilities of existing ground-based databases for an accurate validation of GOME and TOMS ozone columns. This is the purpose of this Chapter, where the focus will be on the average characteristics of existing data records rather than on the accuracy of single measurements. Most of the information presented hereafter is a blend of original work and published material. The reader interested in further details is invited to consult the references provided at the end of the Chapter.

IV.2 CONTRIBUTING GROUND-BASED OZONE COLUMN SENSORS

The three ozone column sensors used in this study rely on the principle of differential absorption. Designed in the 1920s, the Dobson spectrophotometer consists of a double prism monochromator [Dobson, 1957]. Its principle relies on the measurement of the ratio of the direct sunlight intensities at standard wavelengths in the ultraviolet Huggins band, where the absorption by ozone presents large spectral structures. The most widely used wavelength combination, recommended as the international standard, is referred to as the AD pair (305.5-325.4 nm; 317.6-339.8 nm) [Komhyr et al., 1993]. Other pairs are also used, especially at low sun elevation in polar regions when the rapidly decreasing intensity of short wavelength radiation weakens the signal-to-noise ratio.

The Brewer grating spectrophotometer [Brewer, 1973] is similar in its principle to the Dobson, but with an improved design that is fully automated [Kerr et al., 1983]. The ozone column abundance is derived from a combination of four wavelengths between 310 and 320 nm. A fifth wavelength is used to determine the SO_2 column abundance.

Initiated in the 1950s, the international network of more than 300 Dobson and Brewer spectrophotometers forms the world's primary total ozone monitoring network, and is a key component of WMO's Global Ozone Observing System (GO_3OS). A few Dobson and Brewer spectrophotometers are recommended at NDSC sites. More than 300 Dobson and Brewer stations archive total ozone at the World Ozone and UV radiation Data Centre (WOUDC) in Toronto, Canada (http://www.woudc.org). Some data records comprise over 35 years of continuous measurements.

The established procedures for maintaining high quality with the Brewer and Dobson instruments are described in detail by Staehelin et al. [2003]. Both instruments are calibrated by intercomparison with world or regional standard instruments. The Dobson calibrations are organized by WMO and the results are usually printed within a couple of years in relevant WMO reports (WMO/GAW reports 19, 108, 118, 119, 138, 145). The Brewer instruments are calibrated against a travelling standard by two private companies, but there is no official publication of these calibrations [see Staehelin et al, 2003]. However there are various publications [e.g. Fioletov et al., 1999], which provide valuable indications to the user about the quality of the deposited data, either through inter-comparison campaigns, workshops (e.g biennial Brewer workshops), or comparisons with satellite data.

Since the 1980s, the technique pioneered by Dobson for single wavelengths measurements in the ultraviolet has been extended to UV-visible spectroscopy. The retrieval method, usually referred to as the Differential Optical Absorption Spectroscopy (DOAS), consists of studying the narrow absorption features of the species, after removal of the broadband signal associated to scattering processes. A differential optical thickness is calculated as the logarithm of the ratio between the actual spectrum and a reference spectrum recorded at low SZA. Column densities along the optical path, or apparent slant columns, are derived by an iterative least squares procedure, fitting the observed differential optical thickness with high resolution differential absorption cross-sections measured in the laboratory and convolved with the instrument slit function. Apparent slant columns are converted into vertical columns using a geometrical enhancement factor, or air mass factor (AMF). This AMF is calculated with a radiative transfer model assuming vertical distributions of the target absorber and of the atmospheric constituents controlling the path of the solar radiation into the atmosphere. Based on this technique, about 40 UV-visible DOAS spectrometers constitute the backbone of the NDSC for total ozone and nitrogen dioxide monitoring. They measure UV-visible sunlight scattered at the zenith of the instrument. Ozone columns are retrieved using the DOAS technique applied to spectra acquired during twilight, between typically 86° and 91° SZA, when the sensitivity to the stratospheric absorbers is the highest (see IV.4). Among them, the SAOZ grating spectrometer [Pommereau and Goutail, 1988a,b] derives apparent slant column amounts of ozone in the Chappuis band (between 470 and 540 nm) and of NO_2 in the 406-526 nm spectral window. Slant columns retrieved from a real time spectral analysis at the station are converted into preliminary total vertical columns by the use of a standard AMF calculated for 60°N in winter, at sea level [Sarkissian et al., 1995]. Real-time data are reprocessed with state-of-the-art algorithms before submission to the official NDSC

database. Other types of DOAS UV-visible instruments contribute also to the NDSC and are described in Chapter VII.

NDSC-certified ozone column data are archived in the NDSC database (http://www.ndsc.ws), some time-series extending well before the inception of the network in 2001. Procedures to certify the quality of NDSC data are governed by the NDSC Data Protocol, established by experts participating to the different working groups of the network. Contributing teams are committed to participate to blind inter-comparison field campaigns of measurements and to algorithm inter-comparison exercises organised under the auspices of the NDSC and/or WMO. The Data Protocol recognises that, in order to produce a verifiable data product, sufficient time is needed to collect, reduce, calibrate, test, analyse, and inter-compare the streams of preliminary analyses at every NDSC site. Among others, seasonal analyses may be required for observations from both individual and multiple sites. It is expected that such a procedure shall yield the verifiable product referred to as "NDSC data" within a two-year period after acquisition. Working group activities, including consolidation and validation of ground-based measurements, are reported once a year to the NDSC Steering Committee.

IV.3 MUTUAL CONSISTENCY AND KNOWN ERRORS

IV.3.1 Dobson and Brewer

During international inter-comparison campaigns, Dobson instruments can be adjusted to agree within 0.3-1% [Basher, 1994]. The long-term agreement between Dobson and Brewer total ozone at high and moderate sun elevation – that is, at low and moderate air mass – can be better than 1%, while day-to-day fluctuations in the difference are usually small, on average less than ±1.5% [e.g., Kerr et al., 1988; De Backer and De Muer, 1991]. Dobson and Brewer instruments might suffer from long-term drift associated with calibration changes for which corrections are needed. Calibration uncertainties are also responsible for a relative air mass dependence between collocated instruments. Additional problems arise at low solar elevation, when the contributions of diffuse and of direct radiation can be of the same order of magnitude. The contribution of short wavelengths is relatively larger in the diffuse component, leading to an erroneous decrease in measured ozone abundance as the solar zenith angle increases [Josefsson, 1992]. This effect can vary with e.g. the aerosol load and the surface albedo. The design of spectrophotometers is such that internal scattering (straylight) also increases at low solar elevation. For those reasons and a few others mentioned hereafter, at low sun elevation, mean differences of ±5% have been reported between well-calibrated instruments [e.g. Nichol and Valenti, 1993].

According to Van Roozendael et al. [1998], the temperature dependence of the ozone absorption coefficients used in the Dobson and Brewer retrievals might account for a seasonal variation of ±0.9% in the Alps and ±1.7% at Sodankylä (Finland, 67.4°N), and for a systematic offset smaller than 1%. The effect can dramatically increase in extremely cold conditions such as those met in the winter polar vortex, where temperatures in the low stratosphere can be as low as 185 K.

Ozone measurements in the ultraviolet can be affected by interfering species, such as SO_2 and NO_2 [Kerr et al., 1988, and references therein]. The effect of SO_2 on Dobson data is an erroneous increase of total ozone by 0.3% on average, depending on the location of the

station with respect to SO_2 sources. Furthermore, according to De Muer and De Backer [1992], the long-term trend of SO_2 generally ascertained in Western European and North American urban areas would induce, if not properly taken into account, a fictitious Dobson total ozone trend, e.g., of −1.69% per decade in urban stations such as Uccle (Belgium, 50.5°N). The wavelengths used in the Brewer ozone measurement are chosen to avoid interferences by SO_2. Interferences by NO_2 may be neglected for both Dobson and Brewer measurements, except during strong NO_2 tropospheric pollution events which can produce an erroneous increase of total ozone by 0.6% in extreme cases.

Built up from quasi-simultaneous direct sun and zenith-sky measurements, a sky chart can be used to derive total ozone from Dobson and Brewer zenith-sky readings. This method is useful for obtaining data in cloudy conditions, or in regions frequently overcast like polar regions in winter. However, a sky chart is known to be less accurate, depending, among other things, on the optical properties of the cloud cover [Dahlback, 1995]. Moreover, due to the degradation of accuracy at low solar elevation and the mostly cloudy conditions in winter, sky charts at polar latitudes would not be suitable in winter [Taalas and Kyrö, 1992].

IV.3.2 UV-visible DOAS

When the uncertainty of the high-resolution ozone absorption cross-sections and the 1σ confidence level of the least squares fit calculated for each spectrum are taken into account, the overall accuracy of the DOAS ozone apparent slant column amounts is better than 2%. Wavelength calibration changes should not exist for SAOZ instruments since they are self-calibrated permanently by reference to the solar Fraunhofer absorption lines. As shown by Brion et al. [1993] and Burkholder and Talukdar [1994], the temperature dependence of the ozone cross-sections in the visible is too small to have a significant effect on atmospheric observations with the DOAS method.

The main sources of uncertainty on the vertical column are associated with the AMF. The zenith-sky AMF is sensitive to the vertical distribution of pressure and temperature, which control the scattering geometry, to the altitude of the site, and to the ozone density profile. Short-term fluctuations of these parameters might account for a ±1% scatter in the retrieved total ozone. For real time SAOZ data based on the standard AMF calculated at 60°N, seasonal change of the ozone profile and scattering geometry introduces a systematic seasonal bias of about 5-6% amplitude at 67°N, 3-4% at 44°N, and negligible in the tropics [Høiskar et al., 1997; Van Roozendael et al., 1998; Denis et al., 1995]. The use of the standard SAOZ AMF also introduces an average meridian dependence of -3% at 67°N to +2.8% at the tropics, due to the latitudinal drift in altitude of the ozone maximum.

Another source of uncertainty of the AMF arises from the increasing tropospheric contribution during strong pollution events. AMFs are also affected by changes in the effective optical path of the scattered light. Tropospheric multiple scattering, generated by fog, thick clouds, or snow showers, can enhance the tropospheric light path. This enhancement increases the absorption by ozone and interfering species, such as O_4 and H_2O, resulting in a bias in the retrieved ozone [Van Roozendael et al., 1994]. According to Van Roozendael et al. [1998], this contribution does not exceed 1% on average at middle latitudes if erroneous data are rejected after detection by adequate criteria.

The impact of aerosols depends largely on the altitude distribution of both ozone and the aerosols [Sarkissian 1995]. Short-term variations of the background aerosol load should not affect the twilight AMF by more than ±0.5%. The reduced stratospheric aerosol layer observed in the Antarctic vortex in winter might increase the actual AMF by 1%. The effect is expected to be more significant with the strong aerosol load released by major volcanic eruptions, and with dense polar stratospheric clouds of type II.

Finally, a constant offset in the retrieved total ozone can result from the uncertainty of the determination of the residual ozone amount in the low-SZA reference spectrum. The offset depends on the method used to estimate the residual ozone [Vaughan et al., 1997] and it can be significantly reduced with methods based on a coincident ozonesonde measurement, or on a reference spectrum recorded in the direct sun mode if the instrument design allows this viewing mode.

At the Tenth WMO Dobson Intercalibration Campaign held at Arosa in July-August, 1995 [WMO, 1995], the mean bias between the Dobson and Brewer #40 was found to be less than 1%, and less than 1.6% with SAOZ #13 (operated at the same site for intercomparison purposes). Long-term comparisons of SAOZ total ozone with Dobson or Brewer co-located observations at mid-latitudes show an agreement within 0 to 2.4% with a scatter of 3% to 5% [Van Roozendael et al., 1998]. NDSC and European field inter-comparison campaigns of UV-visible spectrometers were held in May 1992 at Lauder in New Zealand [Hofmann et al., 1995]; in September 1994 at Camborne in United Kingdom [Vaughan et al., 1997]; in June 1996 at the Observatoire de Haute Provence in France [Roscoe et al., 1998], and in March 2003 at Andoya in Norway [papers in preparation]. At Camborne, the difference between four SAOZ and other DOAS spectrometers was smaller than 3% for total ozone, as well as with the co-located Dobson and integrated ozonesonde profiles. This result improved by about 1% after the following NDSC inter-comparison campaigns.

IV.4 SMOOTHING ERRORS

Remote sensing gives only a smoothed perception of the true ozone vertical column. Vertical smoothing of the information is a well-known concept to scientists involved in the retrieval of height-resolved data from measurements by both ground-based and orbiting sensors [see e.g. Rodgers 1976,1990]. This concept is applicable to vertical column measurements of ozone by all ozone sensors considered in this report. Indeed, the absorption of sunlight by ozone is not the same at all altitudes, but it varies with the abundance of ozone and with scattering and absorption processes that control the path and the intensity of solar radiation through the atmosphere. The result is that, instead of measuring the exact integral of the vertical distribution of ozone, total ozone instruments report only a weighted average of this distribution, the actual weight being dependent on a list of parameters. In the case of weak absorbers and an optically thin atmosphere, e.g. like for ozone measurements in the visible Chappuis band, the optical path is determined mainly by Rayleigh and Mie scattering. The convolution of this optical path by the ozone profile is a first-order approximation of the weighting function, often referred to as “static” weighting function.

Figure 12 illustrates schematically the optical path of the solar radiation reaching the entrance slit of the Dobson and Brewer spectrophotometers (left) and of the zenith-viewing

SAOZ instrument at twilight (right). **Figure 13** proposes a similar illustration for GOME nadir measurements. Having in mind the standard distribution of ozone with altitude, we can deduce from these figures that the static weighting function for SAOZ twilight data will reach a clear maximum for stratospheric absorptions. Dobson and Brewer direct-sun measurements will increase the relative weight of the troposphere, but again with a maximum weight in the stratosphere. For nadir-viewing satellites, at first glance, the weighting function resembles that of ground-based direct-sun observations for large solar elevations, and that of ground-based twilight observations for low solar elevations.

In the case of strong absorbers and of an optically thick atmosphere, like for ozone measurements in the ultraviolet Huggins band, the approximation of the static weighting functions (convolution of optical path enhancement and ozone profile) can lack of accuracy. The effective optical path can vary rapidly within the spectral fitting window (GOME) or between pairs of wavelengths (Dobson), and absorptions by the target absorber itself add to the loss of solar flux along the optical path, thus to the loss of photons available to measurable absorptions in the remaining part of the optical path. Dynamical weighting functions, including an estimation of the effective optical path as a function of wavelength and the effect of solar flux variations along this effective optical path, have to be calculated by appropriate radiative transfer tools.

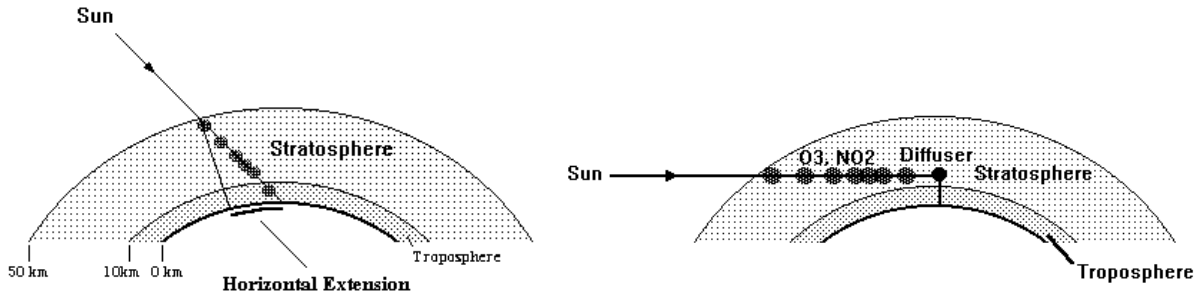

Figure 12 – Schematic view of the optical path of: (left) direct sunlight measured by the Dobson and the Brewer instruments; and (right) single-scattered sunlight observed by the ground-based zenith-sky spectrometer at twilight.

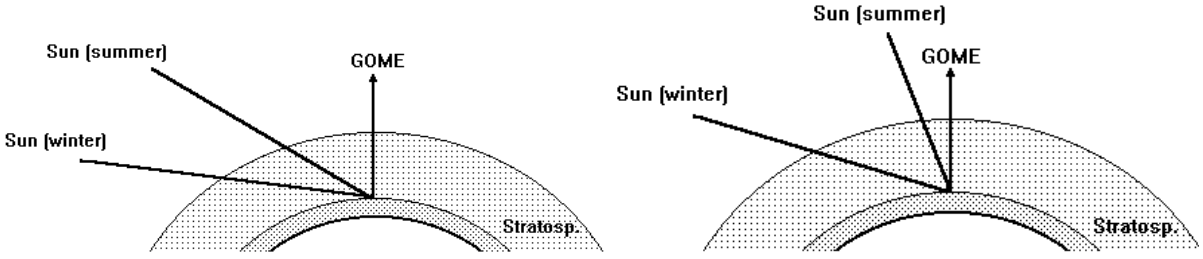

Figure 13 – Schematic view of the optical path of cloud-free, single-scattered sunlight reaching GOME at high (left) and middle (right) latitudes.

To investigate the vertical smoothing inherent to GOME and TOMS, we have calculated dynamical weighting functions for the nadir sounding of the ozone column using a home-made adaptation of the DISORT radiative transfer code [Dahlback and Stamnes, 1991]. The following settings were adopted: 1-km horizontal layers from surface to top of atmosphere at 90 km; full spherical atmosphere; λ = 325 nm; all orders of multiple scattering included; AFGL profile database of atmospheric constituents [Anderson *et al.*, 1986]; background level of aerosols; cloud-free scenario; 64 solar zenith angle values from 30° to 93°; and surface albedo values typical of the ocean (0.05), land with vegetation (0.15), and aged snow (0.75). It is assumed that DISORT and the GOME and TOMS forward models provide mutually consistent results.

Figure 14 shows GOME total weighting functions representative of sub-Arctic winter (top) and the tropics (bottom). As expected, the total weighting function is found to vary with a variety of parameters affecting radiative transfer properties, like the solar zenith angle, the vertical distribution of air density, the vertical distribution of ozone, the surface albedo, the presence of clouds etc. At high and moderate solar elevations, the sensitivity evolves slowly, with a maximum weight remaining in the low stratosphere. At solar elevations lower than 10°, the weight moves rapidly up to the middle stratosphere. Increasing the albedo increases the relative weight of the lower atmosphere. Differences between the polar and tropical atmosphere result mainly, for the tropical case, in a rise of the stratospheric weight towards higher altitudes (by about 5km). In any cases, the maximum weight resides slightly below the ozone density maximum up to 80° of solar zenith angle. Deviations from the simple scenarios illustrated here, e.g. in presence of clouds, can distort the smoothing functions more or less significantly.

Vertical smoothing is only part of the smoothing issue. Much less considered than vertical smoothing, horizontal smoothing can however play a large role in the comparisons of remotely sensed ozone columns. Actually, smoothing can be a three- and sometimes four-dimensional issue. For clarity, we will investigate in this section vertical and horizontal smoothing separately. More generally, smoothing contributes to the problematic of the air mass coincidence. To ensure presumably sufficient coincidence, total ozone comparisons usually start with the selection of data to be compared. A typical example of basic data selection is the widely used time/space distance criteria; in the GOME and TOMS validation literature, this window is found to vary from 100 to 600 km and from 1 hour to 1 day. Assuming implicitly that space- and ground-based measurements both yield the exact integral of the ozone vertical distribution, and that they are concentric when the satellite overpasses the station, the presumed objective of this easy-going method is to reduce the time and distance differences in air mass. Unfortunately, it often underestimates the impact of differences in smoothing and in sensitivity to the actual, fine-scale properties of the atmosphere.

The scanning nature of GOME operation limits its horizontal resolution to its footprint, that is, 40km along track x 320km across track for the three forward scans. The GOME information is smoothed additionally by the fact that the measured radiation passes two times through the atmosphere; the optical path consists of the incoming solar beam and of the scattered beam. According to the results of weighting function studies, the spatial distance between the incoming and scattered beams near the ozone maximum should provide a good estimate of this additional horizontal smoothing of the information, which degrades the horizontal resolution of nadir data in the direction of the sun.

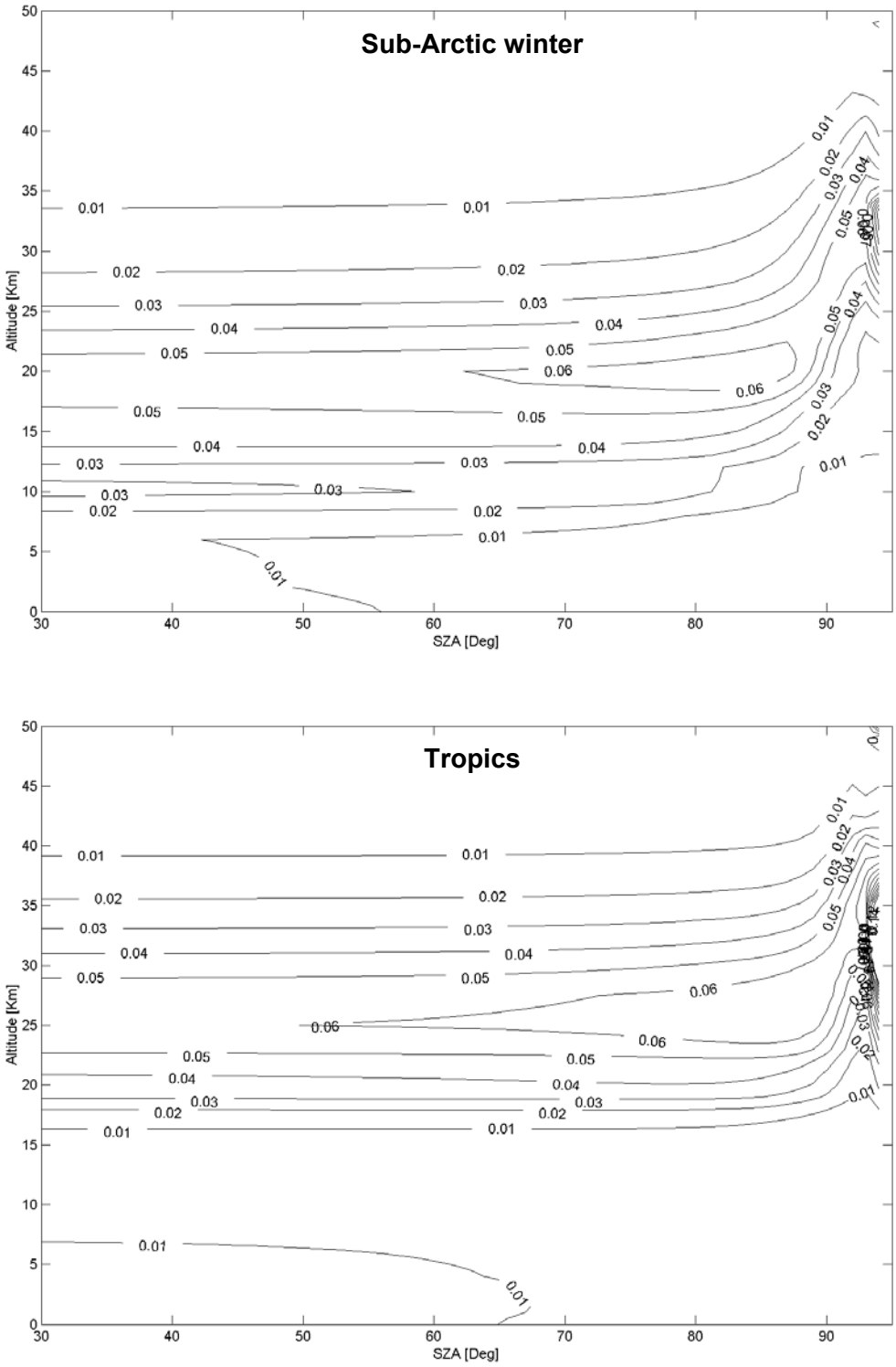

Figure 14 – Weighting functions of GOME nadir ozone column measurements for sub-Arctic winter (top) and the Tropics (bottom), as a function of the altitude and the GOME solar zenith angle.

The right-hand panel of **Figure 15** shows the amplitude of the dilution of the GOME air mass in the direction of the sun, calculated with a ray-tracing radiative transfer model. For solar elevations larger than 15°, the dilution does not exceed 40km. When approaching twilight conditions, it can reach 150 km. Using the same ray-tracing code, and knowing that the zenith-sky geometry is more sensitive to the stratosphere, we have also estimated the horizontal projection of the stratospheric contribution to the SAOZ ozone air mass. As shown in **Figure 15** (left panel), the stratospheric air mass observed at twilight does not comprise the location of the station, but it starts at a distance ranging from about 100 km at 86°SZA to 180 km at 91°SZA. The ending point of the stratospheric SAOZ air mass travels from a distance of 300 km at 86°SZA to 550 km at 91°SZA. The horizontal smoothing occurs in the direction of the rising or setting sun, thus within an azimuth changing with the season, opposite in sign between sunrise and sunset, and changing during twilight slightly at low latitudes but significantly near the Terminator. The horizontal projection of the ozone air mass probed by Dobson and Brewer instruments in direct-sun operation, thus the horizontal resolution of that kind of measurement, is estimated to extend from nearby the station to a maximum distance of about 100 km towards the sun, provided that measurements below 15° of solar elevation are excluded as recommended.

Those estimates of the spatial properties of the probed air masses suggest that selection criteria based on simple time/space window can lead to the comparison of measurements with very different horizontal resolution, and even distant by several hundred of kilometres. As illustrated in the following section, erroneous selection of the total ozone data to be compared can increase dramatically the dispersion of the comparison results, from a few percent at middle latitudes to sometimes 60% percent at Antarctic stations located at the edge of the polar vortex and situated alternatively inside and outside the ozone hole. At stations experiencing stationary gradients, e.g. near high mountains with North-South orientation or in the vicinity of stationary weather patterns, erroneous selection can even conclude to fictitious systematic biases reaching sometimes 10% and more.

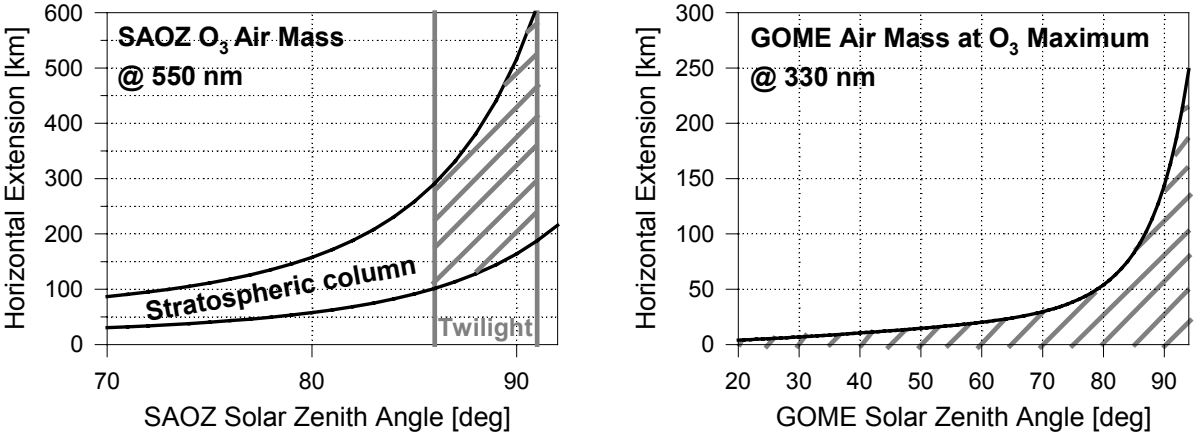

Figure 15 – Estimated horizontal extension (shaded area) of the ozone air mass probed by the SAOZ (left) and the GOME (right).

IV.5 EXAMPLES

IV.5.1 Mutual consistency of UV and UV-visible ozone column data

In Section IV.3, we have mentioned several papers dealing with the issue of the consistency between Dobson and Brewer ozone column measurements, and listed major effects leading to cyclic errors, systematic offsets and fictitious trends. Here, starting from the paper published by Van Roozendael *et al.* [1998], which dealt with the main sources of discrepancy between Dobson/Brewer data and SAOZ/UV-visible data at several NDSC sites in Europe, we will show that their mutual agreement can reach the "percent" level when main sources of discrepancy are properly corrected for.

Assuming that the Dobson and Brewer instruments are well calibrated, and that their data are filtered to avoid any air mass dependence, Dobson and Brewer data can be corrected for their temperature dependence using the formulas given by Komhyr et al. [1993]. Corrections at the stations of Arosa (46°N) and Sodankylä (67°N) are displayed in **Figure 16**. The temperature sensitivity is responsible for a fictitious seasonal variation of ±0.9% in the Alps and ±1.7% at Sodankylä (Finland), and for a systematic offset smaller than 1%.

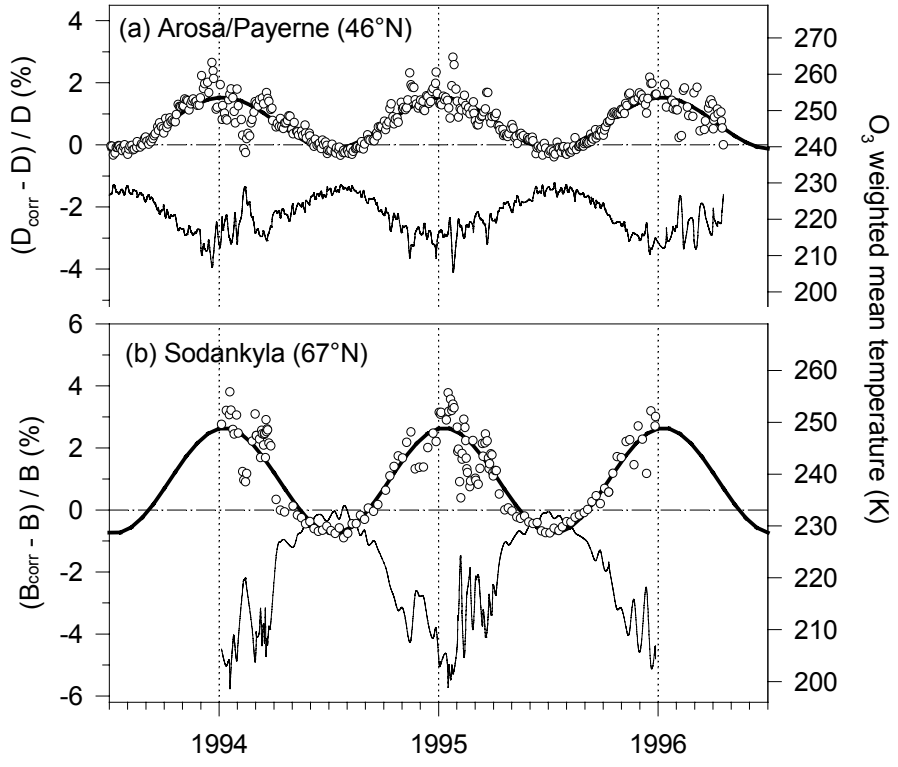

Figure 16 – Time-series of the relative difference in total ozone between corrected and uncorrected Dobson data at Arosa (46°N) and Brewer data at Sodankylä (67°N). Temperature corrections are based on ozone-weighted mean temperatures derived from ozonesonde profile measurements at Payerne and Sodankylä, respectively. (adapted from Van Roozendael *et al.*, 1998).

For the SAOZ, it is essential to calculate air mass factors at the right altitude of the station, otherwise offsets of up to 5% can show up in the case of high mountain stations. The use of the standard SAOZ ozone air mass factor, calculated with fixed pressure, temperature and ozone profiles that can not reproduce the actual variability of the atmosphere, introduces in the time-series seasonally varying offsets, in addition to the ±1% scatter that might result from short-term fluctuations of these parameters. This effect is shown in **Figure 17** at the NDSC stations of Jungfraujoch/Payerne (Switzerland), Uccle (Belgium) and Sodankylä (Arctic Finland).

After due correction for the temperature sensitivity of the Dobson and Brewer instruments (**Figure 16**) and the seasonal variation of the SAOZ air mass factor (**Figure 17**), **Figure 18** shows that apparent seasonalities between Dobson/Brewer and SAOZ ozone column measurements vanish. It is worth mentioning that most of the data archived at WOUDC and NDSC, and used in the comparisons presented in Chapter VI, are based on standard settings and consequently do not include the aforementioned corrections. Therefore corresponding errors will be taken into account in the discussion of comparison results.

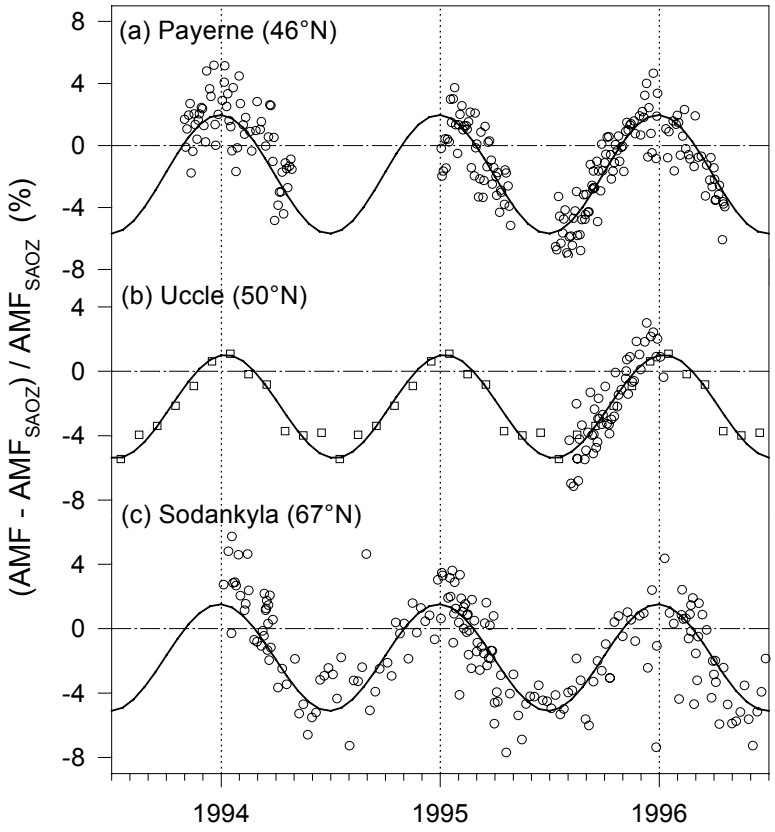

Figure 17 – Time-series of the relative difference between SAOZ ozone air mass factors calculated from ozonesonde data and standard SAOZ air mass factors, at three different latitudes in Europe (adapted from Van Roozendael *et al.*, 1998).

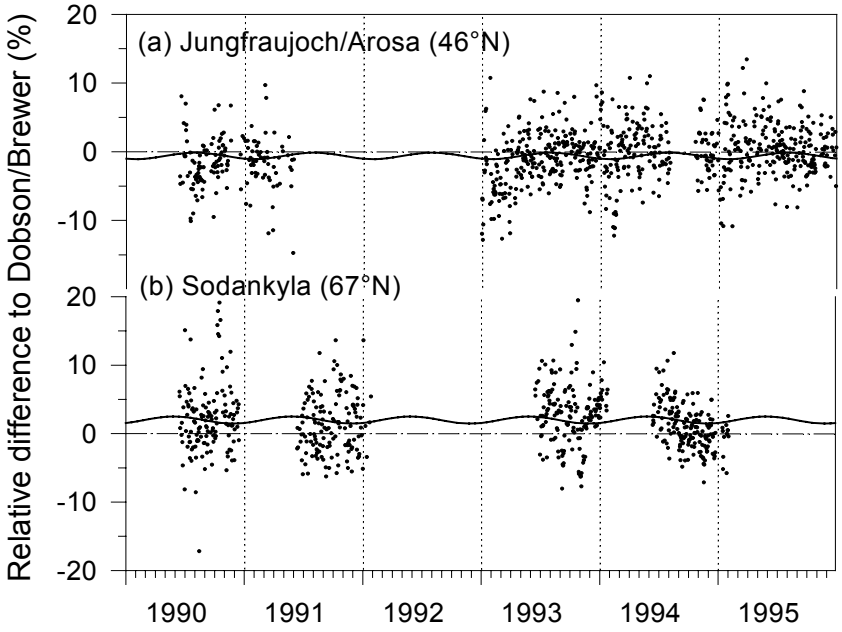

Figure 18 – Time-series of the relative difference of ozone measured by the SAOZ at the Jungfraujoch (a) and at Sodankylä (b) to that measured respectively by the Dobson at Arosa and by the Brewer at Sodankylä, after correction for the temperature sensitivity of the Dobson and Brewer instruments (see **Figure 16**) and for the seasonal variation of the SAOZ air mass factor (see **Figure 17**) (adapted from Van Roozendael *et al.*, 1998).

IV.5.2 Coincidence of effective air masses

The discussion in Section IV.4 suggested that selection criteria based on simple time/space window could lead to the comparison of measurements with very different horizontal resolution, and even distant by several hundred of kilometres. **Figure 19** illustrates this problem with the comparison between GOME and SAOZ total ozone at the Jungfraujoch on a day with spatial gradients and high variability typical of the fall season over the Alps. For this example, comparing the SAOZ sunset data with all GOME pixels acquired within a radius of 500 km around the station would conclude to a systematic offset of nearly 5% and a 1σ scatter of 6%. The same GOME/SAOZ comparison based on the daily average of sunrise and sunset SAOZ data would lead to even worse conclusion since sunrise SAOZ data concern high ozone air masses located several hundred kilometres eastward from the station. On the opposite, if we compare only GOME measurements for which the footprint offers at least 25% of overlap with the effective air mass probed by SAOZ, then the mean agreement for this unstable day falls down to 2.5% and its 1σ scatter down to about 1% [Lambert *et al.*, 1998]. It is not excluded that the remaining 2.5% difference can be partly explained by the 8-hour time distance between sunset (SAOZ acquisition) and mid-morning (GOME overpass). A similar behaviour is obtained when comparing Jungfraujoch SAOZ and Arosa Dobson total ozone data. Comparisons based on sunrise SAOZ data only, which overpass the Arosa station situated Eastern of the Jungfraujoch, are less scattered than comparisons based on sunset data which concern air masses situated several hundred kilometres westward from Arosa.

The difference in air mass extension, thus in horizontal smoothing, can also explain parts of the difference in scatter seen in Chapter VI between GOME/SAOZ, GOME/Dobson, TOMS/SAOZ and TOMS/Dobson comparisons.

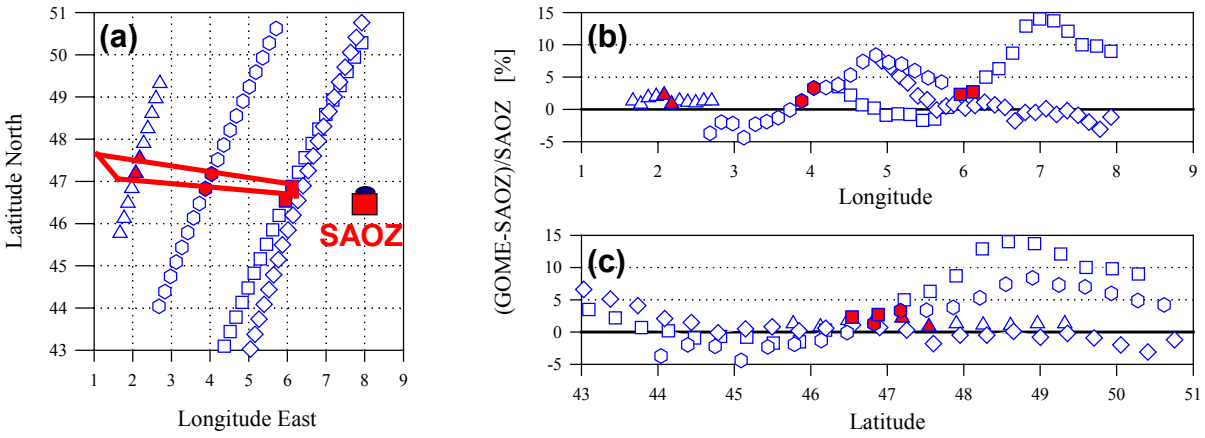

Figure 19 – Effect of air mass differences on the GOME/SAOZ comparisons, illustrated at the Jungfraujoch (Switzerland) on 4 September 1995. Panel (a) displays the horizontal projection of the centres of individual GOME footprints recorded on this day in a radius of 500 km around the station (blue open symbols); the SAOZ location and the horizontal projection of its sunset air mass are represented in red; GOME measurements crossing the SAOZ air mass with at least 25% of area overlap are highlighted in red. Panels (b) and (c) show the corresponding difference between GOME and SAOZ total ozone as a function of the longitude (b) and latitude (c) of the footprint centres; differences corresponding to the GOME footprints overlapping the SAOZ air mass are highlighted in red.

IV.6 CONCLUSION

The main conclusion of this Chapter is that uncertainties in the standard and/or real-time ozone data products as available from existing databases (namely, NDSC, WOUDC and ENVISAT Cal/Val), coupled to smoothing errors, can be larger than the expected agreement between improved satellite (GOME GDP 4.0 and TOMS V8) and ground-based ozone column data. Ground-based validation of satellites at the "1-% level" is nevertheless feasible provided that the interpretation takes major uncertainties into account, as it will be done in Chapter VI when discussing comparison results.

References

Anderson, G. P., S.A. Clough, F. X. Kneizys, J. H. Chetwynd, and E. P. Shettle, AFGL Atmospheric Constituents Profiles (0-120 km), Environmental Research Papers, No. 954, AFGL-TR-86-0110, AFGL (OPI), Hanscom AFB, MA 01736, 1986.

Basher, R.E. Review of the Dobson spectrophotometer and its accuracy, WMO Global ozone research and monitoring project, Report No 13, WMO Geneva, 1982.

Basher, R.E., Survey of WMO-sponsored Dobson spectrophotometer intercomparisons, WMO/GAW Global Ozone research and Monitoring Project, Report No 19, WMO Geneva, 1994.

Brewer, A.W., A replacement for the Dobson spectrophotometer, *Pure and Appl. Geophys.*, 106-108, 919-927, 1973.

Brion, J., A. Chakir, D. Daumont, J. Malicet, and C. Parisse, High Resolution Laboratory Cross-sections of O3, Temperature Effect, *Chem. Phys. Lett.*, 6, 612, 1993.

Burkholder, J. B., and R. K. Talukdar, Temperature dependence of the ozone absorption spectrum over the wavelength range 410 to 760 nm, Geophys. Res. Lett., 21, 581-584, 1994.

Dahlback, A., and K. Stamnes, A new spherical model for computing the radiation field available for photolysis and heating at twilight, *Planet. Space Sci.*, 39, 671-683, 1991.

Dahlback, A., The Influence of Clouds on Dobson Measurements, Proceedings of the 3rd European Symposium on Polar Stratospheric Ozone, Schliersee, Bavaria, Germany, 18-22 September 1995, edited by J.A. Pyle, N.R.P. Harris, and G.T. Amanatidis, published by the European Commission (DG XII, Brussels, Belgium), Air Pollution Research Report 56 (891 pages), 527-531, 1995.

De Backer, H., and D. De Muer, Intercomparison of Total Ozone Data Measured With Dobson and Brewer Ozone Spectrophotometers at Uccle (Belgium) From January 1984 to March 1991, Including Zenith Sky Observations, *J. Geophys. Res.*, Vol. 96, pp. 20,711-20,719, 1991.

De Muer, D., and H. De Backer, Revision of 20 Years of Dobson Total Ozone Data at Uccle (Belgium): Fictitious Dobson Total Ozone Trends Induced by Sulfur Dioxide Trends, *J. Geophys. Res.*, 97, 5921-5937, 1992.

Denis, L., J.-P. Pommereau, F. Goutail, T. Portafaix, A. Sarkissian, M. Bessafi, S. Baldy, J. Leveau, P. V. Johnston, and A. Matthews, SAOZ Total O3 and NO2 at the Southern Tropics and Equator, Proceedings of the 3rd European Symposium on Polar Stratospheric Ozone, Schliersee, Bavaria, Germany, 18-22 September 1995, edited by J.A. Pyle, N.R.P. Harris, and G.T. Amanatidis, published by the European Commission (DG XII, Brussels, Belgium), Air Pollution Research Report 56 (891 pages), 458-462, 1995.

Dobson, G.M.B., Observer's handbook for the ozone spectrophotometer, Ann. Int. Geophys. Year, 5, 46-89, 1957a.

Dobson, G.M.B., Adjustment and calibration of ozone spectrophotometer, Ann. Int. Geophys. Year, 5, 90-114,1957b.

Fioletov, V., J. Kerr, E. Hare, G. Labow, and R. McPeters, An assessment of the world ground-based total ozone network performance from the comparison with satellite data, *Journal of Geophysical Research*, 1999.

Høiskar, B. A. K., A. Dahlback, G. Vaughan, G. O. Braathen, F. Goutail, J.-P. Pommereau, and R. Kivi, Interpretation of ozone measurements by ground-based visible spectroscopy - A study of the seasonal dependence of air mass factors for ozone based on climatology data, J. Quant. Spectrosc. Radiat. Transfer, 57, 569-579, 1997.

Josefsson, W. A. P., Focused Sun observations using a Brewer ozone spectrophotometer, J. Geophys. Res., 97, 15 813-15 817, 1992.

Kerr, J. B., C. T. McElroy, and W. F. J. Evans, The automated Brewer spectrophotometer for measurement of SO_2, O_3, and aerosols, Proceedings of the WMO/AMS/CMOS Symposium on Meteorological Observations and Instrumentation, 470-472, American Meteorological Society, Boston, MA, 1983.

Kerr, J.B., I.A. Asbridge and F.J. Evans, Intercomparison of total ozone measured by the Brewer and Dobson spectrophotometers at Toronto, J. Geophys. Res., 93, 11,129-11,140, 1988.

Komhyr, W.D., R.D. Grass and R.K. Leonard, Dobson spectrophotometer 83: a standard for total ozone measurements, 1962-1987*, J. Geophys. Res.*, 94, 9847-9861, 1989.

Komhyr, W.D., C. L. Mateer, R. D. Hudson, Effective Bass-Paur 1985 Ozone Absorption Coefficients for Use With Dobson Ozone Spectrophotometers, *J. Geophys. Res.*, 98, 20,451-20,465, 1993.

Kyro, E., Intercomparison of total ozone data from Nimbus 7 TOMS, the Brewer UV spectrophotometer and SAOZ UV-visible spectrophotometer at high latitudes observatory, Sodankyla, *Geophys. Res. Lett.*, 20, 571-574, 1993.

Lambert, J-C., M. Van Roozendael, J. Granville, P. Gerard, P. C. Simon, H. Claude, and J. Staehelin, Comparison of the GOME ozone and NO2 total amounts at mid-latitude with ground-based zenith-sky measurements, Atmospheric Ozone - Proc. 18th Quad. Ozone Symp., L'Aquila, Italy, 12-21 September 1996, 2 Vol., edited by Rumen D. Bojkov and Guido Visconti, Vol. I, 301-304, 1998.

Lambert, J.-C., M. Van Roozendael, M. De Mazière, P.C. Simon, J.-P. Pommereau, F. Goutail, A. Sarkissian, and J.F. Gleason, Investigation of pole-to-pole performances of spaceborne atmospheric chemistry sensors with the NDSC, *Journal of the Atmospheric Sciences*, Vol. 56, pp. 176-193, 1999.

Nichol, S. E., and C. Valenti, Intercomparison of total ozone measured at low sun angles by the Brewer and Dobson spectrophotometers at Scott Base, Antarctica, *Geophys. Res. Lett.*, 20, 2051-2054, 1993.

Pfeilsticker, K., D.W. Arlander, J.P. Burrows, F. Erle, M. Gil, F. Goutail, C. Hermans, J.-C. Lambert, U. Platt, J.-P. Pommereau, A. Richter, A. Sarkissian, M. Van Roozendael, T. Wagner, and T. Winterrath, Intercomparison of the influence of tropospheric clouds on UV-visible absorptions detected during the NDSC intercomparison campaign at OHP in June 1996, *Geophysical Research Letters*, 26, pp. 1169-1172, 1999.

Pommereau, J.-P., and F. Goutail, Ground-based Measurements by Visible Spectrometry during Arctic Winter and Spring 1988, *Geophys. Res. Lett.*, 15, 891-894, 1988a.

Pommereau, J. P., and F. Goutail, Stratospheric O_3 and NO_2 observations at the southern polar circle in summer and fall 1988, *Geophys. Res. Lett.*, 15, 895-898, 1988b.

Rodgers, C. D., The Vertical Resolution of Remotely Sounded Temperature Profiles with a priori Statistics, *J. Atmos. Sci.*, 33, pp. 707-709, 1976.

Rodgers, C. D., Characterization and Error Analysis of Profiles Retrieved From Remote Sounding Measurements, *J. Geophys. Res*., 95, pp. 5587-5595, 1990.

Roscoe, H. K., J. A. C. Squires, D. J. Oldham, A. Sarkissian, J.-P. Pommereau, F. Goutail, Improvements to the accuracy of zenith-sky measurements of total ozone by visible spectrometers, J.Q.S.R.T., 52, 639-648, 1994.

Roscoe, H.K., P.V. Johnston, M. Van Roozendael, A. Richter, A. Sarkissian, J. Roscoe, K.E. Preston, J.-C. Lambert, C. Hermans, W. De Cuyper, S. Dzienus, T. Winterrath, J. Burrows, F. Goutail, J.-P. Pommereau, E. D'Almeida, J. Hottier, C. Coureul, D. Ramon, I. Pundt, L.M. Bartlett, C.T. McElroy, J.E. Kerr, A. Elokhov, G. Giovanelli, F. Ravegnani, M. Premuda, I. Kostadinov, F. Erle, T. Wagner, K. Pfeilsticker, M. Kenntner, L.C. Marquard, M. Gil, O. Puentedura, M. Yela, W. Arlander, B.A. Kåstad Høiskar, C.W. Tellefsen, K. Karlsen Tørnkvist, B. Heese, R.L. Jones, S.R. Aliwell, and R.A. Freshwater, Slant column measurements of O_3 and NO_2 during the NDSC intercomparison of zenith-sky UV-visible spectrometers in June 1996, *Journal of Atmospheric Chemistry*, Vol. 32, pp. 281-314, 1999.

Sarkissian, A., H. K. Roscoe, D. Fish, M. Van Roozendael, M. Gil, A. Dahlback, L. Perliski, J.-P. Pommereau, and J. Lenoble, Ozone and NO_2 air-mass factors for zenith-sky spectrometers: intercomparison of calculations with different radiative transfer models, *Geophys. Res. Lett.*, 22, 1113-1116, 1995.

Sarkissian, A., H. K. Roscoe, and D. J. Fish, Ozone measurements by zenith-sky spectrometers: an evaluation of errors in air-mass factors calculated by radiative transfer models, *J.Q.S.R.T.*, 54, 471-480, 1995.

Staehelin J., J. Kerr, R. Evans and K. Vanicek, Comparison of total ozone measurements of Dobson and Brewer spectrophotometers and recommended transfer functions, WMO TD N. 1147, No 149, 2003.

Taalas, P., and E. Kyrö, Two years of regular ozone soundings in the European Arctic, Sodankylä, *J. Geophys. Res.*, 97, 8093-8097, 1992.

Van Roozendael, M., M. De Mazière and P. C. Simon, Ground-based visible measurements at the Jungfraujoch Station since 1990, *J.Q.S.R.T.*, 52, 231-240, 1994.

Van Roozendael, M., P. Peeters, H. K. Roscoe, H. De Backer, A. Jones, G. Vaughan, F. Goutail, J.-P. Pommereau, E. Kyrö, C. Wahlstrøm, G. Braathen, and P. C. Simon, Validation of Ground-based UV-visible Measurements of Total Ozone by Comparison with Dobson and Brewer Spectrophotometers, *J. Atm. Chem.*, 29, 55-83, 1998.

Vaughan, G., H. K. Roscoe, L. M. Bartlett, F. O'Connor, A. Sarkissian, M. Van Roozendael, J.-C. Lambert, P.C. Simon, K. Karlsen, B.A. Kåstad Høiskar, D.J. Fish, R.L. Jones, R.A. Freshwater, J.-P. Pommereau, F. Goutail, S. B. Andersen, D. G. Drew, P. A. Hughes, D. Moore, J. Mellqvist, E. Hegels, T. Klupfel, F. Erle, K. Pfeilsticker, and U. Platt, An intercomparison of ground-based UV-Visible sensors of ozone and NO_2, *Journal of Geophysical Research*, Vol. 102, pp. 1411-1422, 1997.

WMO, 1995: World Meteorological Organization Global Atmosphere Watch (WMO), Report of the tenth WMO international comparison of Dobson spectrophotometers (Arosa, Switzerland, 24 July - 4 August 1995), Environmental Pollution Monitoring and Research Programme Report Series No. 108, 1995.

V SUMMARY OF CHANGES BETWEEN TOMS V7 AND V8

The TOMS instruments provides measurements of Earth's ozone total column by measuring the backscattered Earth radiance at a set of discrete 1-nm wavelength bands in the region 310-380nm. Both absorbing and non-absorbing regions of the backscattered ultraviolet (BUV) are sampled, and the concept of differential absorption is used to derive total column ozone from these measurements. The experiments use a single monochromator and scanning mirror to sample the BUV radiation. TOMS uses periodic measurements of the sun to provide normalisation of the BUV radiances to the solar output, and to remove some instrumental dependence. The TOMS scanning mechanism provides (except for Earth Probe) equatorial inter-orbit overlap so that the entire sunlit portion of the globe is sampled daily. The sun synchronous near-polar orbits (except for Meteor-3) provide these measurements at the same approximate local time, the local equator crossing time over most of the globe throughout the course of the experiment.

For the validation study we used TOMS data from Earth Probe satellite, processed at NASA/GSFC for the period 1996-2003. The absolute calibration of the Earth Probe TOMS data was determined from extensive pre-launch instrument testing. The Earth Probe TOMS time-dependent calibration is maintained by using a series of three on-board diffuser plates. The calibration is directly maintained to high accuracy by analysing the degradation of the cover diffuser relative to the working and reference diffusers. In 2001 a bias in measurements made on one side of the orbital track relative to measurements from the opposite side of the scan was discovered in the Earth Probe TOMS data, and this problem became worse with time. An empirical correction was implemented in the Version 8 Earth Probe TOMS calibration to stabilise it relative to NOAA-16 SBUV/2 in the equatorial zone. Because of continuing changes in the optical properties of the front scan mirror that are not well understood, the TOMS team is however seeing a latitude dependent error that cannot be corrected by a simple calibration correction. The calibration appears to be stable near the equator. But by 50 degrees latitude, there is now a -2% to -4% error in TOMS, a bit larger in the northern hemisphere than in the southern hemisphere. Because of this error, NASA/GSFC recommends that data since 2002 are NOT used for trend analysis.

TOMS version 8 [Bhartia and Wellemeyer, 2004] is the most recent version of the BUV total ozone algorithms. BUV algorithms have undergone 30 years of progressive refinement. Version 8 has corrected several errors that were discovered in its predecessor version 7 [McPeters *et al.*, 1998]. TOMS V8 uses only two wavelengths (317.5 and 331.2nm) to derive total ozone while other 4 wavelengths (depending on the instrument) are used for diagnostics and error corrections. There were several improvements introduced in TOMS v8 [Bhartia and Wellemeyer, 2004], which are described hereafter.

V.1 UPGRADED A PRIORI OZONE PROFILE DATABASE

A set of 21 standard ozone profiles and a single temperature profile are used to generate the basic radiance tables. The ozone profiles have been generated using ozonesonde data below 25 km and SAGE-II satellite data above. The ozone profile data are binned two-dimensionally: in 50 DU total ozone bins, and in 30° latitude bins. The same set of profiles is used in both hemispheres. There are 3 profiles for low latitudes (30S-30N) containing 225-325 DU, 8 for mid latitude (30-60) containing 225-575 DU, and 10 for high latitude (60-pole) containing 125-575 DU.

V.2 SEASONAL AND LATITUDINAL TEMPERATURE DEPENDENCE IN OZONE ABSORPTION PROPERTIES

A single US standard temperature profile is used in constructing the radiance tables, and thus the effect of seasonal and latitudinal variation of temperature on ozone cross-sections is not accounted for. This practice is also consistent with the standard procedures used by the ground-based Dobson and Brewer instruments, which also ignore seasonal and latitudinal variations in atmospheric temperature in retrieving total ozone from their measurements. The previous TOMS algorithms had ignored these effects, since they did not increase the RMS error of a single measurement significantly and had virtually no impact on global ozone trend. TOMS V8 corrects for these errors by incorporating monthly and latitudinally varying ozone and temperature climatologies in the retrieval algorithm. These errors are corrected using Jacobians – defined as dlogI/dx, where I is the TOA (top of atmosphere) radiance, and x is the layer ozone amount in ~4.8 km (Δlogp=log2) atmospheric layers. The month-latitude climatology of temperature profiles is obtained from NOAA/NCEP data.

V.3 UPDATED TROPOSPHERIC OZONE CLIMATOLOGY

The new climatology, based mostly on ozonesonde measurements (enhanced significantly by the SHADOZ programme) follows the seasonal behaviour of tropospheric ozone and its hemispherical asymmetry.

V.4 IMPROVED RADIATIVE TRANSFER IN FORWARD MODEL

The current version of TOMS forward model TOMRAD is a modified version of the original Dave code. The modifications include pseudospherical correction, molecular anisotropy and rotational Raman scattering. The current version of the code handles multiple absorbers, accounts for the effect of temperature on molecular absorption and of the Earth's gravity on the Rayleigh optical depth.

V.5 IMPROVED CORRECTIONS FOR CLOUD, TROPOSPHERIC AEROSOL, SEA GLINT AND ROTATIONAL RAMAN SCATTERING EFFECTS

TOMS v7 in the presence of absorbing aerosols overestimates total ozone. Based on the Aerosol Index (AI), calculated using radiances at 331.2 and 360nm, and an empirical linear relationship between the residues at 360nm and the ozone error [Torres and Bhartia, 1999],

the new algorithm corrects for this effect. The same correction procedure is also applied for sea-glint. It is important however to separate sea-glint from clouds. TOMS v8 distinguishes clouds from sea-glint using the fact that clouds do not produce residues. In cases where geometry indicates the potential for sea-glint retrievals with 360nm >3.5% are flagged. Rotational Raman scattering effects are considered in the forward model calculations [Joiner *et al.*, 1995].

V.6 IMPROVED TREATMENT OF SNOW/ICE SURFACE REFLECTANCE

Initially in the forward model the surface reflectivity is set to 0.15 (although in the UV most surfaces show a reflectivity between 2% and 8%) in order to account for haze, aerosols and fair weather cumulus clouds and the cloud reflectivity is set to 0.8. When in the inverse algorithm the effective reflectivity is calculated and found larger than 0.8 it is assumed that the surface contribution to the radiance is zero. Using a climatological database surfaces containing snow/ice are flagged. When the snow/ice flag is set it is assumed that the cloud contribution to the radiances is negligible.

V.7 REFERENCES

Bhartia P.K, and C. Wellemeyer, TOMS version 8 Algorithm Theoretical Basis Document, http://toms.gsfc.nasa.gov, 2004-11-24.

Joiner, J., P.K. Bhartia, R.P. Cebula, E. Hilsenrath, R. McPeters, and H.W. Park, Rotational Raman Scattering (Ring Effect) in Satellite Backscatter Ultraviolet Measurements, Appl. Opt., 34, 4513-4525, 1995.

Labow G.J., R.D. McPeters, and P.K. Bhartia, A Comparison of TOMS, SBUV & SBUV/2 Version 8 Total Column Ozone Data with Data from Groundstations, Proceedings of QOS2004, Kos, 1-8 June, Kos, Greece, 2004.

McPeters R., P.K. Bhartia, A. Krueger and J. Herman, Earth Probe Total Ozone Mapping Spectrometer (TOMS) Data Products User's Guide, NASA Technical Publication 1998-206895, 1998.

Torres O and P.K. Bhartia, Imapct of tropospheric aerosol absorption on ozone retrieval from backscattered ultraviolet measurements, J. Geophys. Res., 104, 21569-21577, 1999.

WMO, Scientific Assessment of Ozone Depletion, 1998.

WMO, Scientific Assessment of Ozone Depletion, 2002.

VI OZONE COLUMN VALIDATION

VI.1 INTRODUCTION

In the GOME GDP 2.7 ozone column product, there was a pronounced dependence of the differences between GOME and ground-based data on the season, the solar zenith angle, the ozone column value, and the latitude. With the GDP upgrade from version 2.7 to 3.0, the ozone column dependence had nearly disappeared and the amplitude of all other dependences had reduced by about 50% on an average. With TOMS V7, seasonally varying errors showed a lower amplitude, but a systematic offset affected the whole Southern hemisphere, increasing with latitude from a few percent in the Tropics to about 10% in Antarctica. An ozone column dependence was also found in TOMS V7. Effects of instrumental degradation were noted with both TOMS V7 and GDP 2.7, but not with GDP 3.0. Present upgrades of GOME GDP to version 4.0 and TOMS to version 8 aim at reducing drastically all remaining dependences.

The main objective of this Chapter is to verify and quantify changes in the GOME ozone column product as expected from the GDP upgrade to version 4.0. The study will rely on comparisons of GOME validation orbits to ground-based measurements acquired by ground-based networks. Similar studies will be conducted with the TOMS ozone algorithm upgrade to version 8. For TOMS, comparisons will be based on the overpass data files available from NASA/GSFC.

In this Chapter, we will take advantage of the complementary capabilities offered by the different NDSC techniques as well as the statistical capabilities offered by the WOUDC worldwide network data, to investigate a list of expected improvements. The investigation will address the following aspects:

- Global agreement between satellite and ground-based network total ozone data;
- Cyclic errors associated with the season, solar zenith angle, and temperature;
- Meridian structures;
- Long-term stability;
- Dependence on the ozone column value;
- Dependence on the fractional cloud cover.

Correlative data records and their quality control will be described in Section VI.2. In Section VI.3, test case studies at the Alpine station of the NDSC will illustrate how validation at the "percent level" is feasible thanks to the integrated interpretation of complementary measurement types. Taking into account the error budget of ground-based ozone validation presented in Chapter IV and the results obtained at all the individual stations, Sections VI.4 to VI.7 will use large-scale capabilities of ground-based networks to investigate major characteristics of GDP 4.0 and TOMS V8 on the global scale and in the long term: global agreement, seasonal dependences, meridian structure, and long-term stability. Sections VI.8 to VI.10 will focus on dependences on the solar zenith angle, the ozone column value in ozone 'hole' conditions, and the fractional cloud cover, respectively.

VI.2 CORRELATIVE DATA RECORDS

The present study is based on archived total ozone measurements provided by two major contributors to World Meteorological Organization's Global Atmosphere Watch programme (WMO/GAW): Dobson and Brewer total ozone data records, as these are deposited at the World Ozone and UV Data Center (WOUDC) in Toronto, Canada (http://www.woudc.org); and UV-visible DOAS, Dobson and Brewer total ozone data records acquired as part of the international Network for the Detection of Stratospheric Change (NDSC, public archive available via http://www.ndsc.ws). WOUDC and NDSC operate scientific databases containing a variety of ozone-related data sets to the international scientific community. There are over 300 stations represented in the archives, some of which comprise over 35 years of continuous data. WOUDC data sets include total column ozone, surface ozone, ultraviolet irradiance data, and vertical profile data from electrochemical ozonesonde flights, differential lidar measurements, and the Umkehr technique. NDSC data sets include total columns and profiles of ozone, of the nitrogen, chlorine and bromine families, of greenhouse gases, and of aerosols, as well as ultraviolet irradiance data, acquired by ultraviolet, visible, infrared and millimetre wave spectrometry with a variety of complementary observation techniques. Total ozone data from a large number of WOUDC and NDSC stations have already been used extensively both for trend studies (e.g. WMO 1998, 2002) as well as for validation of satellite total ozone data (e.g. McPeters and Labow, 1996; Lambert et al., 1999; Fioletov et al., 1999; Lambert et al., 2000; Bramstedt et al, 2003; Labow et al., 2004,).

WOUDC contains total ozone data mainly from Dobson and Brewer UV spectrophotometers and from M-124 UV filter radiometers. NDSC database contains total ozone data from DOAS UV-visible and Fourier Transform infrared spectrometers, plus Dobson and Brewer instruments at selected stations that usually upload their preliminary data to WOUDC. As stressed in Chapter IV, before performing any comparison between satellite and ground-based total ozone data, it is essential to assess the quality of the ground-based data in both qualitative and quantitative terms. As declared at the WOUDC website, the data residing in the database must be considered preliminary and the originator(s) of data sets should always be contacted directly for detailed information. On the opposite, NDSC affiliated teams are committed to submit to the NDSC data archive only consolidated data sets duly recalibrated and validated; nevertheless, the existing literature should always be consulted to ensure that documented errors for NDSC-certified instruments are taken properly into consideration in the validation analysis, and the originator(s) of consolidated NDSC data sets should also always be contacted directly for detailed information.

Although of great value, we did not consider, for the present comparisons with satellite data, ground-based measurements performed with FTIR spectrometers and with M-124 radiometers, mainly for the following reasons: (a) coincidences offered by the Dobson, Brewer and UV-visible networks with the list of validation orbits are sufficient to investigate the effects of current GDP upgrades; (b) compared to ozone data records acquired by ultraviolet and visible instruments, FTIR ozone data records are sparser, resulting in too few coincidences with the considered delta validation orbits; (c) the network of M-124 instruments operated by Russia and the Community of Independent States (former USSR republics) add significantly to the geographical coverage over Eurasia, however, comparison results based on those instruments are found to lead to a slightly larger scatter and of show a negative offset of about 2% relative to Dobson and Brewer data of neighbouring stations.

To prepare ground-based data sets for the sake of GOME and TOMS validation, we investigated in this study the quality of the total ozone data of each station and instrument that deposited data at NDSC and WOUDC for any period during 1995-2004. Ground-based data from all the reporting stations have been compared with various versions of GOME and TOMS satellite data: GDP 2.7, GDP 3.0, GDP 4.0, the GOME fast delivery product generated by KNMI, and assimilated fields generated by KNMI and DLR (see GOA and STREAMER EU projects) for GOME; and TOMS versions 7 and 8 provided by NASA/GSFC. In order to verify the quality of the ground-based data, we examined for each station a series of plots and statistics based on GOME and TOMS comparisons. A sample of these plots is shown in **Figure 20** for the Dobson station of Potsdam in Germany. Comparisons using only direct sun ultraviolet measurements, which offer a greater accuracy (~1%) than zenith-sky data, are also performed separately (right panel). We examined for each station monthly time-series of the percent relative differences with the satellite data, the distribution of these differences, the scatter of the differences and the correlation between the satellite and the ground-based data, the mean annual course of the differences, and finally the dependence of the difference on the solar zenith angle of the satellite observation for each season of the year. The results indicated in some cases systematic inconsistencies of the comparison results with the respective ones of neighbouring stations. In certain cases unreasonable and unexpected small correlation was systematically found between the ground-based and the satellite data. Concerning the Dobson instruments some of these inconsistencies were explained when considering the results reported from international comparisons.

For NDSC data, a specific problem arises from the 2-year delay between the data acquisition and the upload of consolidated data to the central archive. The NDSC Data Protocol recognises that, in order to produce a verifiable data product, sufficient time is needed to collect, reduce, calibrate, test, analyse, and inter-compare the streams of preliminary analyses at every NDSC site. Among others, seasonal analyses may be required for observations from both individual and multiple sites and it is expected that such a procedure shall yield the verifiable product referred to as "NDSC data" within a two-year period after acquisition. To enable long-term stability studies intended in the present study, we have to augment NDSC-endorsed data records with data reported in near real time and thus not consolidated yet. For those near real time data, an additional verification is based on climatological grounds. At ground stations where long enough time-series are available in the NDSC and/or WOUDC databases, the verification procedure consists in comparing fresh data to climatological means and standard deviations that we calculate on low-pass filtered time-series acquired, if possible, since 1995. A log file is created, which identifies in a first time aberrant data, e.g. Dobson data erroneously referred to as polar night data, or sunrise NO_2 columns exceeding systematically sunset NO_2 columns. Then, column values deviating from the climatological mean by more than 2σ and 3σ are pointed out. Trains of consecutive values falling out of the $\pm 3\sigma$ interval are looked at carefully to determine whether such persistent deviations may be due to data quality issues, to natural atmospheric variability, or to unexpected atmospheric features like e.g. the 2002 Antarctic vortex split. Single values falling out of the $\pm 3\sigma$ interval without belonging to a justifiable 2σ train are flagged accordingly but are not rejected systematically since they could reflect natural atmospheric variability (e.g. high frequencies near the polar vortex boundary) or indicate interesting events like tropospheric pollution episodes enhanced by multiple scattering within clouds.

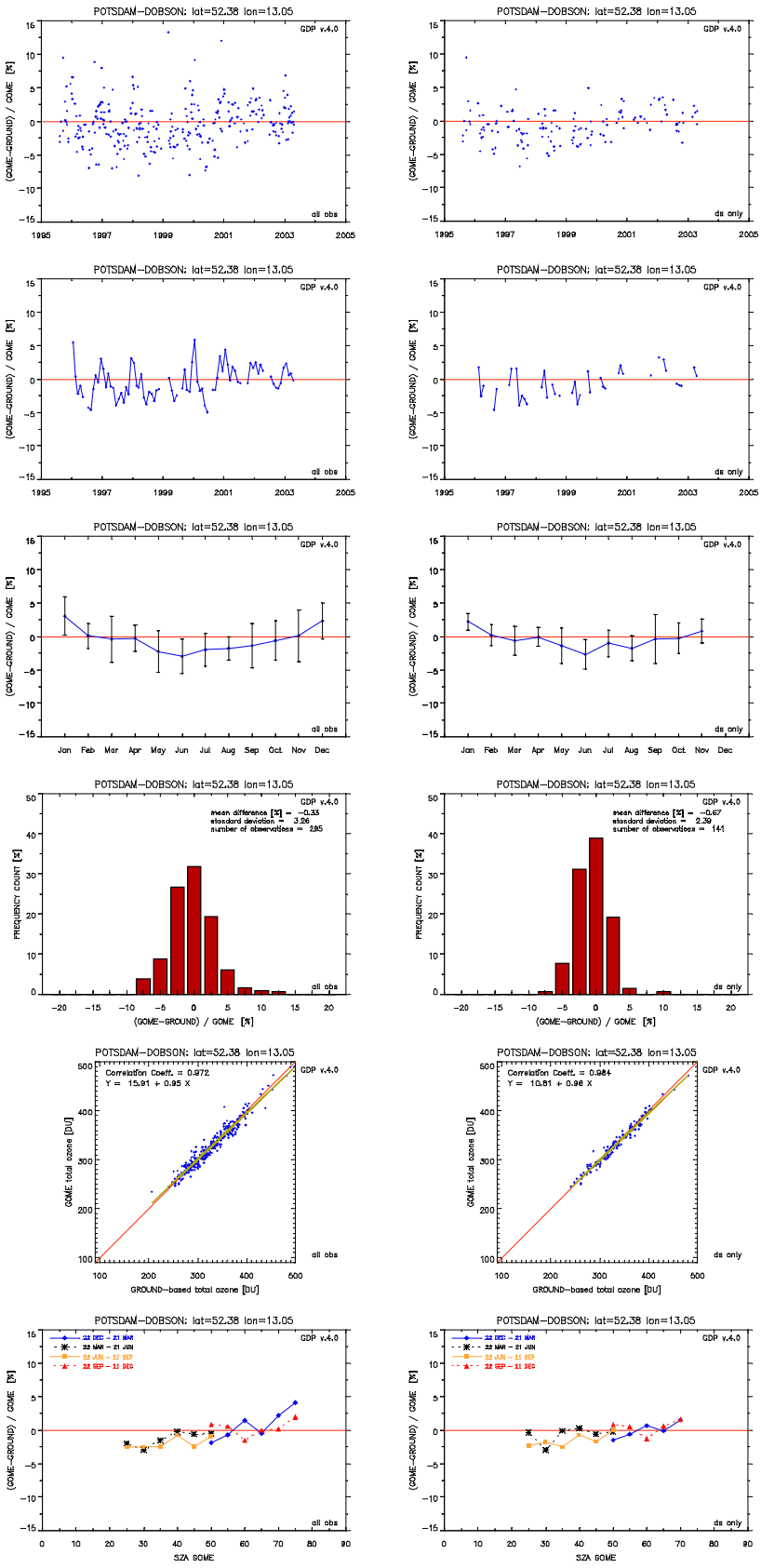

Figure 20 - Sample of individual station statistics and plots carried out for all the stations and satellite data set examined (see text). Left: all direct-sun and zenith-sky Dobson data included; right: direct-sun data only.

Finally, 41 Brewer, 61 Dobson and 27 UV-visible DOAS instruments were considered for the comparisons with GDP 3.0, GDP 4.0, and TOMS V8. The locations of these instruments are listed in **Table 1**, **Table 2** and **Table 3** for the Brewer, Dobson, and DOAS instruments, respectively.

Table 1 - List of Brewer stations selected for comparisons with GOME and TOMS ozone data sets.

ID	NAME	LATITUDE	LONGITUDE	ELEVATION	COUNTRY
314	BELGRANO	-77.87	-34.63	255	Antarctica
322	PETALING JAYA	3.10	101.65	46	Malaysia
287	FUNCHAL	32.65	-17.05	59	Portugal
332	POHANG	36.03	129.38	0	Korea
295	MT.WALIGUAN	36.17	100.53	3816	China
213	EL ARENOSILLO	37.10	-6.73	41	Spain
346	MURCIA	38.00	-1.17	69	Spain
82	LISBON	38.77	-9.13	105	Portugal
308	MADRID	40.45	-3.55	0	Spain
261	THESSALONIKI	40.52	22.97	4	Greece
305	ROME UNIVERSITY	41.90	12.52	0	Italy
282	KISLOVODSK	43.73	42.66	2070	Russia
65	TORONTO	43.78	-79.47	198	Canada
326	LONGFENSHAN	44.75	127.6	0	China
321	HALIFAX	44.90	-63.5	0	Canada
319	MONTREAL	45.47	-73.75	0	Canada
301	ISPRA	45.80	8.63	0	Italy
35	AROSA	46.77	9.67	1860	Switzerland
100	BUDAPEST	47.43	19.18	140	Hungary
99	HOHENPEISSENBERG	47.80	11.02	975	Germany
290	SATURNA	48.78	-123.13	0	Canada
331	POPRAD-GANOVCE	49.03	20.32	0	Slovakia
320	WINNIPEG	49.91	-97.24	0	Canada
96	HRADEC KRALOVE	50.18	15.83	285	Czech Rep.
338	REGINA	50.21	-104.67	0	Canada
53	UCCLE	50.8	4.35	100	Belgium
318	VALENTIA	51.93	-10.25	0	Ireland
316	DEBILT	52.00	5.18	0	Netherlands
241	SASKATOON	52.10	-105.28	550	Canada
174	LINDENBERG	52.22	14.12	98	Germany
50	POTSDAM	52.38	13.05	89	Germany
76	GOOSE	53.32	-60.38	44	Canada
21	EDMONTON	53.57	-113.52	668	Canada
279	NORKOPING	58.58	16.12	0	Sweden
77	CHURCHILL	58.75	-94.07	35	Canada
123	YAKUTSK	62.08	129.75	98	Russia
284	VINDELN	64.25	19.77	0	Sweden
267	SONDRESTROM	67.00	-50.98	150	Greenland
262	SODANKYLA	67.37	26.65	179	Finland
24	RESOLUTE	74.72	-94.98	64	Canada
315	EUREKA	79.89	-85.93	10	Canada

Table 2 - List of Dobson stations selected for the comparisons with GOME and TOMS ozone data sets.

ID	NAME	LATITUDE	LONGITUDE	ELEVATION	COUNTRY
111	AMUNDSEN-SCOTT	-89.98	-24.80	2835	Antarctica
268	ARRIVAL HEIGHTS	-77.83	166.40	250	Antarctica
101	SYOWA	-69.00	39.58	21	Antarctica
232	VERNADSKY (FARADAY)	-65.25	-64.27	7	Antarctica
339	USHUAIA	-54.85	-68.31	7	Argentina
29	MACQUARIE ISLAND	-54.48	158.97	6	Australia
342	COMODORO RIVAD.	-45.78	-67.50	43	Argentina
256	LAUDER	-45.03	169.68	3701	N. Zealand
253	MELBOURNE	-37.48	144.58	125	Australia
91	BUENOS-AIRES	-34.58	-58.48	25	Argentina
159	PERTH	-31.95	115.85	2	Australia
343	SALTO	-31.58	-57.95	31	Uruguay
340	SPRINGBOK	-29.67	17.90	1	S. Africa
27	BRISBANE	-27.47	153.03	5	Australia
265	IRENE	-25.25	28.22	1524	S. Africa
200	CACHOEIRA-PAULIS.	-22.68	-45.00	573	Brazil
191	SAMOA	-14.25	-170.57	82	USA
84	DARWIN	-12.47	130.83	0	Australia
219	NATAL	-5.83	-35.20	32	Brazil
175	NAIROBI	-1.27	36.80	1710	Kenya
214	SINGAPORE	1.33	103.88	14	Singapore
216	BANGKOK	13.73	100.57	2	Thailand
2	TAMANRASSET	22.80	5.52	1395	Algeria
245	ASWAN	23.97	32.45	193	Egypt
209	KUNMING	25.02	102.68	1917	China
190	NAHA	26.20	127.67	29	Japan
152	CAIRO	30.08	31.28	35	Egypt
11	QUETTA	30.18	66.95	1799	Pakistan
7	KAGOSHIMA	31.63	130.60	283	Japan
14	TATENO	36.05	140.13	31	Japan
106	NASHVILLE	36.25	-86.57	182	USA
341	HANFORD	36.32	-119.63	73	USA
213	EL ARENOSILLO	37.10	-6.73	41	Spain
252	SEOUL	37.57	126.95	84	Korea
107	WALLOPS ISLAND	37.87	-75.52	4	USA
293	ATHENS	38.00	23.70	15	Greece
82	LISBON	38.77	-9.13	105	Portugal
208	SHIANGHER	39.77	117.00	13	China
67	BOULDER	40.02	-105.25	1634	USA
12	SAPPORO	43.05	141.33	19	Japan
40	HAUTE PROVENCE	43.92	5.75	580	France
201	SESTOLA	44.22	10.77	1030	Italy
226	BUCHAREST	44.48	26.13	92	Romania
19	BISMARCK	46.77	-100.75	511	USA
35	AROSA	46.77	9.67	1860	Switzerland
20	CARIBOU	46.87	-68.02	192	USA
100	BUDAPEST	47.43	19.18	140	Hungary
99	HOHENPEISSENBERG	47.80	11.02	975	Germany
96	HRADEC KRALOVE	50.18	15.83	285	Czech R.
36	CAMBORNE	50.22	-5.32	88	UK
53	UCCLE	50.80	4.35	100	Belgium
68	BELSK	51.83	20.78	180	Poland
50	POTSDAM	52.38	13.05	89	Germany
116	MOSCOW	55.75	37.57	187	Russia
165	OSLO	59.92	10.72	50	Norway
43	LERWICK	60.15	-1.15	90	UK
51	REYKJAVIK	64.13	-21.90	60	Iceland
284	*VINDELN*	*64.25*	*19.77*	*0*	*Sweden*
105	FAIRBANKS	64.8	-147.89	138	USA
199	BARROW	71.32	-156.60	11	USA
89	NY ALESUND	78.93	11.88	0	Norway

Table 3 - List of UV-visible DOAS stations selected for comparisons with GOME and TOMS ozone data sets.

ID	NAME	LATITUDE	LONGITUDE	ELEVATION	COUNTRY
na	BELGRANO	-77.87	-34.63	255	Antarctica
sy	SYOWA	-69.00	39.58	21	Antarctica
ne	NEUMAYER	-70.65	-8.25	0	Antarctica
ro	ROTHERA	-67.57	-68.13	0	Antarctica
dd	DUMONT D'URVILLE	-66.67	140.01	0	Antarctica
fa	FARADAY	-65.25	-64.27	7	Antarctica
mb	MARAMBIO	-64.28	-56.72	1	Antarctica
ke	KERGUELEN	-49.36	70.26	1	Kerguelen Island
ba	BAURU	-22.35	-49.03	10	Brazil
re	SAINT-DENIS	-20.85	55.47	50	Reunion Island
nr	NAIROBI	-1.27	36.80	1710	Kenya
tw	TARAWA	1.37	172.93	1	Kiribati
iz	IZANA	28.29	-16.49		Spain
ik	ISSYK-KUL	42.63	76.98		Kyrgyzstan
oh	HAUTE PROVENCE	43.92	5.75	580	France
ju	JUNGFRAUJOCH	46.55	7.98	3580	Switzerland
ab	ABERYSTWYTH	52.42	-4.07		UK
Br	BREMEN	53.11	8.86		Germany
ha	HARESTUA	60.22	10.75		Norway
zg	ZHIGANSK	66.72	123.40		Siberia
sl	SALEKHARD	66.7	66.7		Siberia
sk	SODANKYLA	67.37	26.65	179	Finland
an	ANDOYA	69.28	16.18		Norway
sc	SCORESBYSUND	70.48	-21.96		Greenland
th	THULE	76.51	-68.76		Greenland
ly	LONGYEARBYEN	78.12	15.40	0	Norway
na	NY ALESUND	78.93	11.88	0	Norway

VI.3 TEST CASE STUDIES IN THE ALPS

Figure 21 and **Figure 22** show the percent relative difference between GOME and ground-based total ozone data recorded by three well-documented instruments of the NDSC/Alpine station: the Dobson and Brewer operated by MCH/ETHZ at Arosa (46.78°N, 9.68°E) and the SAOZ/UV-visible spectrometer operated by IASB-BIRA at the Jungfraujoch (46.55°N, 7.98°E). The Dobson and Brewer comparisons presented here are based on GOME data acquired in a radius of 150 km around the station. The ground-based data selected for the comparisons are based on recalibrated records of direct-sun measurements only. In order to reduce the impact of air mass dependence differences, a filter is applied to the individual measurements to rule out Dobson and Brewer data recorded at solar elevation lower than 15°. Dobson and Brewer time-series are also filtered by a time window of two hours around the GOME overpass to gain the best time coincidence possible. Processed with standard WMO recommendations, the Arosa Dobson and Brewer data used hereafter are based on absorption coefficients at the fixed temperature of –46.3°C, and will thus be affected by the temperature dependence of the ozone absorption coefficients. Therefore, a seasonally varying offset of about ±0.9% in amplitude is expected with the Dobson data, with a maximum of 2% offset in winter and no offset in summer. The temperature effect on Brewer data is believed to be less significant. The SAOZ ozone column data at the nearby station at the Jungfraujoch have been derived from measurements of the zenith-scattered UV-visible sunlight twice daily during sunrise and sunset. Compared to the standard SAOZ analysis procedure used for near real time processing, the data reprocessing performed at IASB-BIRA includes a list of improvements. Among the improvements relevant to satellite ozone validation, is the fact that the conversion of the fitted slant columns to vertical columns is corrected for the seasonal

variation of the zenith-sky air mass factor (associated to seasonal changes in the profile of ozone, pressure and temperature) and for the high altitude of the station. A filter based on the observed (fitted) absorptions by O_4 and H_2O is also applied to the data to rule out pollution events coupled to multiple scattering within thick clouds or snow showers, an effect not corrected for in the air mass factor calculation. GOME data are selected for comparison with SAOZ data when crossing the effective air mass sampled from the ground in the zenith-sky twilight geometry [1]. The latter is calculated by a ray tracing method. This technique of air mass matching reduces the dispersion due to horizontal smoothing differences and limits the risk of offsets in case of stationary gradients in the ozone field. The agreement of the three (nearly) collocated measurements at Arosa and at the Jungfraujoch is studied in details in [2] and [3]. Provided that Dobson and Brewer data are corrected for their temperature and air mass dependences, and provided that the SAOZ is corrected for variations of the air mass factor and for the altitude of the station, the average agreement can be better than 1%.

GOME/ground relative differences are presented in **Figure 21** and **Figure 22** as a function of the GOME solar zenith angle, and separately for the four seasons and the three instruments. Open circles represent results with the previous GDP 2.7 (grey open circles) and 3.0 (black open circles), while plain black circles show results for GDP 4.0. With the Brewer (upper panels of **Figure 21** and **Figure 22**), it is clear that the GDP 4.0 upgrade is an improvement: the seasonal dependence of +4% to –3% with GDP 2.7 and of ±2% with GDP 3.0 has fallen with GDP 4.0 below the estimated accuracy limit of the ground-based data. With the Dobson (middle panels of **Figure 21** and **Figure 22**), GDP 4.0 performs certainly better than GDP 2.7 but it is difficult to conclude that the agreement has improved between GDP 3.0 and GDP 4.0: a small seasonal variation persists, with a mean offset negligible in summertime but reaching a maximum of +3% in late fall and early winter (GOME SZA beyond 60°). Actually, this seasonally varying overestimation is comparable (but not equal) in phase and amplitude with the Dobson temperature effect (maximum offset of in winter) calculated at this station in [2]. Finally, with the SAOZ (lower panels of **Figure 21** and **Figure 22**), the improvement of GDP 4.0 compared to GDP 3.0, and *a fortiori* to GDP 2.7, is again clear: the mean agreement does not exceed ±1% and does not change with the season. From one 2.5°SZA-bin to another, the mean GOME/SAOZ agreement ranges between +2.5% and –2%, while Brewer comparisons show only a limited range of ±1%. This apparent difference in dispersion can be explained by the less amount of coincidences offered by SAOZ data (with the air mass matching technique, only one SAOZ value per individual GOME pixel) compared to the amount of GOME/Brewer coincidences (several Dobson values per individual GOME pixel), and also by residual smoothing effects related to the large tilt between of GOME and SAOZ air masses.

Taking into account the documented error budget of ozone column measurements at Arosa and the Jungfraujoch, we can conclude that the average agreement between GOME and ground-based measurements falls with GDP 4.0 within what we will call the “percent level”.

It is important to note that, in addition to Arosa in Switzerland, the same comparative study was performed at 5 other stations equipped with both Dobson and Brewer instruments, all known to keep a well-maintained calibration: Vindeln (Finland, 64°N), Oslo (Norway, 60°N), Uccle (Belgium, 51°N), Hradec Kralove (Czech Rep., 50°N), Hohenpeißenberg (Germany, 48°N), and Toronto (Canada, 44°N). Similar conclusions about GDP 4.0 were drawn for all of them.

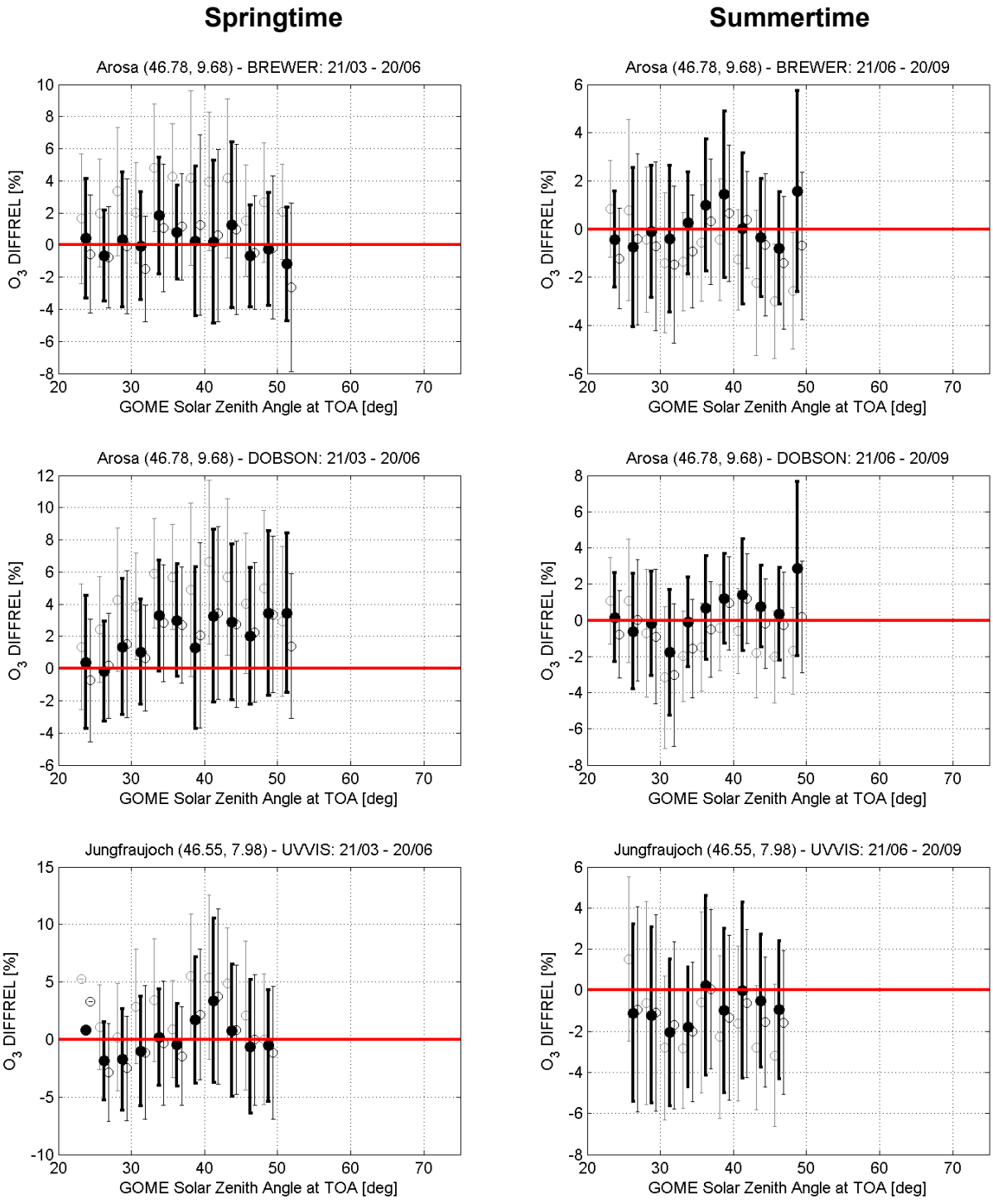

Figure 21 – Percent relative difference between GOME and ground-based total ozone at two NDSC/Alpine sites in Switzerland, averaged over 2.5°-bins and plotted as a function of the GOME solar zenith angle. From top to bottom: comparisons with MCH/ETH Brewer and Dobson at Arosa, and with BIRA-IASB SAOZ at the Jungfraujoch. Left: springtime; right: summertime. Open grey circles relate to GDP 2.7 (light grey) and GDP 3.0 (dark grey) results while plain black circles relate to GDP4. Error bars show the 1σ standard deviation around the average agreement over the 2.5°SZA-bin.

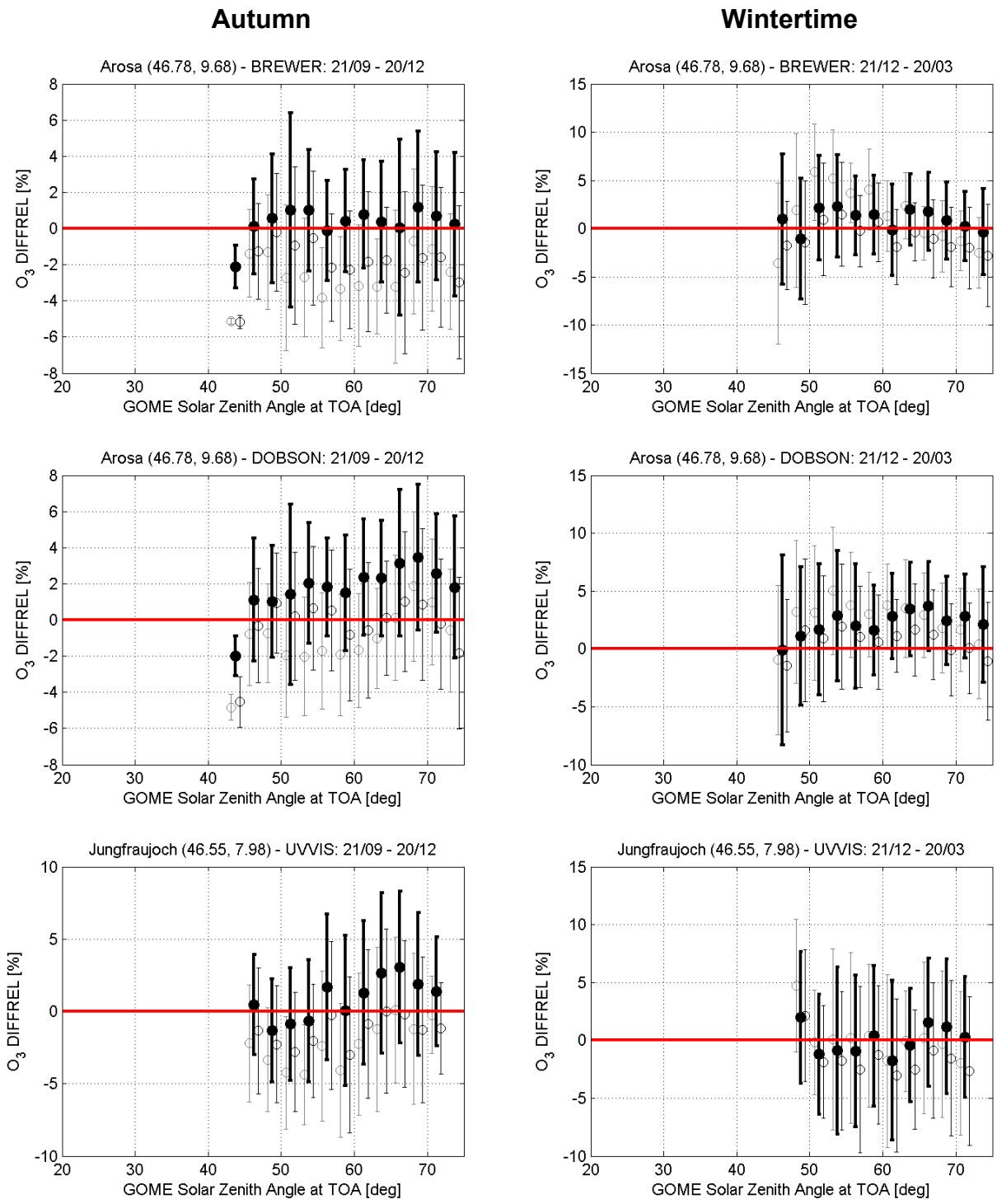

Figure 22 – Same as **Figure 21**, but for autumn (left) and wintertime (right).

VI.4 GLOBAL AGREEMENT

Figure 23 shows the month-latitude cross-sections of the differences between GOME (GDP 2.7 and GDP 3.0) and direct sun Brewer-Dobson total ozone measurements. Over the middle and high latitudes of both hemispheres, GOME GDP 2.7 overestimated ground-based total ozone during winter-spring by 2% while during summer-autumn it underestimated ground-based ozone values by down to 4% resulting to an amplitude of about 3%. In the tropics there was no significant seasonal dependence of the differences observed but in general ozone was underestimated by GOME by 1%-2%. As shown in the right panel of the same **Figure 23**, with GDP 3.0, the amplitude of the seasonal dependence over the middle and high latitudes was reduced by almost 50%. The remaining dependence was found almost in phase with the one found with GDP2.7. The change was mainly reflected in the winter-spring season where overestimation by GOME was minimised. In the tropics, GDP 3.0 showed again a negative bias of about 2%, similar to that observed with GDP 2.7. In addition, GOME underestimated ground-based total ozone by 2% to 4% over desert areas. The changes introduced in GDP 4.0 result in a different picture of the month-latitude cross sections of the differences between GOME and ground-based stations. The comparison results are shown in **Figure 24** separately for the Dobson (left panel) and the Brewer (right panel) and are based on the selected validation orbits (see Chapter III).

Figure 25 shows the same month-latitude cross-sections as in **Figure 24**, but here direct-sun Dobson (left panel) and Brewer (right panel) data are compared to TOMS V8 overpass data records. The figure indicates that TOMS has almost no bias against the Dobson total ozone observations and shows no seasonality almost in every latitude belt. The systematic TOMS V7 overestimation of the Southern Hemisphere total ozone values has disappeared. At first glance, we can conclude that both GDP 4.0 and TOMS V8 are an improvement compared to their previous operational versions. Remaining structures in time and latitude are still visible and will be discussed hereafter in Sections VI.5 and VI.6, respectively.

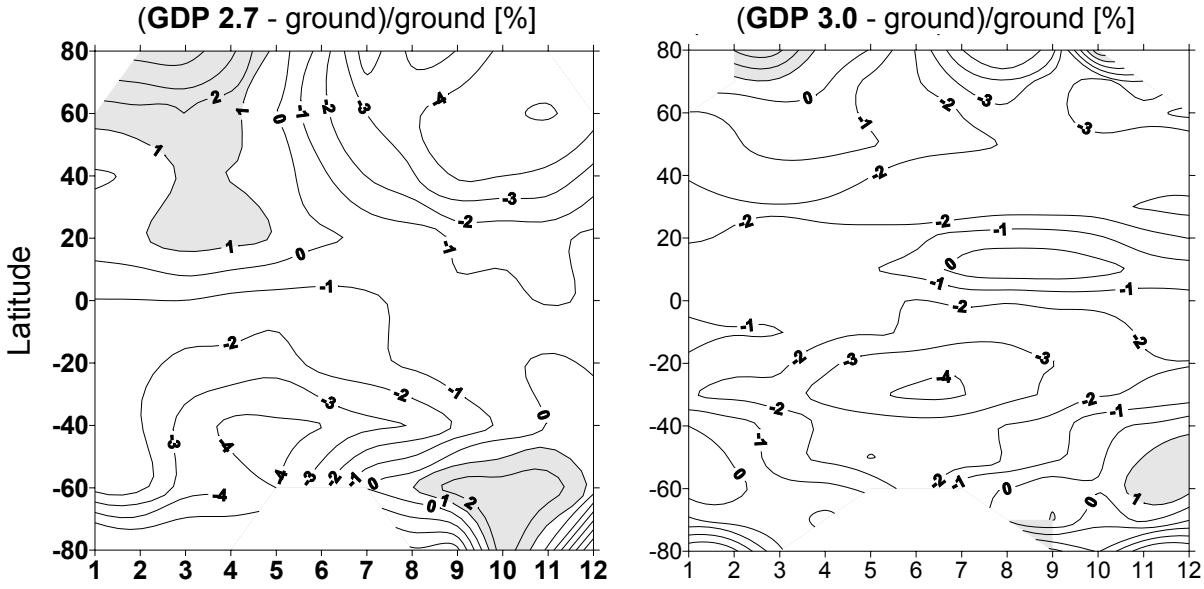

Figure 23 – Month-latitude cross-section of the relative difference between GOME ground-based total ozone (Brewer and Dobson direct sun data), based on all orbits available to the public. Left: GDP 2.7; right: GDP 3.0.

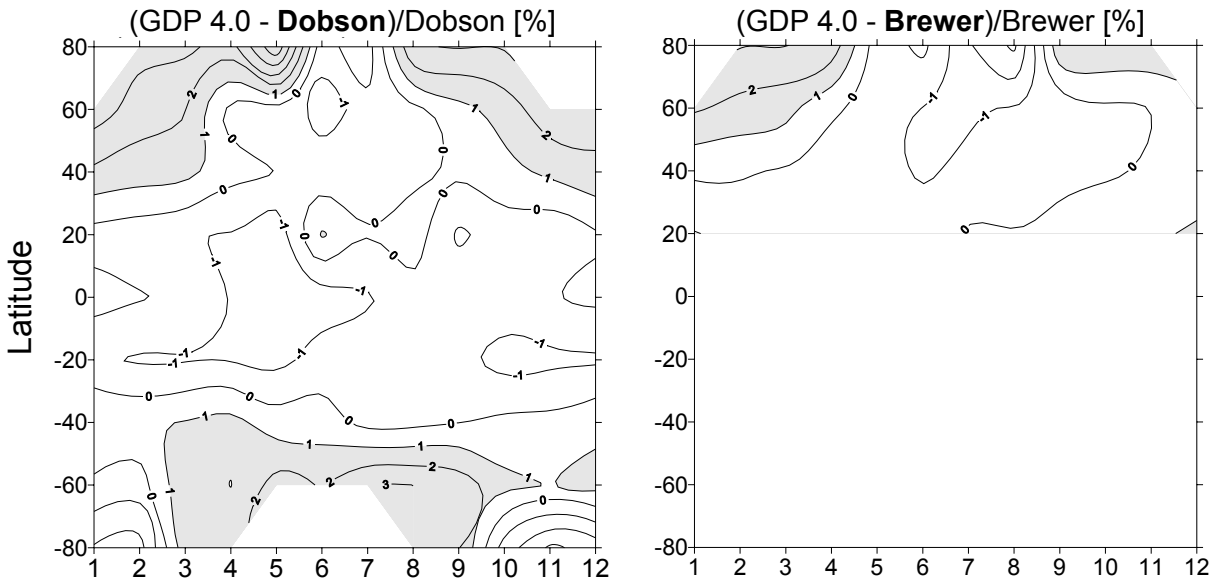

Figure 24 – Same month-latitude cross-sections as **Figure 23**, but here GOME total ozone data are the 4900 validation orbits processed with new GDP 4.0, and results obtained by comparison with Dobsons (left) and Brewers (right) are also presented separately.

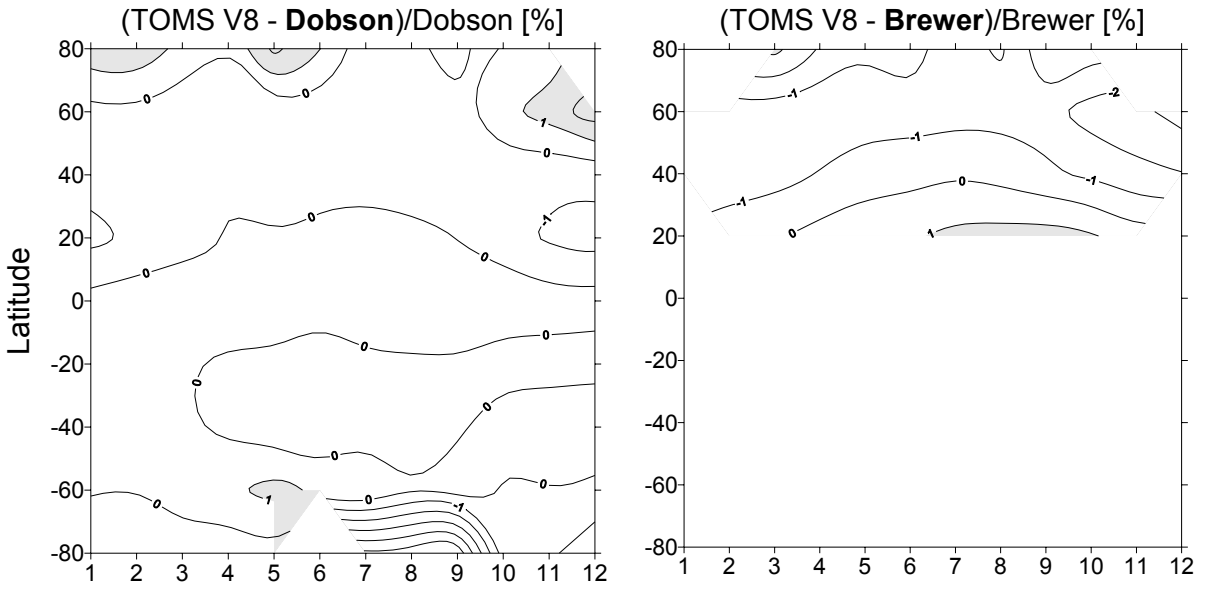

Figure 25 – Same as **Figure 24**, but here satellite total ozone data are TOMS v8 overpass data provided by NASA/GSFC. Results obtained by comparison with Dobsons (left) and Brewers (right) are again separated.

VI.5 SEASONAL DEPENDENCE

From **Figure 24** it can be concluded that there is still a mean seasonal dependence remaining in the comparisons with the ground-based measurements north of 40°N and south of 40°S. The amplitude of this seasonality does not exceed 1%-1.5% for the Dobson comparisons and is even less for the Brewer comparisons. Over the tropics, the comparisons show results between 0 and 1% with nearly no seasonal variation. When comparing **Figure 23** with **Figure 24**, we see that the GDP 4.0 seasonality is not in phase with the one observed in GDP3.0 but is rather in phase with the variation of the stratospheric temperatures (see 25°N-65°N Zonal mean temperatures at 50 hPa displayed in **Figure 26**): there is almost no bias to date during the warm period, while a positive bias of about 2% occurs during the cold period (including ozone hole conditions).

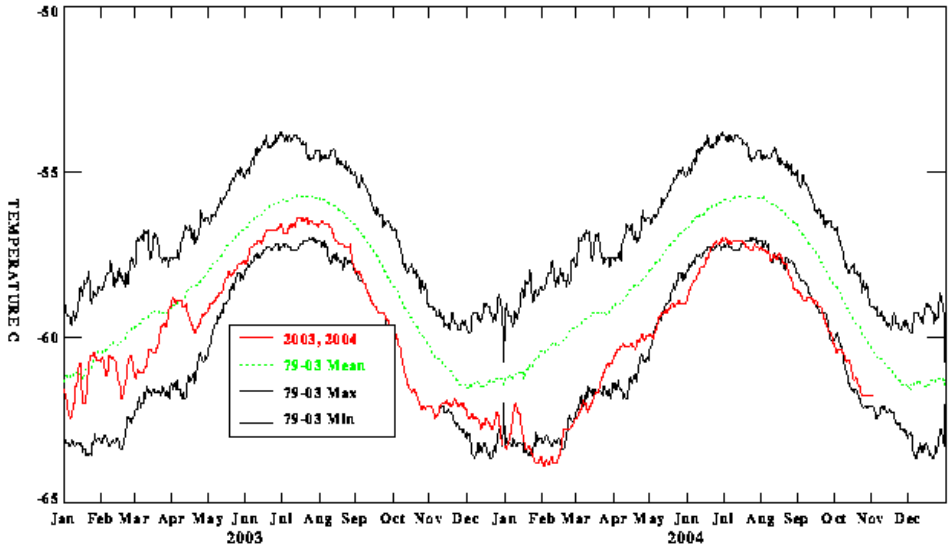

Figure 26 – 25°N-65°N zonal mean temperature time-series at 50 hPa for the years 2003-2004 (in red), and climatological temperatures (minimum, mean and maximum) over the 1979-2003 period (image courtesy NOAA/NWS/CPC http://www.cpc.ncep.noaa.gov/products/stratosphere).

As discussed in Chapter IV and in Section VI.3, both Dobson and Brewer total ozone measurements assume constant stratospheric temperature in their standardised retrieval algorithms, although absorption coefficients in the Huggins band are temperature-dependent. This approximation results in ozone column values dependent on stratospheric temperature variations. The latter includes day-to-day fluctuations, seasonal cycles, and inter-annual variability. The stratospheric temperature dependence of ground-based ozone measurements in the UV is believed to be more pronounced in the Dobson than in the Brewer due to the different wavelengths used. On the other hand, as discussed earlier, the GDOAS approach adopted in GDP 4.0 includes the spectral fitting of effective temperatures at which the cross-sections are inferred. Therefore GDP 4.0 should not depend significantly on the variability of stratospheric temperatures. A seasonal signature with similar phase and amplitude is found when comparing co-located Brewer and Dobson measurements from well-calibrated instruments for a long period (see examples at Hradec Kralove and Hohenpeißenberg in Staehelin *et al.*, 2003).

The smaller amplitude of the Brewer comparisons relative to the Dobson comparisons, the fact that the seasonal behaviour of the differences between GOME GDP4.0 and ground-based measurements is in phase with the variability of the stratospheric temperatures, and the fact that comparisons between collocated Brewer and Dobson measurements show similar in phase and in amplitude seasonality, indicate that a large part the observed differences could be attributed to the characteristics of the algorithms of the ground-based measurements rather than to algorithm implications of GDP4.0. A further indication for that is provided by the comparisons between Dobson, Brewer and TOMS version 8 total ozone. Comparison results displayed in **Figure 25** indicate that TOMS has almost no bias against the Dobson total ozone observations and shows no seasonality almost in every latitude belt. On the other hand the Brewer comparisons indicate over the middle latitudes a small negative bias of -1% and a seasonal behaviour with an amplitude of 0.5% in phase with the one found in GDP4.0. Considering that: (a) the forward model of TOMS v8 uses a single temperature profile for calculating radiances, and (b) the wavelengths used are close to the Dobson AD ones, can allow us to suggest that TOMSv8 and Dobson measurements have similar dependence on the lower stratospheric temperature. Their temperature-related errors might consequently cancel out when calculating their differences, which is partly valid in the Brewer comparisons.

VI.6 MERIDIAN STRUCTURE

We have already remarked in Section VI.4 that both GDP 4.0 and TOMS V8 show a reduction of their previous dependences on the latitude. **Figure 27** compares the yearly mean meridian dependence of GDP 3.0 and GDP 4.0 with respect to Dobson and Brewer network data. It is again evident that GDP 4.0 has improved its performance in all latitudes. Systematic offsets of GDP 3.0 vs. Brewer (-1.89%) and Dobson (-2.06%) data have vanished with GDP 4.0 to -0.17% for Brewer and 0.11% for Dobson comparisons. Zonal mean agreement varies within ±1-2%, with no marked meridian structure. Over the polar latitudes of both hemispheres, GDP 4.0 results are based on few measurements, especially at large SZA, and therefore they do not have the same significance with the results at the other latitudes. Studies relevant to the high latitude and large SZA are detailed in Section VI.8.

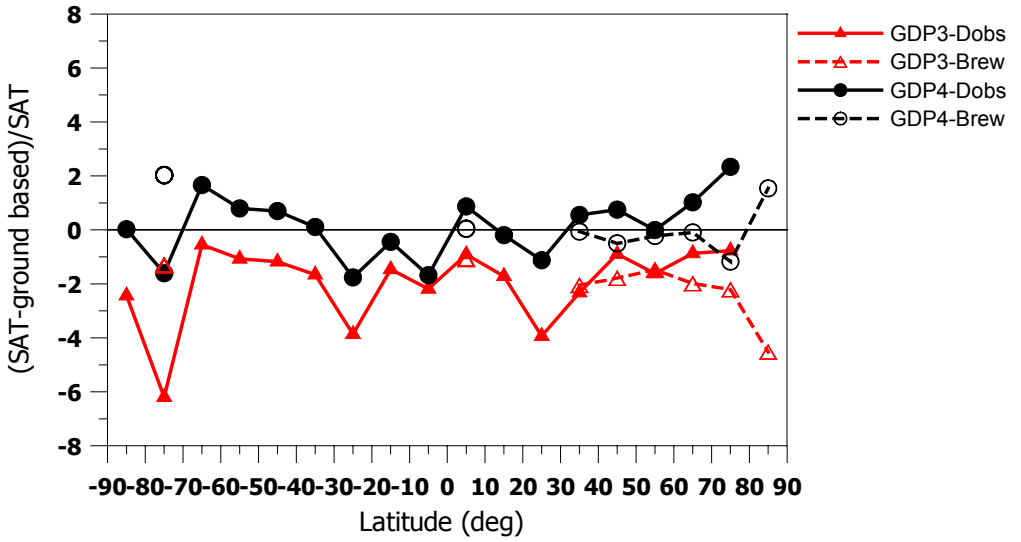

Figure 27 – Meridian variation of the percent relative difference between GOME (GDP 3.0 and GDP 4.0) and ground-based (Dobson and Brewer separately) total ozone.

Figure 28 shows the same type of results as **Figure 27**, but here the ground-based data are compared to TOMS V7 and TOMS V8. Again, it is evident that TOMS has improved with version 8 its performance in all latitudes. TOMS V8 data, when compared with Dobson instruments, have almost no offset (-0.3%), while they show a negative bias of about 1.5% compared with Brewer instruments. There is no meridian dependence of the differences, which vary within 1%. This was not case for TOMS V7, where especially in the southern hemisphere TOMS overestimated total ozone up to 6% on an average and even more at individual stations in the Antarctic. It is interesting to note in **Figure 29**, which reproduces the GDP4.0/Dobson and TOMS V8/Dobson comparison results already presented in **Figure 28** and **Figure 29**, that Dobson comparisons with the two different satellites yield similar meridian patterns and offsets.

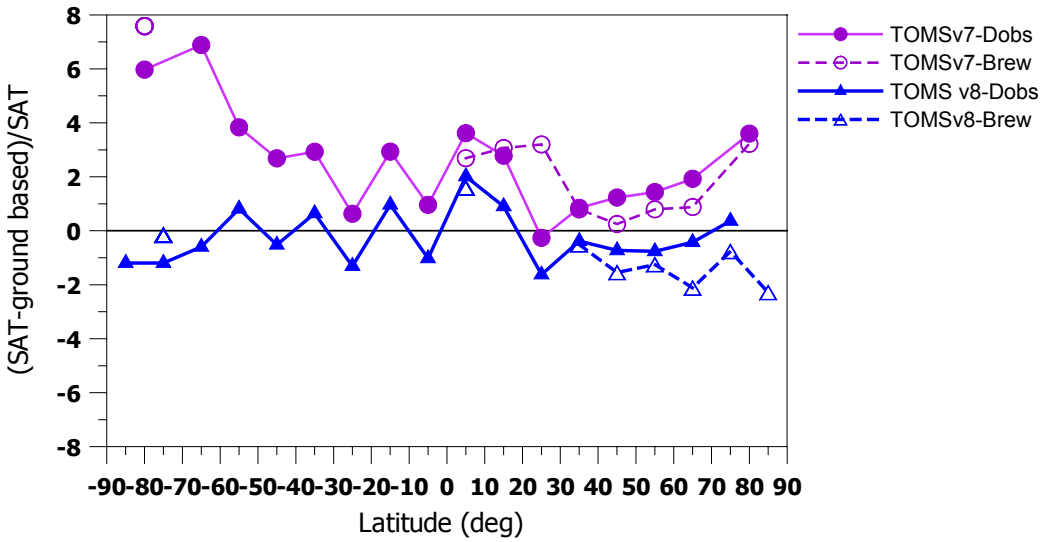

Figure 28 – Meridian variation of the percent relative difference between TOMS and ground-based total ozone.

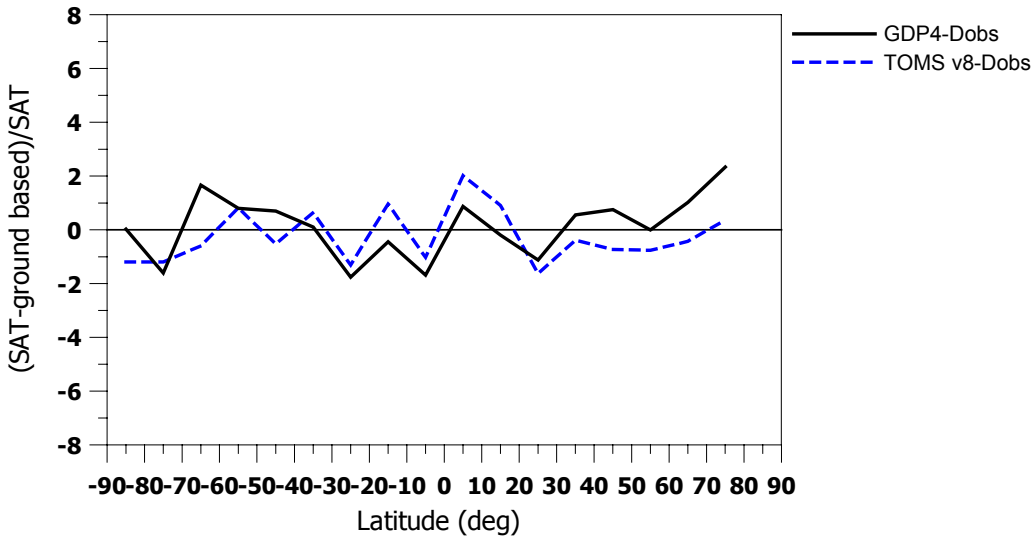

Figure 29 – Meridian variation of the percent relative difference between satellite total ozone (GDP 4.0 and TOMS V8) and ground-based Dobson direct-sun observations.

VI.7 LONG-TERM STABILITY

In order to examine and compare the long-term stability of GDP 3.0, GDP 4.0 and TOMS V8, we averaged the individual station comparisons (based on all available orbits) separately over the Northern and Southern Hemisphere. Comparison results with Dobsons and with Brewers were also separated. Results are shown in **Figure 30** and **Figure 31** for the Southern and Northern Hemisphere, respectively. It is evident from **Figure 30** that both GOME GDP 3.0 and GDP 4.0 total ozone data do not show any drift with respect to the ground-based data till 2003. We see in the upper panel of this figure the known GDP 3.0 seasonal dependence of the differences with half amplitude of 1.5%, consistent when compared either with Brewer or with Dobson instruments. A systematic bias close to –2% is also evident with GDP 3.0. In the middle panel of the same **Figure 30**, the respective time-series for GDP 4.0 are presented. It is evident that both (Brewer and Dobson) comparisons have no systematic bias anymore. However sampling issues (less ground-based data available during 2003-2004 and less validation orbits) might increase the noise at the end of the time series. There is still a seasonal dependence of differences remaining, however different in phase compared to GDP3.0 and also different in amplitude (1-1.5%) when considering Brewer or Dobson comparisons. This remaining seasonal dependence is likely related to the one discussed in previous Section VI.3.2.

In the lower panel of **Figure 30**, TOMS V8 time-series for the Northern Hemisphere do not show any drift till mid 2001. After that period, TOMS/ground differences show an increasing bias, evident both in the Dobson and Brewer comparisons. Dobson comparisons, as discussed earlier, do not show any bias or significant seasonal variability, while the Brewer comparison show a small negative bias and a seasonal structure similar to that observed with GDP 3.0.

In **Figure 31** we show the time-series of the Dobson comparisons with GDP 3.0, GDP 4.0 and TOMS V8 averaged for both the Northern (as discussed before) and the Southern hemisphere. There are very few Brewer instruments in the Southern Hemisphere to allow a similar comparison. In the Southern Hemisphere, GDP 3.0 is consistent with Northern Hemisphere results; however there are fewer measurements available for comparison and therefore the noise in the time-series is large. Differences in the size of the GOME and TOMS footprints, hence in spatial smoothing of the ozone field by the satellites, could also explain partly why the scatter in the comparisons depends on the couple satellite/ground.

VI.8 DEPENDENCE ON SOLAR ZENITH ANGLE

Errors linked to the estimation of AMF and the correction for Raman scattering can result in a significant dependence of the vertical column product on the solar zenith angle at which the observation was acquired. The solar zenith angle dependence of GDP 2.7 ozone columns had an amplitude from a few percent to ±15% on an average, varying with the latitude, the season, the vertical column amount, and sometimes from year to year. With GDP 3.0, where the improved AMF calculation was based on a iterative neural network approach and the use of an ozone profile climatology instead of modelling results, the amplitude of the SZA dependence was cut down by about 50% on an average. With GDP 4.0, major improvements in the Raman correction and additional improvements in the AMF calculation are expected to result in a drastic reduction of the SZA dependence. The present section aims at assessing this expected reduction.

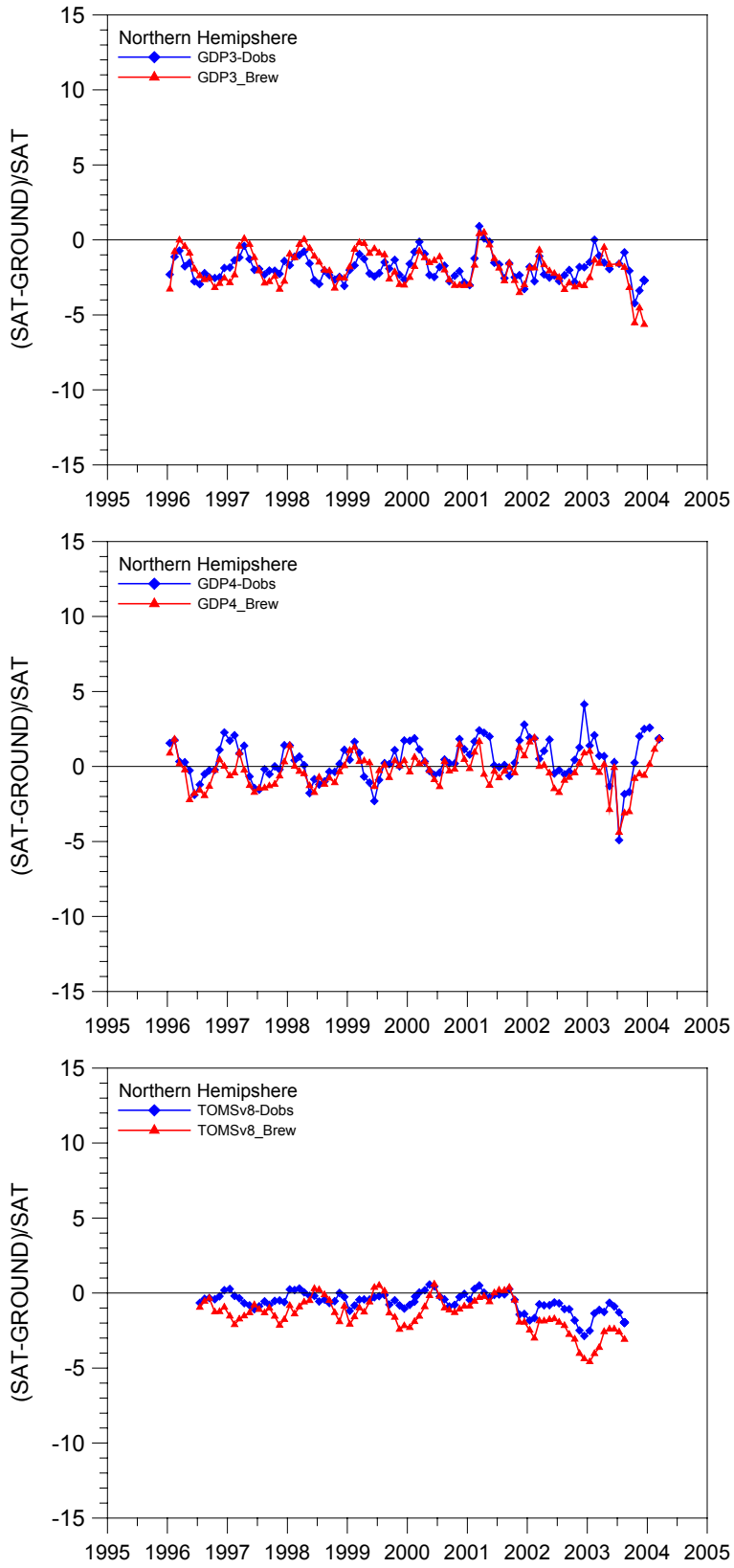

Figure 30 – Time-series of the percent relative differences between satellite (GDP 3.0, GDP4.0 and TOMS V8) and ground-based ozone data for the period 1996-2004 averaged for the Northern Hemisphere. Dobson and Brewer comparisons are plotted separately.

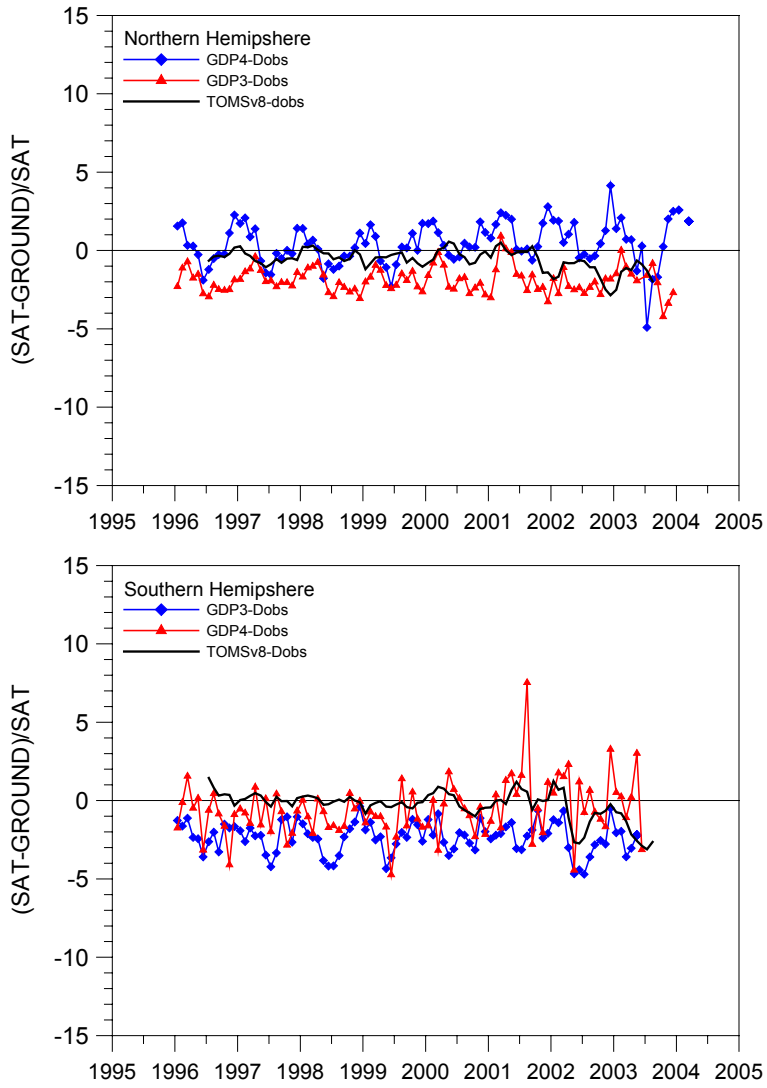

Figure 31 – Time-series of the percent relative differences between satellite (GDP 3.0, GDP4.0 and TOMS V8) and ground-based Dobson ozone data for the period 1996-2004, averaged over the Northern Hemisphere (top) and the Southern Hemisphere (bottom).

We had already remarked in previous sections that it is more difficult to conclude to a clear reduction of the SZA/season dependence at high latitudes. This difficulty arises from the decreasing amount of delta validation coincidences with latitude and the increasing uncertainties on both the satellite and ground-based measurements at such large latitudes and/or solar zenith angle. To detect and quantify possible improvements in the solar zenith angle dependences of GOME, we have first applied the so-called polar day technique. At high latitudes, the polar orbit of ERS-2 combines with the polar convergence of the meridians to result in several daily overpasses. During polar summer, when the poles are illuminated permanently, GOME acquires measurements over the same high latitude stations at least two times a day under different solar elevations, as illustrated in **Figure 32** for both the North and South Poles. As the ozone field usually is relatively stable around summer solstice, this multiple daily overpass allows the detection of the SZA dependence between GOME data acquired in the mid-morning (medium SZA) and GOME data closer to the midnight sun conditions (large SZA). Ground-based data are used in the comparison as a standard transfer.

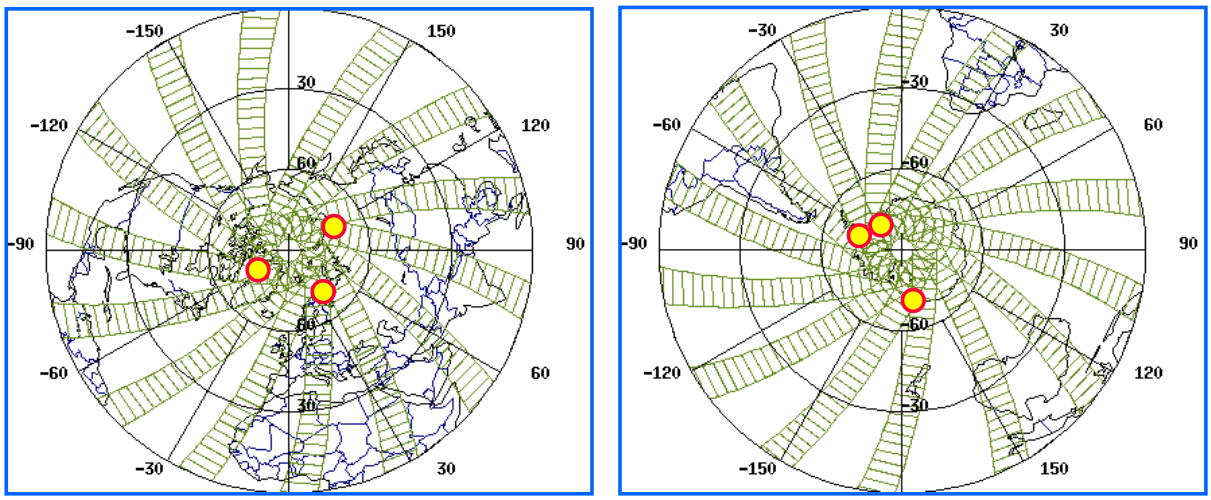

Figure 32 - Polar projection of the GOME orbit tracks acquired after one day of operation (14 orbits), and geolocation of the six ground-based stations considered for the study of the GOME polar day SZA dependence. Around summer solstice, GOME overpasses those polar stations at least two times a day under different solar elevations, allowing the detection of the SZA dependence. Left: NDSC/Arctic sites of Sodankylä (Finland), Zhigansk (Siberia) and Thule (Greenland); right: NDSC/Antarctic sites of Dumont d'Urville (Terre Adélie), Rothera (Antarctic Peninsula) and Halley Bay (Weddell Sea).

For the present study, the polar day technique was applied to 6 polar stations in both hemispheres (identified in **Figure 32**), for which the amount of coincidences with the delta validation orbits was sufficient. **Figure 33** shows GOME polar day SZA dependences with respect to two ground-based sensors operated at the NDSC/Arctic station of Sodankylä (67°N). Comparison with the FMI Brewer instrument (upper panel) demonstrates that the average bias of about 6% observed between mid-morning (moderate SZA) and midnight sun (large SZA) data with GDP 3.0 has reduced to the 1.5% with GDP 4.0. Comparison with the collocated CNRS/FMI SAOZ UV-visible instrument confirms this improvement. **Figure 34** shows similar comparisons with the BAS Dobson instruments operated at the Antarctic stations of Rothera (68°S) and Halley (76°S). At Rothera, the decrease of the polar day SZA dependence from 5.4% with GDP 3.0 to 0.9% with GDP 4.0 is similar to that reported in the Arctic. At Halley, where there was already no clear polar day SZA dependence with GDP 3.0, we observe no change with GDP4.0.

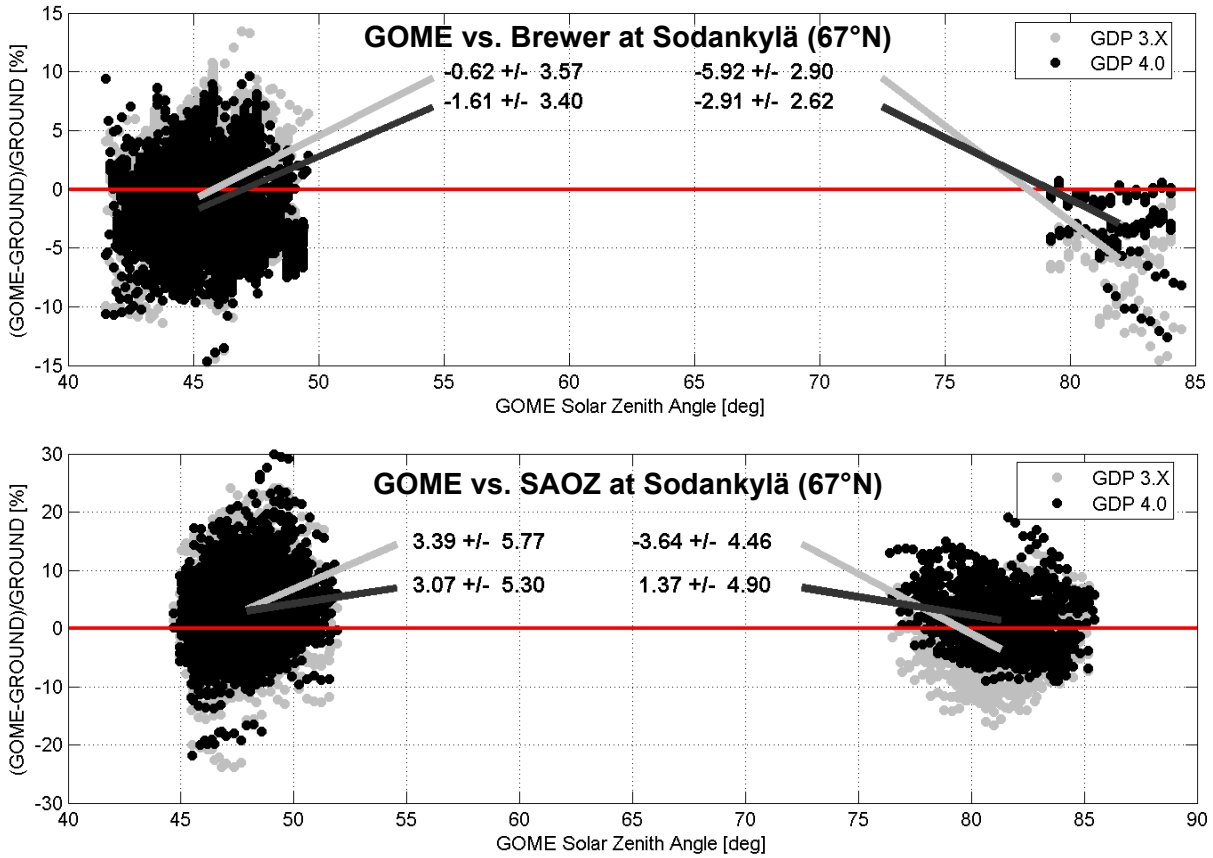

Figure 33 - Comparison of the polar day SZA dependence of GDP 3.0 and GDP 4.0 total ozone at Sodankylä (Arctic Finland), using the FMI Brewer (top) and CNRS SAOZ (bottom) as standard transfers. The percentage relative difference between GOME and ground-based total ozone around summer solstice, plotted as a function of the GOME SZA, demonstrates that the average bias of about 6% observed between mid-morning (moderate SZA) and midnight sun (large SZA) data with GDP 3.0 has reduced to the 1.5% level with GDP4.0.

The polar day technique could not be applied successfully to TOMS overpass data files provided by NASA/GSFC, as multi-overpass data sets acquired during polar day are already filtered to provide only the ozone value acquired at the lowest SZA. In order to investigate the TOMS SZA dependence as well, we have also carried out global studies relying on the statistical significance offered by network data. In **Figure 35**, GOME total ozone data generated by both GDP 3.0 and GDP 4.0 are confronted to Dobson and Brewer total ozone measurements on the global scale, as a function of the GOME SZA. It seems that in GDP 4.0 there is an overestimation of GOME for SZA between 60° and 70°. However, when examining the different latitude zones, this result corresponds to the measurements of the cold period and therefore these differences also include the possible temperature dependence of the comparisons, which is consistent with the fact that the Brewer comparisons show a smaller feature. It is worth mentioning that this feature was not evident in GDP 3.0, which had a different seasonal dependence. For SZA larger than 80°, there were only occasional data available from the ground stations for the GDP 4.0 comparisons, so the results should not be considered as statistically significant.

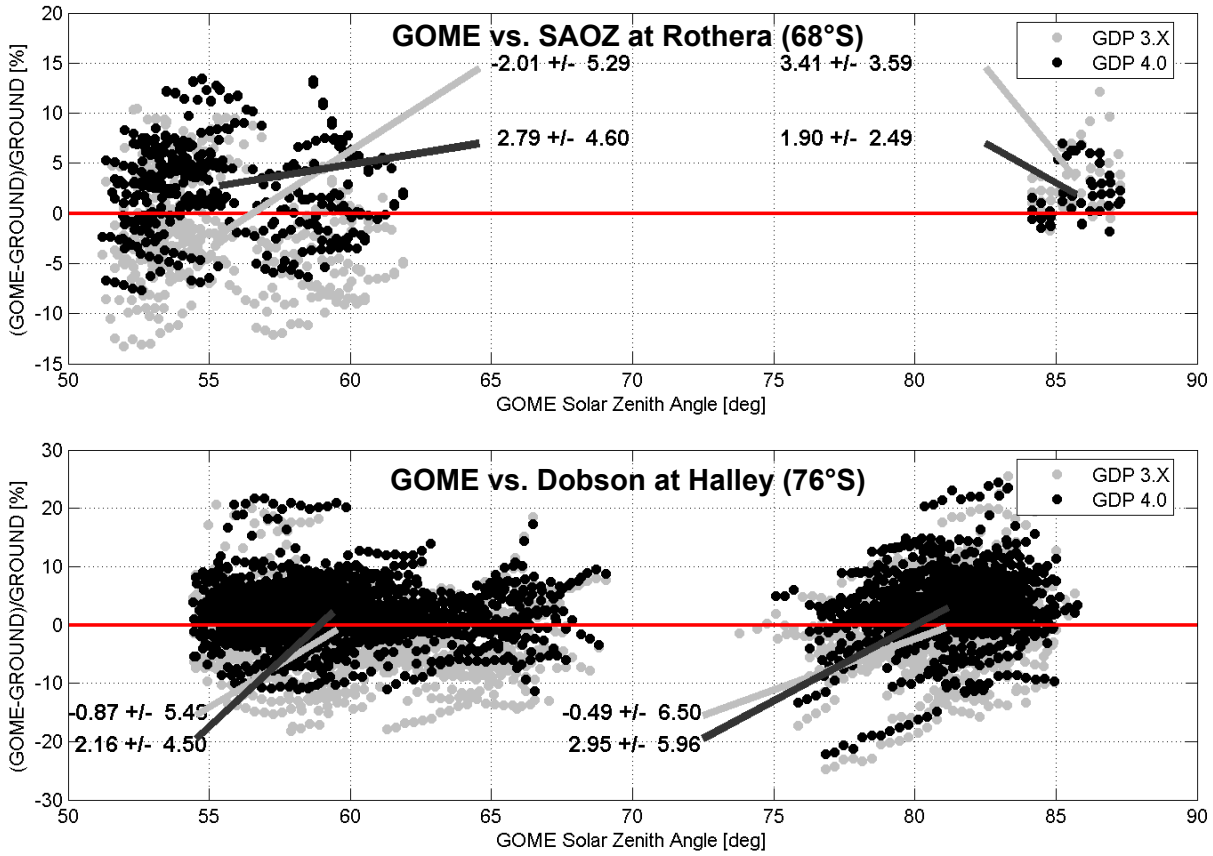

Figure 34 – Same as **Figure 33**, but at the NDSC/Antarctic sites of Rothera (Antarctic Peninsula) and Halley Bay (Weddell Sea), using the BAS/NERC SAOZ (top) and BAS/NERC Dobson (bottom) as standard transfers. At Rothera, the decrease of polar day SZA dependence from 5.4% to 0.9% is similar to that observed in the Arctic. At Halley, where there was already no clear polar day SZA dependence with GDP 3.0, we observe no change with GDP 4.0.

Figure 36 is similar to **Figure 35**, but here TOMS V7 and TOMS V8 are confronted to Dobson and Brewer observations. Global comparisons show no significant SZA dependence, while this is not the case with the Brewer comparisons, where TOMS overestimates by 2% for small SZA and underestimates by -2% for large SZA. This behaviour is similar when comparing Dobson and Brewer observations as a function of air mass without any temperature correction and therefore it could be probably attributed also partly to the temperature dependence of the comparisons.

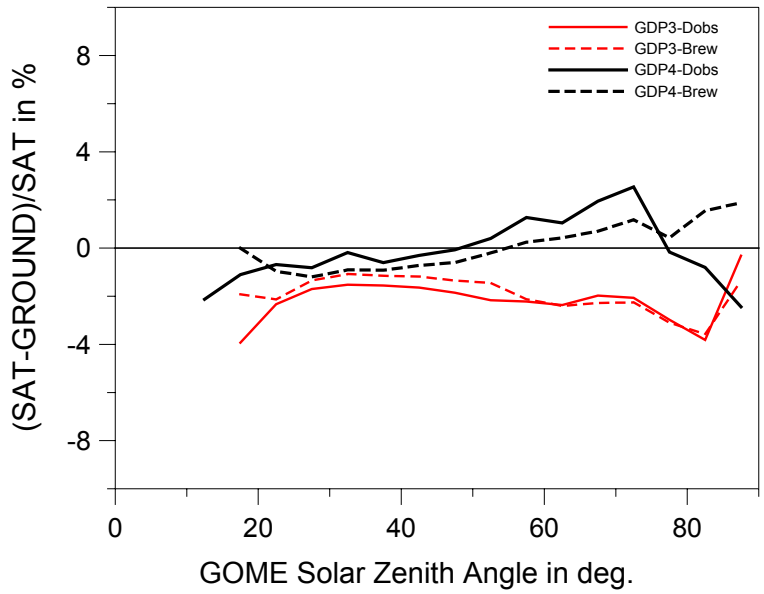

Figure 35 - Percentage relative difference between GOME (GDP 3.0 and GDP 4.0) and ground-based total ozone as a function of the GOME solar zenith angle (SZA). Dobson and Brewer comparisons are presented separately.

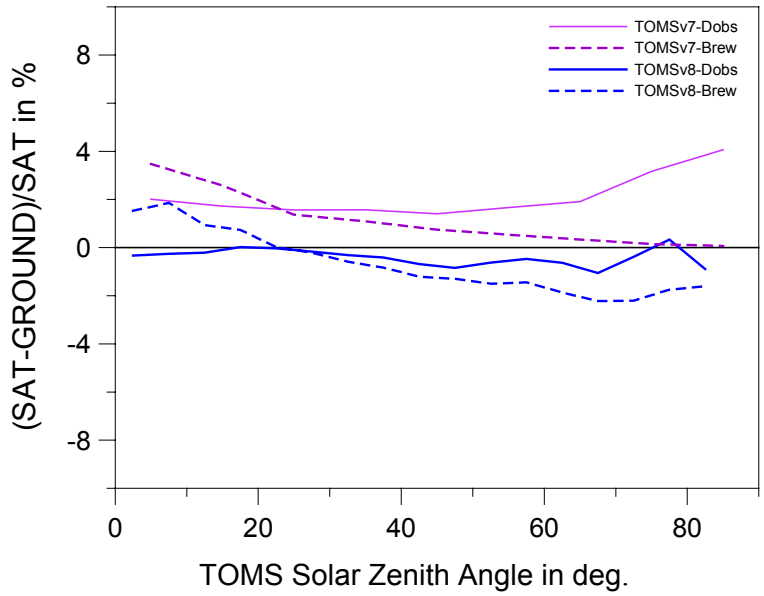

Figure 36 - Percentage relative difference between TOMS (V7 and V8) and ground-based total ozone as a function of the TOMS solar zenith angle (SZA). Dobson and Brewer comparisons are presented separately.

VI.9 DEPENDENCE ON OZONE COLUMN

Both GOME GDP 2.7 and TOMS V7 presented a significant overestimation of the low ozone column values observed during Antarctic springtime ozone depletion. A similar effect was also detected in the Arctic, although more difficult to quantify due to the less stable conditions of the Arctic winter [4]. With the GDP upgrade to version 3.0, the large 10-20% overestimation of low column values (below 200 DU) by GDP2.7 had reduced significantly to the 5% level for very low column values (below 130 DU), as illustrated in **Figure 37** at the Antarctic station of Halley. This Section will track changes in the ozone column dependence that could be associated with the GDP 4.0 upgrade. It is anticipated that the TOMS V7 column dependence will reduce with TOMS V8.

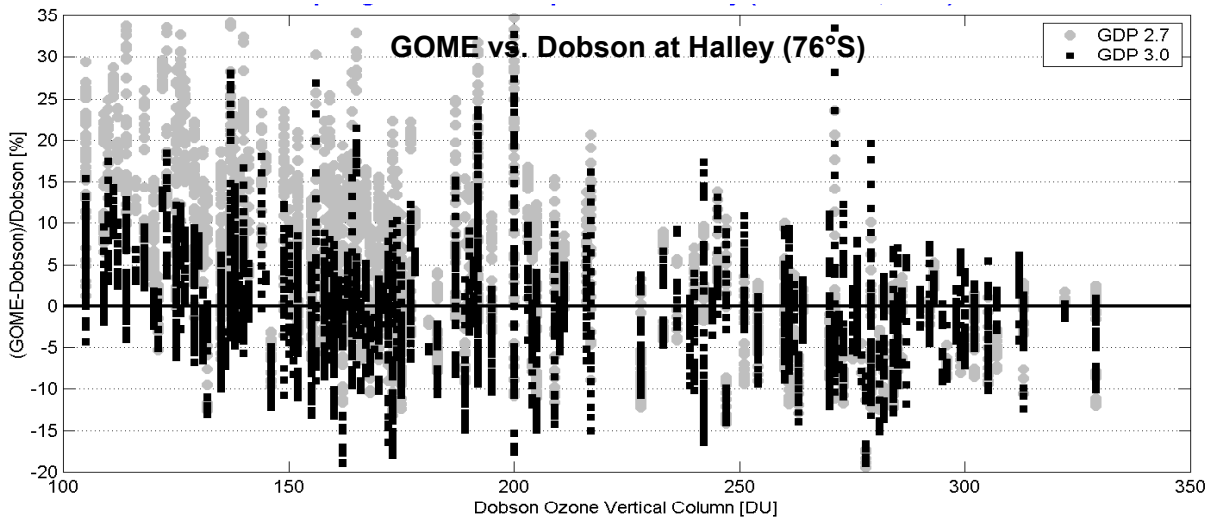

Figure 37 - Percentage relative difference between GOME (GDP 2.7 and GDP 3.0) and BAS Dobson total ozone during ozone hole conditions at the NDSC/Antarctic site of Halley, as a function of the ground-based Dobson ozone column value. The large 10-20% overestimation of low column values (below 200 DU) by GDP 2.7 had reduced significantly to the 5-10% level for very low column values (below 130 DU) with GDP 3.0.

In **Figure 38**, the column dependence of the difference between GOME and ground-based total ozone is presented for three different instruments (two Dobson and one SAOZ) operated in the Antarctic. Comparisons are limited to the ozone hole period, from September 1 till November 1, in order to avoid interferences with possible SZA and seasonal dependences. At all stations, compared to GDP 3.0, the upgrade to GDP 4.0 produces a constant decrease of the ozone column value by about 3% over the entire ozone column range; there is thus no perceptible change in the ozone column dependence.

Figure 39 presents the column change from TOMS V7 to TOMS V8 using again three different instruments operated in the Antarctic. Here, the strong column dependence of TOMS V7, of about 15% below 130 DU, is cut down to a low level difficult to quantify due to the scarcity of relevant TOMS/ground coincidences. Nevertheless, it is clear that TOMS V8 is an improvement with respect to the ozone column dependence.

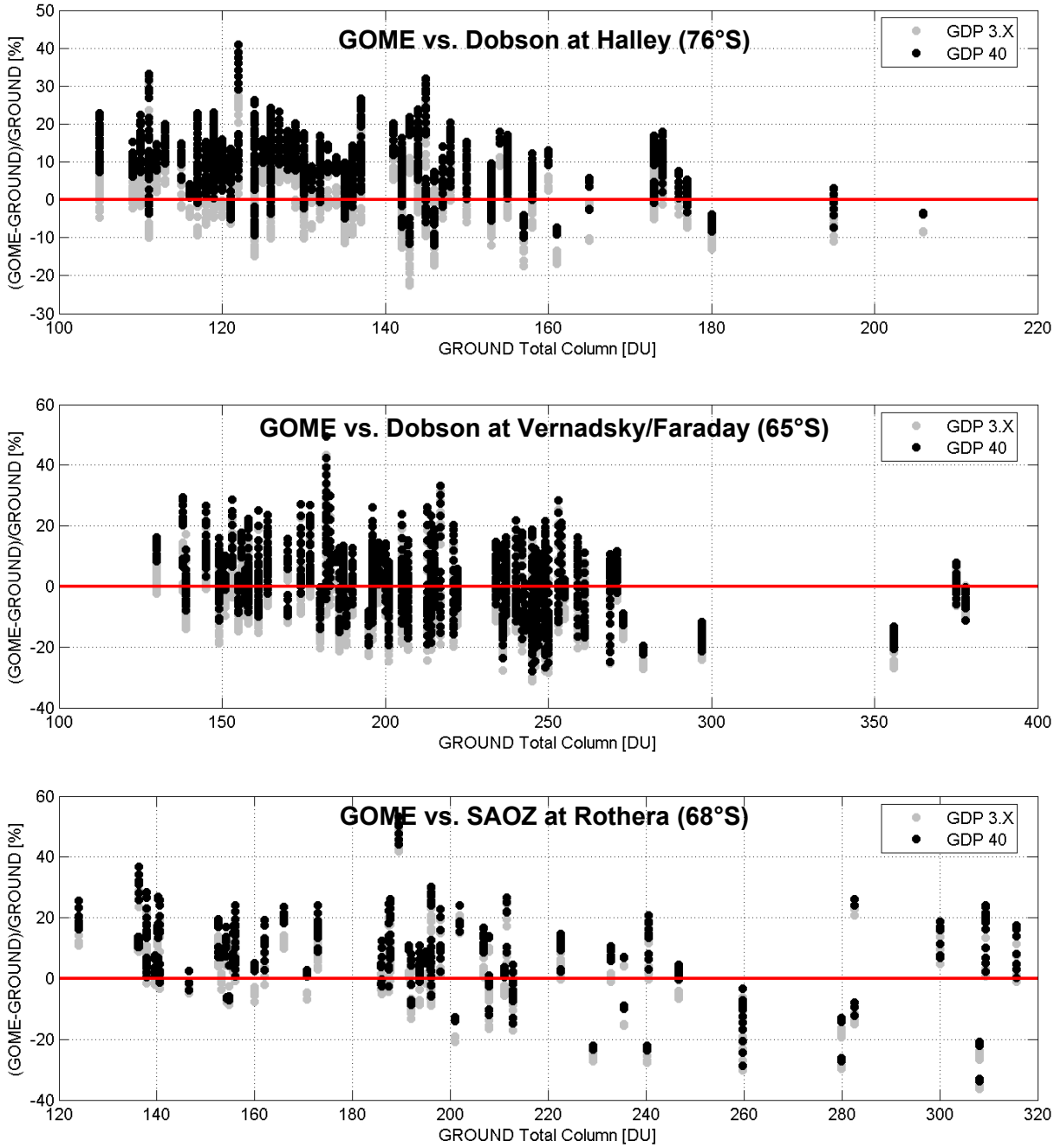

Figure 38 - Percentage relative difference between GOME and ground-based total ozone during ozone hole conditions at three NDSC/Antarctic sites, as a function of the ground-based ozone column value: BAS Dobson at Halley, BAS/KTSU Dobson at Vernadsky (formerly Faraday), and BAS SAOZ at Rothera. The main difference between GDP3.x and GDP4 total ozone consists in an offset of a few percent, but there is no change to date in the GDP column dependence from one version to another.

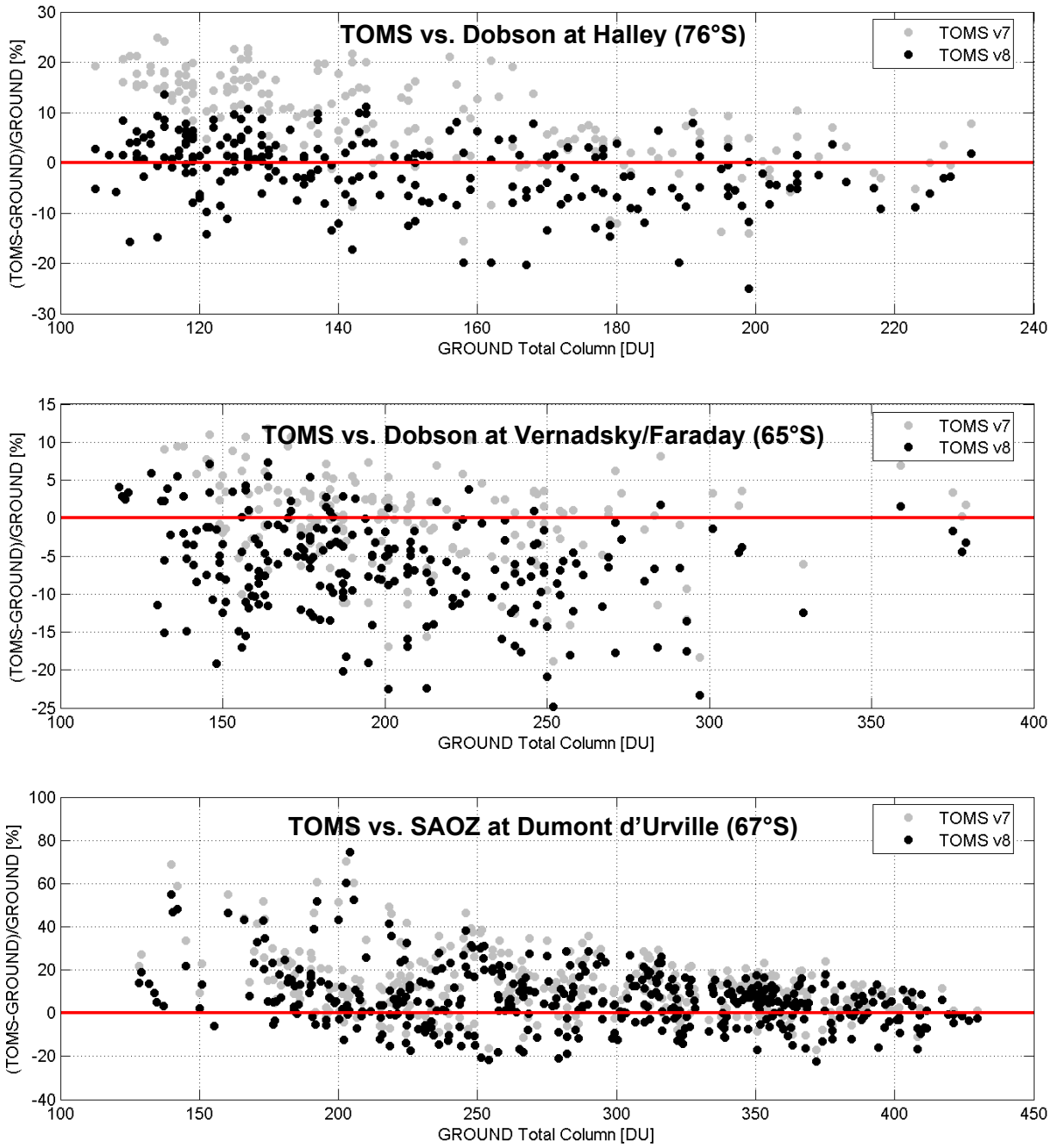

Figure 39 – Same as **Figure 38**, but with TOMS and at the three following NDSC/Antarctic sites: BAS Dobson at Halley, BAS/KTSU Dobson at Vernadsky (formerly Faraday), and CNRS SAOZ at Dumont d'Urville. The large 15% overestimation of low column values (below 170 DU) by TOMSv7 has reduced significantly with TOMSv8.

VI.10 DEPENDENCE ON FRACTIONAL CLOUD COVER

In the GDP total ozone retrieval, reflecting clouds interfering with the air mass probed by GOME, play explicitly a role in the calculation of the AMF and in the estimation of the so-called ghost column hidden by the cloud cover and added to the actually measured vertical column. Therefore, uncertainties in the GOME fractional cloud cover can generate significant errors in the retrieved total ozone value. The largest effect to date with GDP 2.7 was the 6% average offset identified in the Antarctic springtime, due to the combined effects of: (a) the use of an unsuitable ozone profile database with too high tropospheric ozone values for the given conditions; (b) a fractional cloud cover systematically set to 1, thus with a maximum application of the ghost column correction; and (c) a significant contribution of tropospheric ozone to the vertical column when stratospheric ozone is depleted. With GDP 3.0, this particular offset had disappeared thanks to the use of a more suitable ozone profile database for both AMF and ghost column estimations. More generally, GDP 3.0 was not know to be affected by obvious dependences on the fractional cloud cover.

Compared to GDP 3.0 results, the agreement between GDP 4.0 and ground-based total ozone data – in terms of dispersion – has improved sometimes by a factor of two under clear skies, while the situation is unchanged under cloudy skies. This change in cloud fraction dependence between GDP 3.0 and GDP 4.0 is illustrated at the NDSC/Alpine station of Arosa in **Figure 40** and at high latitude stations in **Figure 41** for the Arctic (first three graphs) and the Antarctic (fourth graph). The reduction of the dispersion under clear skies is believed to be the result of the improved Raman treatment and AMF calculation. Unlike the dispersion, the mean value of the agreement does not vary with the cloud fraction, except at a few equatorial stations like Singapore (**Figure 42**) and Nairobi where the cloud fraction dependence correlates with the long-term variation (which is not a drift!) of the agreement between the GOME and ground-based ozone values.

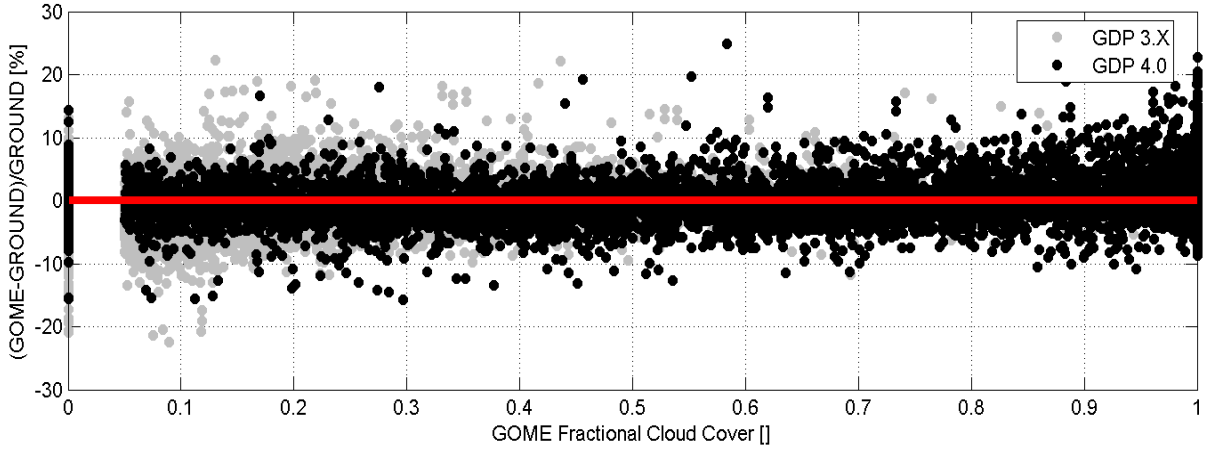

Figure 40 - Percentage relative difference between GOME and ETH/MCH Brewer total ozone at the NDSC/Alpine station of Arosa (Switzerland), as a function of the GOME fractional cloud cover. From GDP 3.0 to GDP 4.0, the main change in cloud fraction dependence is a clear reduction of the dispersion under clear skies.

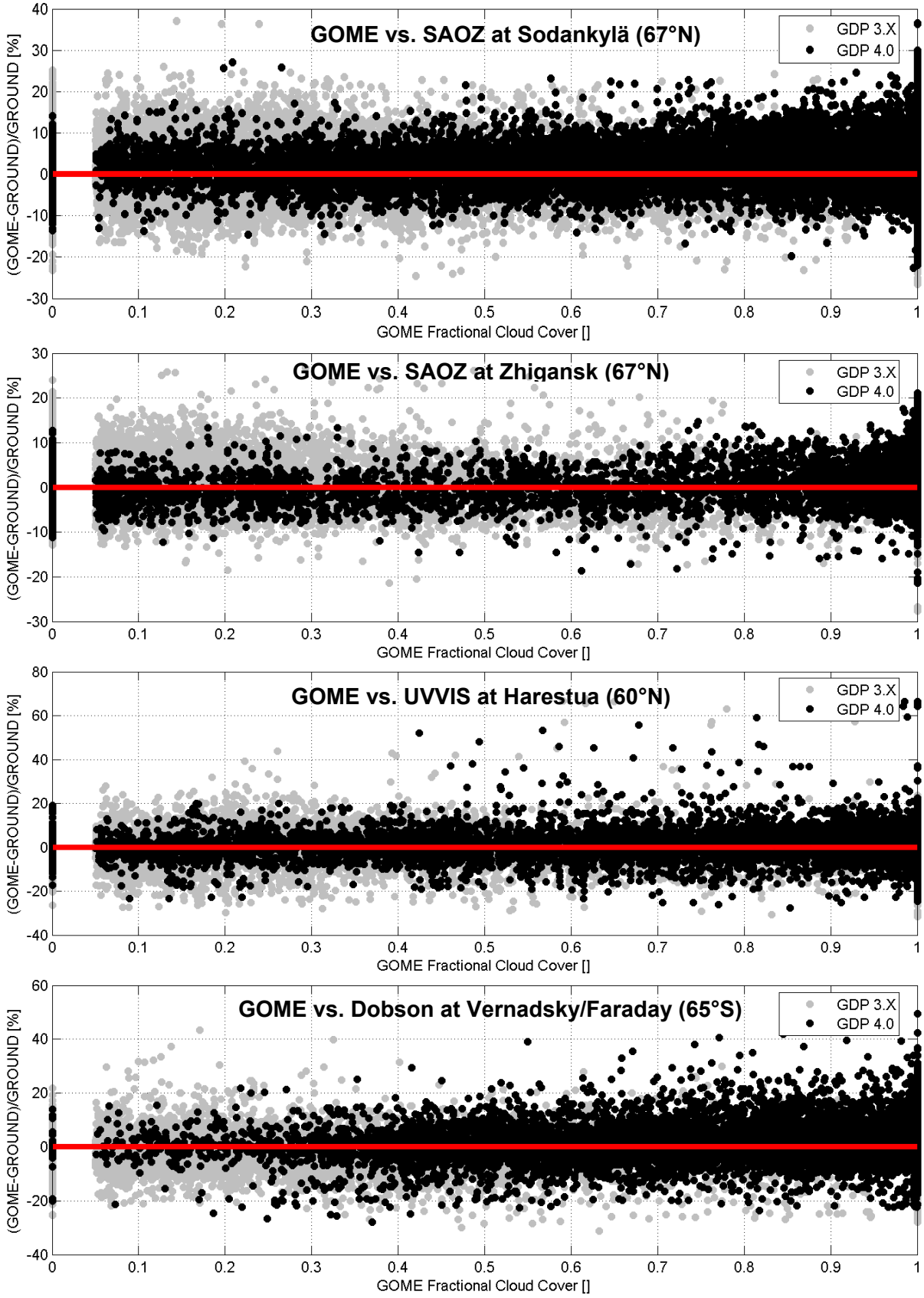

Figure 41 - Same as **Figure 40**, but here at four high latitudes stations. From top to bottom: CNRS/FMI SAOZ at Sodankylä (Finland), CNRS/CAO SAOZ at Zhigansk (Siberia), BIRA-IASB UVVIS at Harestua (Norway), and BAS/KTSU Dobson at Vernadsky/Faraday (Antarctic Peninsula).

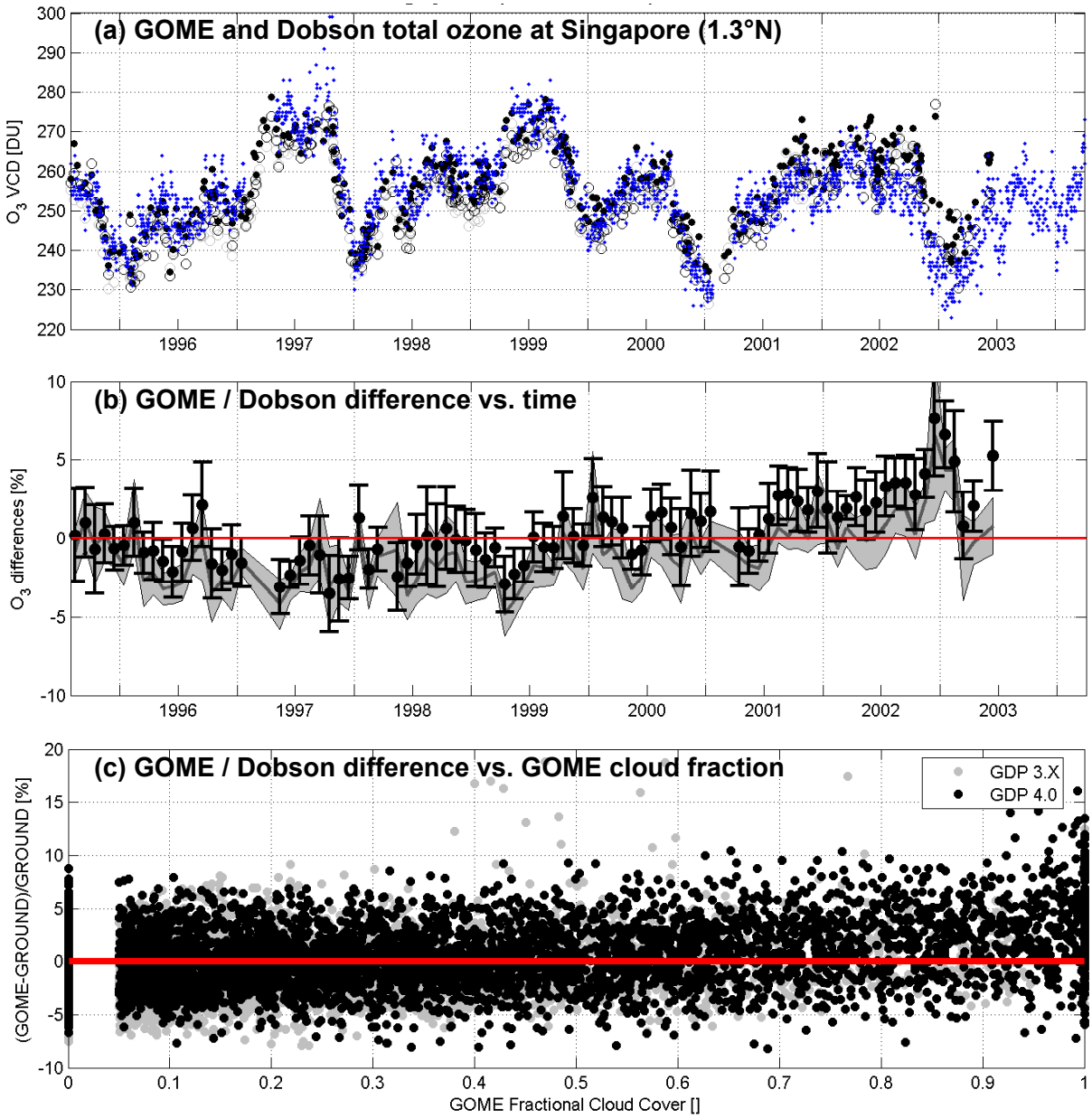

Figure 42 – From top to bottom: (a) GOME (open grey circles for GDP3 and plain black circles for GDP4.0) validation data sets and Dobson (blue dots) total ozone data recorded from 1995 to 2004 at the equatorial station of Singapore; (b) percentage relative difference and 1σ standard deviation between GOME (GDP 3.0 as grey line and shaded area, and GDP 4.0 as black circles and error bars) and Dobson total ozone, again as a function of time; and (c) same GOME/Dobson percent relative difference but plotted here as a function of the GOME fractional cloud cover determined by OCRA/ROCINN.

In **Figure 43** we present the differences between GDP 4.0 and Dobson direct-sun measurements as a function of the GOME cloud fraction. The scatter of the comparisons is larger with increasing cloud fraction, however, there is no evidence for a significant cloud fraction dependence of the mean differences from a global point of view.

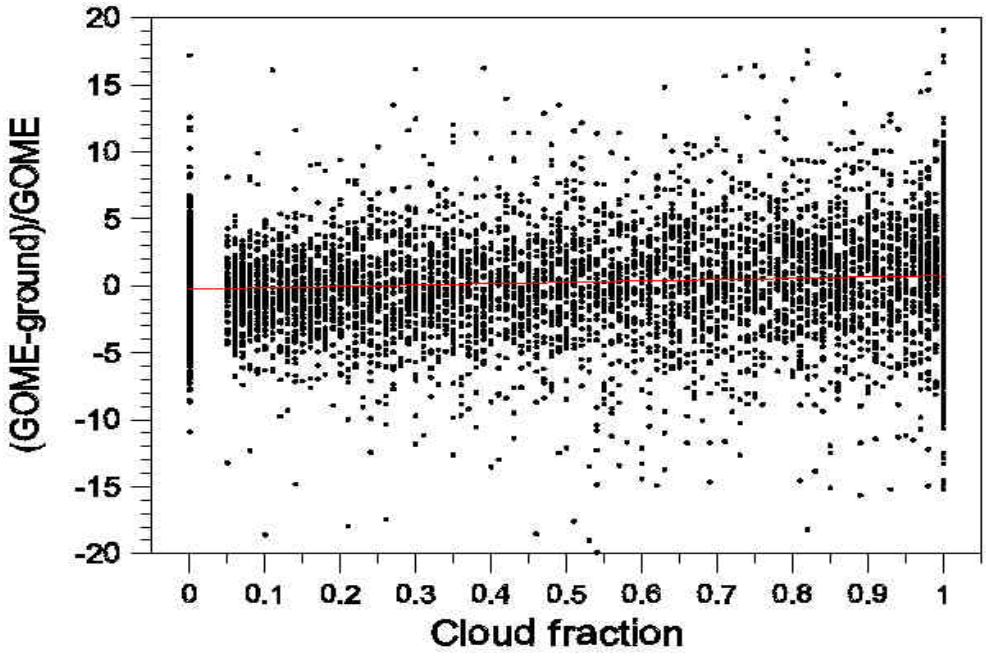

Figure 43 – Percentage relative difference between GDP4.0 and Dobson direct sun total ozone as a function of the GOME GDP 4.0 cloud fraction determined by OCRA/ROCINN.

VI.11 CONCLUSION

GOME total ozone data processed with different versions of the GOME Data Processor (GDP) have been validated from pole to pole through comparisons with ground-based measurements from Brewer and Dobson UV spectrophotometers and SAOZ/DOAS UV-visible spectrometers, as available from the WOUDC and NDSC data archives. TOMS V7 and V8 ozone column data have been studied similarly. Special care has been given to the quality control and the documentation of ground-based data sets.

Compared to GDP 2.7, GDP 3.0 included already a new determination of effective absorption temperature derived by spectral analysis, better atmospheric databases, and AMFs determined iteratively using a neural network trained on column- and latitude-classified atmospheric profiles and measurement parameters. GDP 3.0 upgrades resulted in a reduction by about 30-50% of the amplitude of the GOME total ozone dependence on the SZA, the latitude, the season, and the ozone column amount. Simultaneous upgrades of the Level-1 product resulted in a notable reduction of the sensitivity of the GDP column products (both ozone and nitrogen dioxide) to instrumental degradation. Compared to GDP 3.0, current version GDP 4.0 includes now an improved correction for ozone absorption distortion due to inelastic Raman rotational scattering by atmospheric N_2 and O_2, a new cloud treatment by the OCRA/ROCINN cloud recognition algorithm, and further improvements to the AMF calculation. The main achievement with GDP 4.0 is the drastic reduction to the "percent level" of nearly all the remaining dependences on the latitude, SZA and season that persisted with GDP 3.0. The reduced ozone column dependence of GDP 3.0 has not changed with GDP 4.0.

In general, the average agreement of GDP 4.0 with correlative ozone column measurements falls to the "percent level", that is, within the precision level of ground-based sensors when the latter are corrected for their own dependences on the season, temperature etc. At polar latitudes, and at solar zenith angles beyond 80°, preliminary validation indicates that the agreement degrades slightly, however, average differences at low solar elevation usually do not exceed 5%. A remarkable feature is that, despite the normal degradation of the instrument with time, the total column products do not suffer from any long-term drift of quality, even in 2004 with a degradation of 42.9% in the UV ozone channel. More qualitatively, GOME gives a consistent picture of the global ozone field with temporal signals and spatial structures similar to those observed by other high-quality sensors.

The TOMS ozone algorithm upgrade to version 8 is also a clear improvement compared to the previous operational version 7. TOMS V8 does not seem to be affected anymore by the systematic offset of TOMS V7 over the whole Southern Hemisphere. The TOMS V7 ozone column overestimation of the extremely low ozone column values observed in the Antarctic springtime has also vanished with TOMS V8. Seasonal and meridian dependence still persist with TOMS V8 but their amplitude has reduced. A weak aspect of both TOMS V7 and TOMS V8 is their obvious sensitivity to instrumental degradation. As a consequence, compared to more stable measurement systems, TOMS reports systematically lower ozone column values by a few percent from the second part of 2001 onwards. This result confirms the recommendation expressed by NASA/GSFC that EP-TOMS ozone data acquired after 2000 should not be used for trend assessments.

References

[1] Lambert, J.-C., M. Van Roozendael, J. Granville, P. Gerard, P. Peeters, P.C. Simon, H. Claude and J. Staehelin, Comparison of the GOME ozone and NO_2 total amounts at mid-latitude with ground-based zenith-sky measurements, in *Atmospheric Ozone - Proc. 18th Quad. Ozone Symp., L'Aquila, Italy, 1996*, R. Bojkov and G. Visconti (Eds.), Vol. I, pp. 301-304, 1997.

[2] Van Roozendael M., P. Peeters, H. K. Roscoe, H. De Backer, A. Jones, G. Vaughan, F. Goutail, J.-P. Pommereau, E. Kyrö, C. Wahlstrøm, G. Braathen, and P. C. Simon, Validation of Ground-based UV-visible Measurements of Total Ozone by Comparison with Dobson and Brewer Spectrophotometers, *J. Atm. Chem.*, 29, 55-83, 1998.

[3] Staehelin J, J. Kerr, R. Evans and K. Vanicek, Comparison of total ozone measurements of Dobson and Brewer spectrophotometers and recommended transfer functions, WMO TD N. 1147, No 149, 2003.

[4] Lambert, J.-C. , M. Van Roozendael, P.C. Simon, M. De Mazière, J.-P. Pommereau, F. Goutail, A. Sarkissian, S.B. Andersen, P. Eriksen, B.A. Kåstad Høiskar, W. Arlander, K. Karlsen Tørnkvist, V. Dorokhov, and E. Kyrö, GOME and TOMS Total Ozone in Northern Winter 1996/1997: Comparison with SAOZ/UV-visible Ground-based Measurements in the Arctic and at Middle Latitude, in *Polar Stratospheric Ozone 1997*, N.R.P. Harris, I. Kilbane-Dawe, and G.T. Amanatidis (Eds.), Air Pollution Research Report 66 (CEC DG XII), 696-699, 1998.

[5] ERS-2 GOME GDP3.0 Implementation and Validation, ESA Technical Note ERSE-DTEX-EOAD-TN-02-0006, 138 pp., Ed. By J.-C. Lambert (IASB), November 2002.

VII NITROGEN DIOXIDE COLUMN VERIFICATION

VII.1 INTRODUCTION

Improving the nitrogen dioxide column product was not the focus of this new GDP upgrade. Only a few of the current GDP changes might alter this product, among them the use of a new NO_2 profile climatology and of on-the-fly LIDORT for the AMF calculation, and the improved correction for Raman scattering. Possible changes due to the processing in the new UPAS environment system cannot be excluded *a priori*. Therefore the aim of this Section is mainly to verify that the quality of the GDP 3.0 nitrogen dioxide column product has not changed significantly GDP 4.0. The basis of this study will be the Delta Validation Report of the GDP upgrade to version 3.0 issued in November 2002, thus limited to time-series ending in summer 2002. Here, validations will be extended to 2004 with the aim to investigate long-term stability.

VII.2 SUMMARY OF THE QUALITY OF GDP 3.0 NO_2 COLUMNS

During the Delta Validation of the GDP upgrade to version 3.0, the GOME total nitrogen dioxide product was validated from pole to pole on the basis of comparisons to ground-based measurements of the NDSC network of DOAS UV-visible spectrometers and Fourier Transform Infrared spectrometers, and to global data from the UARS HALOE and SPOT-3/4 POAM-2/3 satellite sensors and tropospheric and stratospheric modelling tools. GDP retrievals had also been compared with GOME NO_2 retrievals performed with the WinDOAS software package.

NO_2 absorption in the usual fitting window (425-450 nm) is optically thin, and retrieval using the two-step DOAS approach is suitable for total column retrieval of this species. Already implemented in GDP 2.7, the inclusion of interfering absorptions by O_4 and H_2O in the DOAS fit reduces uncertainties in the tropical areas. GOME total nitrogen dioxide is found in reasonable agreement with ground-based and other satellite measurements: within $\pm 5\ 10^{14}$ molec.cm^{-2} in areas of low tropospheric NO_2 and within $\pm 8\ 10^{14}$ molec.cm^{-2} in areas of very low slant column of NO_2. Atmospheric parameters in use in the NO_2 AMF calculation introduce a fictitious latitudinal/seasonal variation of a few percent superimposed on the geophysical variations in NO_2. Although it is difficult to make a precise evaluation of the NO_2 total column accuracy (due to various problems such as the photochemical diurnal cycle of NO_2), the overall accuracy is estimated to fall within the 5% to 10% range provided that the contribution of tropospheric NO_2 to the vertical column remains low. GDP total NO_2 has larger errors under certain circumstances, e.g., in the South Atlantic Anomaly and over polluted areas. In the latter case, current NO_2 AMF values and effective absorption temperatures calculated for pure stratospheric scenarios do not account for variations in the tropospheric burden of NO_2 and are consequently subject to systematic errors. For scenarios of extreme pollution, modelling results suggest that AMF errors can lead to an underestimation of the actual NO_2 vertical column amount by a factor of two.

VII.3 CORRELATIVE DATA SETS AND METHODOLOGY

For the present verification exercise, we have conducted correlative studies at 40 ground-based stations listed in **Table 4** and highlighted on the map of **Figure 44**. Contributing ground-based stations are equipped with well-maintained DOAS UV-visible spectrometers monitoring the NO_2 column at sunrise and at sunset, some of them since the early 1980s. Others have provided correlative data for a limited period only, but still of interest for GOME validation. Due to their twilight measurement geometry, NO_2 column UV-visible instruments are mostly sensitive to the stratospheric contribution to the vertical column. Contributing sensors consist in a series of scanning instruments developed by NIWA since the late 1970s [McKenzie and Johnston, 1982], a series of SAOZ grating instruments (Système d'Analyse par Observation Zénithale) developed by CNRS and performing automated network operation since the late 1980s [Pommereau and Goutail, 1988], and spectrometers of a similar design developed at IASB [Van Roozendael *et al.*, 1995], IFE/IU¨P [Richter *et al.*, 1998], INTA, IUP/Heidelberg, and NILU [Arlander *et al.*, 1998]. NO_2 vertical column is inferred from recorded zenith-scattered spectra using a two-step approach of the Differential Absorption Optical Spectroscopy (DOAS) technique similar to that used in the GOME processing chain: apparent slant columns are retrieved from a spectral analysis and then converted into vertical columns by means of a geometrical enhancement factor, or air mass factor (AMF).

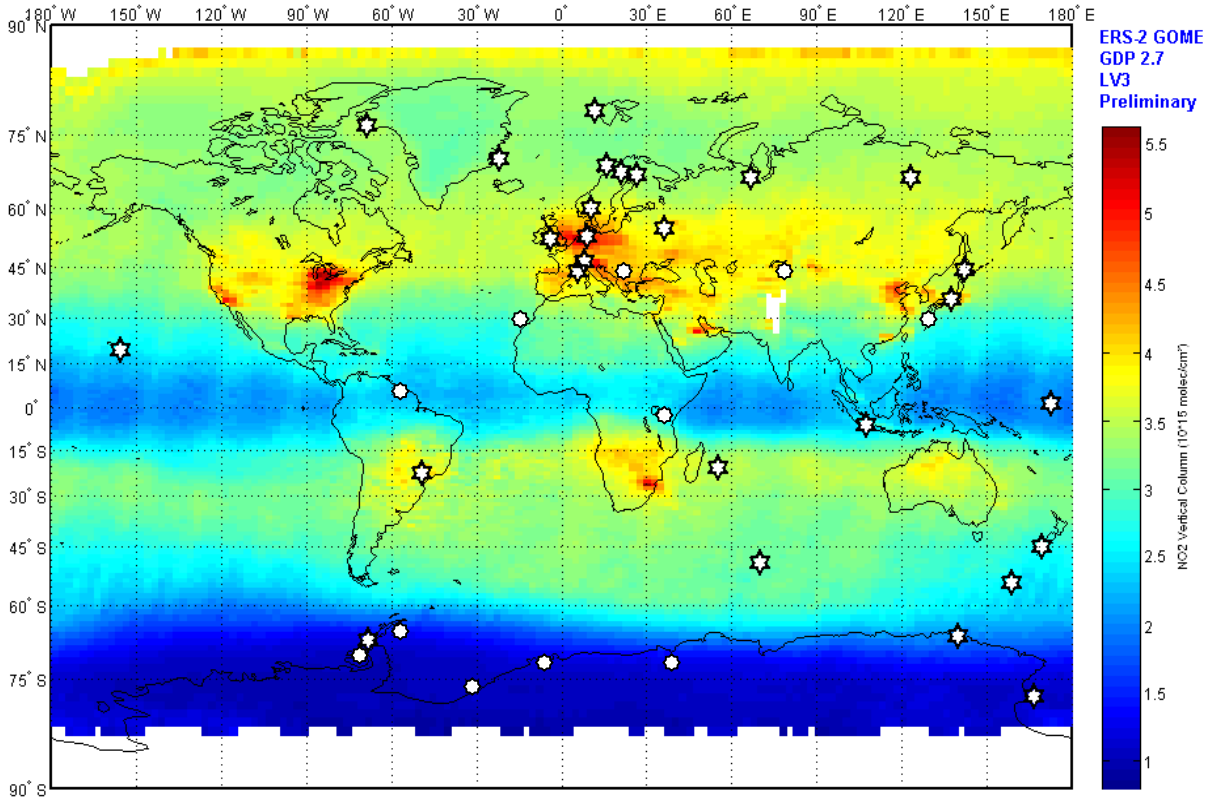

Figure 44 – Geographical distribution of contributing UV-visible DOAS spectrometers monitoring the vertical column amount of NO_2. Stations are identified on top of the September 2000 monthly mean field derived from GOME data.

All contributing UV-visible sensors have been certified for the NDSC after fruitful participation to major inter-comparison campaigns organised through the NDSC and/or the EC Environment Programme. During such campaigns, the agreement between the various instruments generally falls within the 5% to 10% range [e.g., Hofmann *et al.*, 1995; Vaughan *et al.*, 1997; Roscoe *et al.*, 1999]. Long-term comparisons of nearly co-located instruments conclude to a mean agreement of 3% in summer and 9% in winter [e.g., Koike *et al.*, 1999]. The figure is consistent with an estimated 5-10% accuracy of the retrieved slant column amount taking into account the 5% uncertainty of the NO_2 absorption cross-sections [Merienne *et al.*, 1995], their temperature dependence [Harwood and Jones, 1994; Coquart *et al.,* 1995], and the average 1.5% one sigma confidence level of the least-squares spectral fit. The zenith-sky NO_2 AMF exhibits periodic signatures related to seasonal, latitudinal, and sunrise/sunset change of the vertical distribution of atmospheric constituents [Lambert *et al.*, 1999c]. Not taken into account in the ground-based data processing yet, those features generate in the resulting vertical columns fictitious cyclic signatures of a few percent, superimposed on the real total NO_2 variations observed by the instrument. As shown in an NDSC-based study of GOME NO_2 data [Lambert *et al.*, 1999c], those cyclic biases should not affect current GOME validation studies.

Table 4 - List of UV-visible DOAS instruments contributing to the present verification of GOME NO_2 columns.

ID	STATION NAME	LOCATION	LATITUDE	LONGITUDE	INSTITUTE
bg	BELGRANO	Antarctica	-77.87	-34.63	INTA
ah	ARRIVAL HEIGHTS	Antarctica	-77.82	166.66	NIWA
ne	NEUMAYER	Antarctica	-70.65	8.25	IUP/Heidelberg
sy	SYOWA	Antarctica	-69.01	39.59	U. Tokyo/NIWA
ro	ROTHERA	Antarctic Peninsula	-67.57	-68.13	BAS/NERC
dd	DUMONT D'URVILLE	Antarctica	-66.67	140.01	CNRS
fa	FARADAY	Antarctic Peninsula	-65.25	-64.27	BAS/NERC
mm	MARAMBIO	Antarctic Peninsula	-64.28	-56.72	INTA
ma	MACQUARIE	Australia	-54.48	158.97	NIWA
ke	KERGUELEN	Kerguelen Island	-49.36	70.26	CNRS
la	LAUDER	New Zealand	-45.03	169.68	NIWA
ba	BAURU	Brazil	-22.35	-49.03	CNRS/UNESP
re	SAINT-DENIS	Reunion Island	-20.85	55.47	CNRS/U. Réunion
bd	CIATER/BANDUNG	Java (Indonesia)	-6.4	107.4	U. Tokyo/NIWA
nr	NAIROBI	Kenya	-1.27	36.80	IUP/Bremen
tw	TARAWA	Kiribati	1.37	172.93	CNRS + NIWA
pr	PARAMARIBO	Suriname	5.75	-55.2	IUP/Heidelberg
ml	MAUNA LOA	Hawaii	19.54	-155.58	NIWA
iz	IZANA	Tenerife (Spain)	28.29	-16.49	INTA
ks	KISO	Japan	35.8	137.6	STELab/U. Nagoya/NIWA
sz	STARA ZAGORA	Bulgaria	42	25	BAS/STEL
ik	ISSYK-KUL	Kyrgyzstan	42.63	76.98	KSNU/IEM
ri	RIKUBETSU	Japan	43.5	143.8	STELab/U. Nagoya/NIWA
oh	HAUTE PROVENCE	France	43.92	5.75	CNRS
mc	MONTE CIMONE	Italy	44.18	10.7	ISAC/CNR
ms	MOSHIRI	Japan	44.4	142.3	STELab/U. Nagoya/NIWA
ju	JUNGFRAUJOCH	Switzerland	46.55	7.98	BIRA-IASB
ab	ABERYSTWYTH	UK	52.42	-4.07	U. Wales
Br	BREMEN	Germany	53.11	8.86	IUP/Bremen
zv	ZVENIGOROD	Russia	55.7	36.8	IAP/Moscow
ha	HARESTUA	Norway	60.22	10.75	BIRA-IASB
zg	ZHIGANSK	Eastern Siberia	66.72	123.40	CNRS/CAO
sl	SALEKHARD	Western Siberia	66.7	66.7	CNRS/CAO
sk	SODANKYLA	Finland	67.37	26.65	CNRS/FMI
ki	KIRUNA	Sweden	67.84	21.06	NIWA
an	ANDOYA	Norway	69.28	16.18	NILU
sc	SCORESBYSUND	Western Greenland	70.48	-21.96	CNRS/DMI
th	THULE	Eastern Greenland	76.51	-68.76	DMI
ly	LONGYEARBYEN	Spitsbergen (Norway)	78.12	15.40	NILU
na	NY ALESUND	Spitsbergen (Norway)	78.93	11.88	IUP/Bremen + NILU

The comparison method is described e.g. in [ESA 2002] and takes into account the diurnal cycle of the NO_x family and the impact of measurement time differences on the comparison between GOME daytime data and ground-based twilight data.

VII.4 VERIFICATION OF GDP 4.0 NO_2 COLUMNS

Figure 45 illustrates the comparison results obtained at the Southern mid-latitude NDSC station of Macquarie Island. In Part (a), the following GOME and ground-based time-series are compared from 1995 through 2003: GDP 3.0 (open circles), GDP 4.0 (black dots), ground-based dawn (blue dots) and ground-based dusk (red dots). As predicted by photochemical models, GOME mid-morning readings agree fairly with the sunrise values recorded from the ground. At this clean-air station, GDP 3.0 and GDP 4.0 capture the same NO_2 features, which here consist mainly in a smooth seasonal cycle and in weak day-to-day fluctuations, both of stratospheric origin. Part (b) of **Figure 45** shows the absolute difference in NO_2 column between three GDP versions and the ground-based sunrise values: GDP 2.7 (grey line), GDP 3.0 (open black circles and thin black line) and GDP 4.0 (plain black dots and thick black line). From 1996 to 2001, the mean agreement between all GDP versions and the ground-based NO_2 data remains within the accuracy limits of the comparison method, that is, a few 10^{14} molec.cm^{-2} at this station (see [1]). The main change from one version to another is a constant offset of a few 10^{14} molec.cm^{-2}. It is not easy to determine which version is the more accurate since the amplitude of this offset falls itself within the accuracy limit of the validation method. While both GDP 3.0 and GDP 4.0 seem to be stable in the long term, in the second half of 2001, GDP 2.7 starts overestimating other data records – by sometimes more than 10^{15} molec.cm^{-2} – as a consequence of instrumental degradation effects on the Level-1 data quality. With GDP 3.0 and GDP 4.0, this sensitivity of the NO_2 column product vanishes thanks to improved corrections implemented in the Level-0-to-1 processor version 2.2. Linear fitting of the comparison time-series (quite noisy and therefore not shown here) suggests a slight long-term increase of the mean agreement, but its low value of only a few 10^{14} molec.cm^{-2} over 7.5 years calls for verification over the full GOME data record – instead of the validation orbits used here – in order to improve the statistical significance of the trend assessment. Finally, Parts (c)-(f) of **Figure 45** show the GOME/ground difference in total NO_2 sorted by season and plotted as a function of the GOME solar zenith angle. Knowing that ground-based values are acquired at a constant SZA range from 91° to 86/87°, the GOME SZA can be used as a photochemical coordinate to separate partly diurnal cycle and seasonal cycle effects in the interpretation of the comparisons. The main conclusion to draw at this stage is that changes from one GDP version to another produce only a constant offset of a few 10^{14} molec.cm^{-2} independently of the GOME SZA and the season. A more detailed interpretation of the results falls beyond the scope of this verification exercise.

Figure 46 shows similar comparisons at the Brazilian station of Bauru, on the Southern Tropic. The mean agreement varies from –0.3 to +0.5 10^{14} molec.cm^{-2}, that is, within the accuracy limits of the validation method. Again, the present GDP upgrade to version 4.0 produces only a constant offset of a few 10^{14} molec.cm^{-2}, and as expected no significant change is to date in the agreement with ground-based data.

Finally, **Figure 47** illustrates typical results obtained in the Arctic. After photochemical correction for the diurnal cycle during polar day, there is no bias between mid-morning and midnight sun GOME NO_2 data. Again, there is no significant change compared to GDP 3.0.

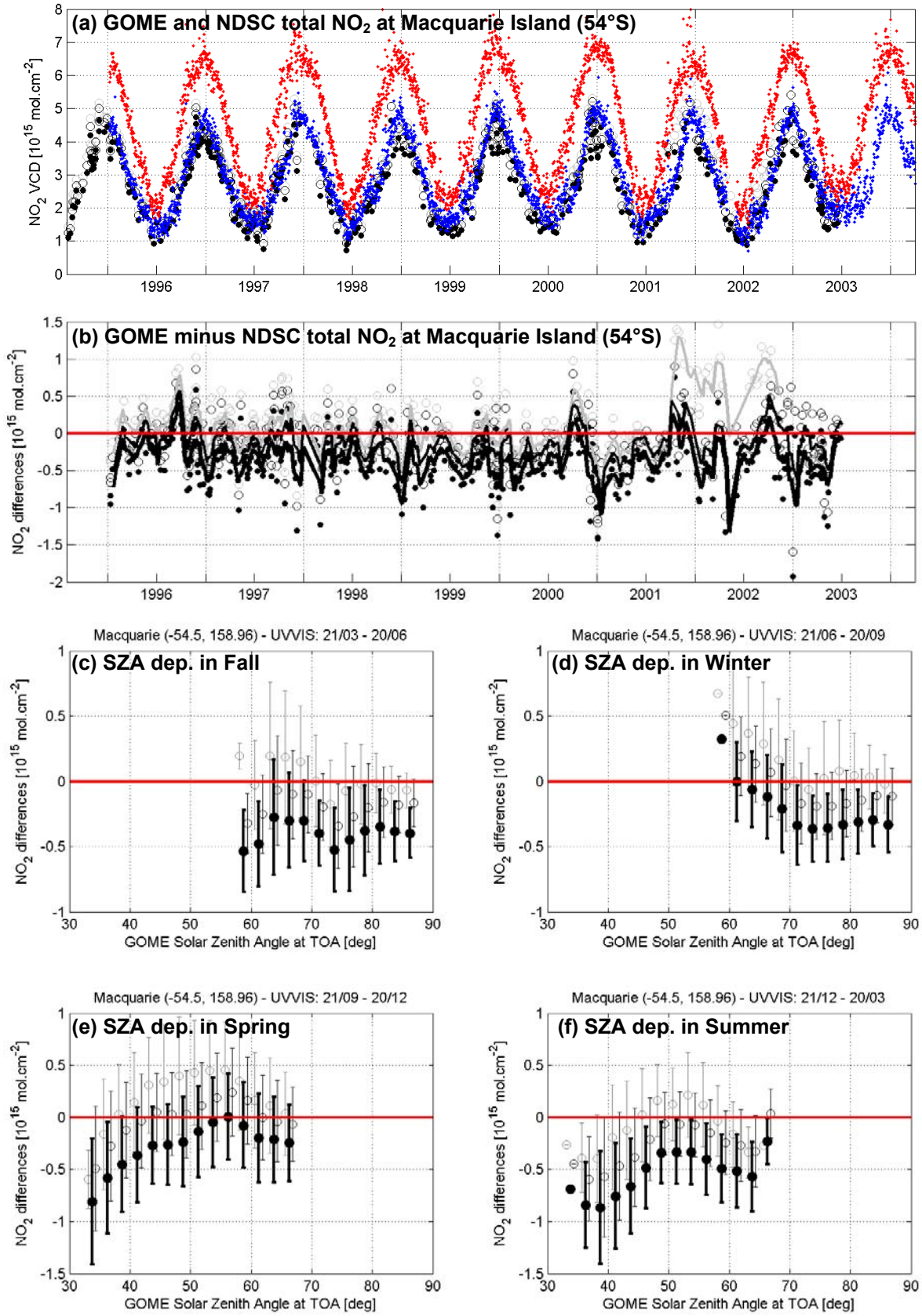

Figure 45 – Comparison of GOME and ground-based DOAS NO_2 column measurements at the Southern mid-latitude NDSC site of Macquarie Island (Australia, 54°S, 159°E). See text for explanations.

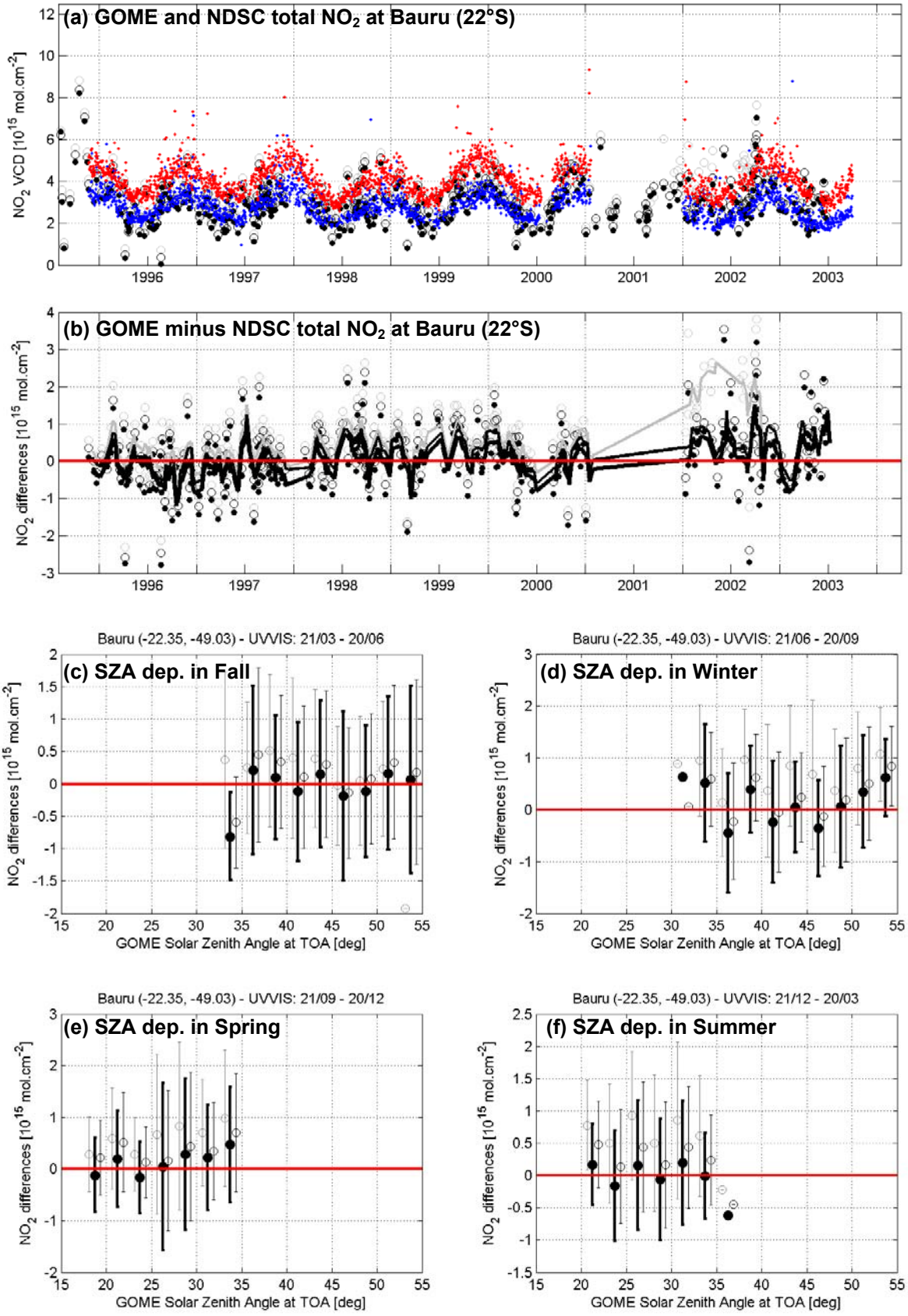

Figure 46 – Comparison between GOME and CNRS/UNESP ground-based DOAS NO_2 column measurements at the Southern tropical NDSC site of Bauru (Brazil, 22°S, 49°W). See text for explanations.

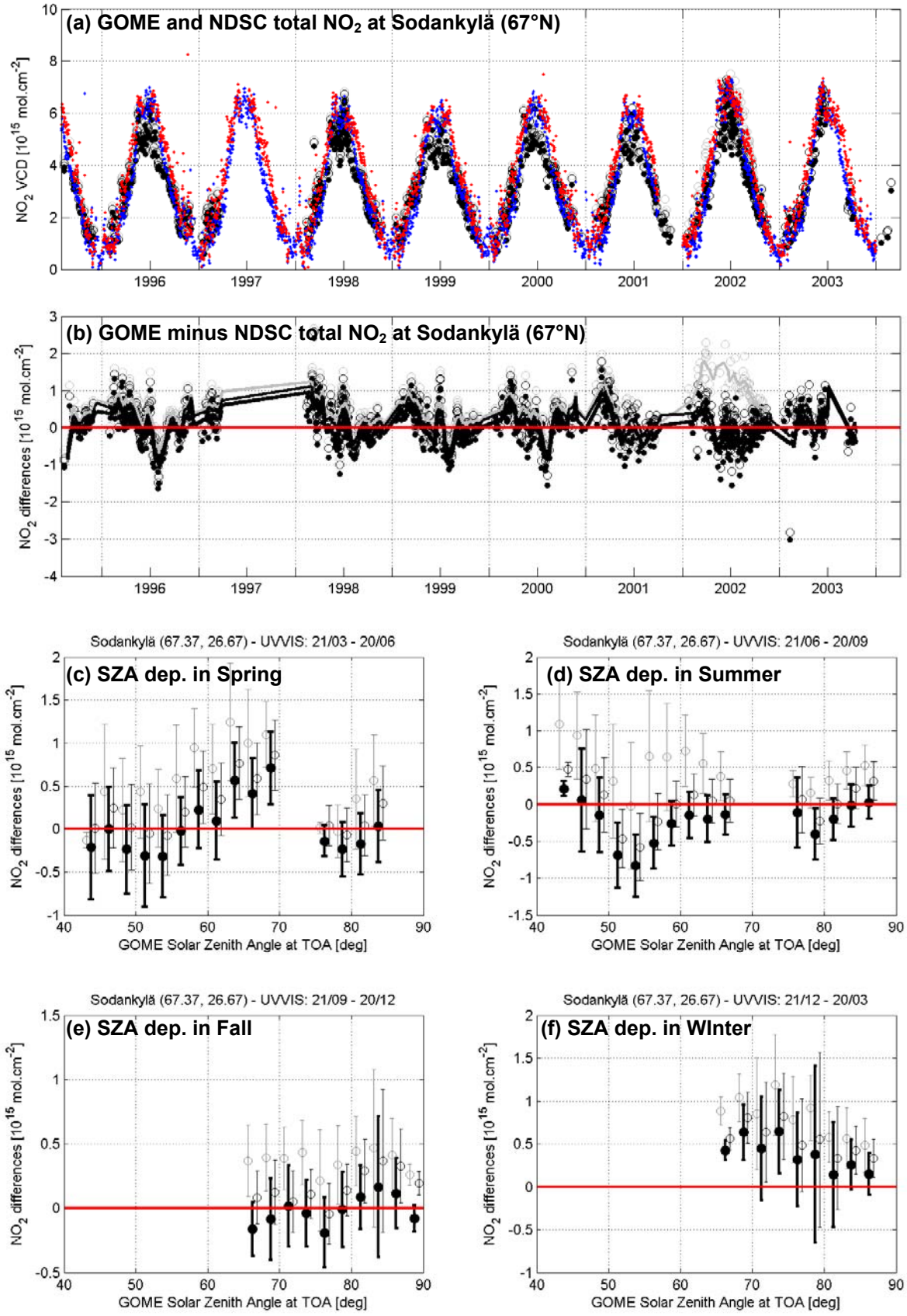

Figure 47 - Comparison between GOME and CNRS/FMI ground-based DOAS NO_2 column measurements at the Arctic Circle NDSC site of Sodankylä (Finland, 67°N, 27°E). See text for explanations

VII.5 CONCLUSION

NO_2 product changes between GDP 2.7, GDP 3.0 and GDP 4.0 have been investigated through comparisons with ground-based NO_2 column data acquired at 40 NDSC stations from pole to pole. Between two different versions of GDP, the main difference to date is a general decrease, of about 1-5 10^{14} molec.cm^{-2} from GDP 2.7 to GDP 3.0 (until 2002 when instrumental degradation effects appear in GDP 2.7 data) and of a similar amplitude from GDP 3.0 to GDP 4.0. GDP 4.0 NO_2 columns offer a remarkable stability in the long term and do not seem to suffer from instrumental degradation effects. The study concludes that previous validation results based on comparisons with data from the NDSC/FTIR ground-based network, the HALOE and POAM satellites, the IMAGES chemical-transport model of the troposphere, and the PSCBOX/SLIMCAT coupled model of the stratosphere, remain valid with GDP 4.0.

References

Arlander, D.W., K.K. Tørnkvist, and G.O. Braathen, Ground-based UV-Vis Validation Measurements of Stratospheric Molecules above Spitsbergen, in Proc. 24th Annual European Meeting on Atmospheric Studies by Optical Methods, Andenes 1997, ISBN 82-994583-0-7, pp. 185-188, 1998.

ESA 2002: ERS-2 GOME GDP3.0 Implementation and Validation, ESA Technical Note ERSE-DTEX-EOAD-TN-02-0006, 138 pp., Ed. By J.-C. Lambert (IASB), November 2002.

Johnston, P.V., and R.L. McKenzie, NO2 Observations at 45°S during the Decreasing Phase of Solar Cycle 21, from 1980 to 1987, J. Geophys. Res., Vol. 94, pp. 3473-3486, 1989.

McKenzie, R.L., and P.V. Johnston, Seasonal variations in stratospheric NO2 at 45°S, Geophys. Res. Lett., 9, pp. 1255-1258, 1982.

Pommereau, J.P. and F. Goutail, O3 and NO2 Ground-Based Measurements by Visible Spectrometry during Arctic Winter and Spring 1988, Geophys. Res. Lett., 891, 1988.

Richter, A., M. Eisinger, F. Wittrock, S. Schlieter, A. Ladstätter-Weißenmayer, and J. P. Burrows, Zenith sky and GOME DOAS measurements of atmospheric trace gases above Bremen, 53°N: 1994 - 1997, in Polar Stratospheric Ozone - Proc. 4th European Workshop, Schliersee 1997, N.R.P. Harris, I. Kilbane-Dawe, and G.T. Amanatidis (Eds.), Air Pollution Research Report 66 (CEC DG XII), pp. 482- 485, 1998.

Roscoe, H. K., et al., Slant column measurements of O3 and NO2 during the NDSC intercomparison of zenith-sky UV-visible spectrometers in June 1996, J. Atmos. Chem., 32, pp. 281-314, 1999.

Van Roozendael, M., C. Hermans, Y. Kabbadj, J.-C. Lambert, A.-C. Vandaele, et al., Ground-Based Measurements of Stratospheric OClO, NO2 and O3 at Harestua, Norway (60°N, 10°E) during SESAME, in Proc. 12th ESA Symp. on European Rocket and Balloon Programmes & Related Research, Lillehamer 1995, ESA SP-370, pp. 305-310, 1995.

Vaughan, G., et al., An intercomparison of ground-based UV-Visible sensors of ozone and NO2, J. Geophys. Res., 102, 1411-1422, 1997.

VIII CONCLUDING REMARKS

The correctness of upgrades of GOME Data Processor level-1-to-2 to version 4.0, as well as their effect on GOME data products, have been investigated using different methods based on comparisons with correlative measurements from ground-based networks, with substantial support from the teams in charge of retrieval algorithm developments and operational implementation.

In general, it is confirmed that modifications implemented in GDP 4.0 produce expected changes in the data products. However, it must be kept in mind that reported studies rely on a representative but limited set of orbits and therefore unverified effects cannot be ruled out.

GOME total ozone: Two main objectives of this GDP upgrade to version 4.0 have been fulfilled. First, seasonal, meridian, and solar zenith angle dependences between GOME and ground-based network total ozone data have been cut down to the "percent level" at low and moderate SZA, and does not exceed an average 5% amplitude at solar zenith angles larger than 80°. This clear improvement allows the use of GOME data for accurate polar studies. Second, the remarkable stability of the GOME GDP 4.0 ozone data record from 1995 till 2004 allows its use for ozone trend monitoring.

TOMS total ozone: The upgrade of the TOMS algorithm to version 8 is an improvement with respect to the seasonal, meridian, and zone column dependences of the previous operational version 7. TOMS V8 is nevertheless sensitive to instrumental degradation and calibration issues, which impact the stability of the EP-TOMS ozone data record after 2001.

GOME total nitrogen dioxide: As expected, the total nitrogen dioxide data product has not significantly changed. Previous validation results based on extended data records and on other sources of correlative data remain valid.

Documentation: Existing documentation on GDP and on the quality of GDP data products was updated: DLR Technical Notes, GOME Data Disclaimer 2004, GOME validation web site. The Algorithm Theoretical Basis Document (ATBD) for GDP 4.0 includes a validation summary based on the present validation results.

Operation: As a result of the general improvement of GOME data products, the complete GOME data record from July 1995 onwards has been reprocessed with GDP 4.0 and is available to the public via the ERS Help & Order desk (see Contact Point below in the GOME Data Disclaimer 2004 provided in the Annexe).

Applications: The present quality of level-2 data products makes them suitable for a wide variety of geophysical research applications, including ozone trend monitoring and polar process studies. All reprocessed products can be used within the limitations outlined in the existing literature and updated in the present report.

ANNEXE – DISCLAIMER FOR GOME LEVEL-1 AND LEVEL-2 DATA PRODUCTS: DECEMBER 2004

1. Introduction

Operational GOME data products are generated by the GOME Data Processor (GDP) at the German Processing and Archiving Facility (D-PAF) at DLR on behalf of ESA. Quality assessment of these products is aimed at improving their accuracies, to the point of achieving theoretical minimum error values. The improvement of operational algorithms and their associated data products is a continuous activity, ongoing since the start of GOME operations in July 1995. This process has benefited from a number of validation campaigns, involving specialist groups in the atmospheric science community with expertise in the retrieval of trace constituents from ground-based and other instrumentation appropriate to GOME validation.

The operational products produced by the GDP are defined as:

- Level-1 data: Earthshine spectral radiance at the Top of the Atmosphere at the GOME viewing solid angle; Extra-terrestrial solar spectral irradiance.
- Level-2 data: Vertical Column amount of O3 (Dobson Unit); Vertical Column amount of NO_2 (molecule cm-^{2}); Cloud Fractional Coverage; Cloud-top Height (km); Cloud-top Albedo.

The first dedicated validation campaign for GOME products was conducted during the commissioning phase in the second half of 1995. As reported in an ESA publication (ESA WPP-108), studies carried out by more than 20 different groups highlighted a number of critical issues for prototype GDP data products. Recommendations were made for modifications to the developmental GDP, to data analysis and instrument operation procedures, and to data processing and distribution policies. Some of these recommendations were implemented during the first months of 1996, and the first public version (GDP 2.0) was released later in that year.

Since then, a number of additional recommendations have been made regarding GDP modifications, and most changes to GDP have been implemented in successive versions, from GDP 2.4 (operational in the 1998-2000 time frame), to GDP 2.7 (2000-2002), GDP 3.0 (2002-2004), and lastly to the current version GDP 4.0 (from December 2004 onwards).

Before implementation of major GDP changes in the operational processing chain and subsequent reprocessing of all historical data, it is essential not only to verify the accuracy and effectiveness of the proposed modifications but also to assess the quality of the new data product. This has been done by means of so-called 'delta' validation campaigns executed by a sub-group of the GOME validation group; such campaigns use a limited but representative subset of validation orbits selected to test expected changes. Results from delta validation campaigns were reported at dedicated meetings in May and June 1996, in January 1998, in May and July 1999, in January and April 2002, and most recently in November 2004 at ESRIN.

At the same time, detailed validation and algorithm improvement studies have been carried out by a wider segment of the atmospheric science community and reported on many occasions, both at international conferences and workshops and in the open literature.

The present disclaimer summarises the status of the current GDP data quality, with reference to version 2.2 for GDP level-0-to-1 processing, and version 4.0 for GDP level-1-to-2 algorithms.

2. Current Data Quality of GOME level 1-Product

GOME level-1 data products possess good wavelength stability, indicating a high instrument precision. Level-1 products are affected by spectral and radiometric distortions of instrumental origin. The solar irradiance measurements exhibit an anticipated slow degradation in the ultraviolet (channels 1 and 2); there is an option to correct for this degradation in the GDP extraction software. In addition, there is a seasonal variation of sensitivity depending on the solar azimuth at the sun diffuser. For retrievals of ozone column amounts using the DOAS technique, these degradation and instrumental errors are relatively minor in importance. The accuracy of the Earth's reflectivity (i.e., the ratio between Earth radiance and solar irradiance) is considered to be about 3%, except in the ultraviolet.

2.1 Solar Irradiance

Validation of GOME solar irradiance data is based in part on comparisons with SOLSTICE and SSBUV measurements in the 240-400 nm spectral range, in part on auto-correlation studies of GOME data, and additionally on comparisons with high-resolution solar spectrum atlas data.

Deviations at the beginning of the GOME Instrument lifetime:

Despite the relatively good agreement with SOLSTICE measurements, the GOME irradiance measurement in channel 1 is considerably lower, by 5 % to 10 %. In channel 2, the agreement is better, but etalon features limit the accuracy of GOME data with modulations of ±2%.

The average deviations of GOME data from SOLSTICE data on 3 July 1996 and the rates of linear decay between 3 July 1995 and 14 January 1996 are given in the following table:

Wavelength range	Average deviation	Linear decay
240 - 250 nm	5.8 %	3.5%/100 days
250 - 300 nm	5.1 %	1.5%/100 days
300 - 370 nm	0.8 %	0.5%/100 days
370 - 400 nm	2.4 %	0%/100 days

Deviations at mid 1999:

The average deviations of GOME data from SOLSTICE V12 data on 1 January 1999 and the rates of linear decay in 1998 are given in the following table:

Wavelength range	Average deviation	Linear decay
240 - 250 nm	-51 %	4.7 %/100 days
250 - 300 nm	-25 %	1.7 %/100 days
300 – 350 nm	-9 %	0.7 %/100 days
350 - 400 nm	-4 %	0.3 %/100 days

The observed degradation in the ultraviolet was expected and is similar to that observed in other remote sensing instruments measuring solar irradiance in the ultraviolet (e.g. TOMS). It can be corrected by the extraction software. Note that the solar azimuth on the solar diffuser differs between January and July data; this affects the sensitivity in the spectral region below 260nm by about 6%. Therefore, the linear decay presented in the tables above must be considered as an upper limit.

Yearly deviations up to and including 2004:

The following table shows the yearly mean percentage degradations of GOME channels (starting point on 3 July 1995 for reference) from 1996 to 2004.

Wavelength (nm)	240-250	250-300	300-350	350-400	400-600	600-790
1996	-0.2 %	-0.1 %	0 %	0 %	0 %	0 %
1997	-9.4 %	-3.0 %	-1.6 %	-0.5 %	-0.6 %	-0.1 %
1998	-22.8 %	-7.6 %	-3.5 %	-1.4 %	-1.3 %	-1 %
1999	-48.8 %	-16.9 %	-5.3 %	-1.8 %	-0.7 %	-2.2 %
2000	-60.6 %	-35.7 %	-9.1 %	-2.3 %	+1.2 %	-1.4 %
2001	-55.6 %	-47.8 %	-25.1 %	-7.7 %	+1.7 %	+2.3 %
2002	-77.9 %	-53.0 %	-36.9 %	-21.7 %	-1.6 %	+3.5 %
2003	-82.0 %	-63.1 %	-37.3 %	-26.7 %	-4.9 %	+7.1 %
2004	-86.3 %	-71.7 %	-42.9 %	-31.8 %	-11.5 %	+4.1 %

2.2 Earthshine Radiance

The Level-1 Earthshine radiance product suffers from the same instrument degradation as the Solar Irradiance product.

A correction for the GOME instrumental response to polarisation is required for the radiance products. This polarisation correction (PC) of the up-welling radiation from the atmosphere is determined as follows:

i. For wavelengths below 300 nm, it is assumed that the Rayleigh single scattering determines the degree of polarisation.

ii. For wavelengths larger than 300 nm, three instrument-derived values for the degree of polarisation have been deduced from integrated detector array measurements in channels 2, 3 and 4 and the corresponding broad-band measurements from the three Polarisation Monitoring Devices (PMDs).

iii. To estimate individual values of the degree of polarisation at all channel wavelengths, a polynomial is then fitted to these four determinations of the degree of polarisation; the fitting includes a parameterisation based on model calculations between 300 and 325 nm.

Allowing for degradation corrections of the polarisation measurements, the accuracy of the radiometric calibration of GOME between 350 and 790 nm is considered to be about 3% except in the ultraviolet, where it is limited to 5% because of additional pre-flight calibration uncertainties and to remaining uncertainties of atmospheric polarisation. Below 350 nm the Earth's radiance has not yet been fully validated.

A significant source of radiance error arises from inadequacies in the polarisation-correction procedure implemented in the level-1 extractor software. Interpolation of polarisation values between 350 nm (PMD1 polarisation value) and 300 nm (single scatter polarisation value) is problematic due to the paucity of polarisation information.

Discontinuities in the absolute radiance values are observed between channels. This is caused by the serial read-out of the detectors, which means that although all array pixel detectors have the same integration time, the read-out of the first array detector pixel is 93 ms shifted in time compared with that for the 1024^{th} detector pixel. This aliasing effect is pronounced for earthshine scenes having significant albedo changes in the field of view between the first and last detector pixel. An option in the extraction software is available to create an effective average scene for the four channels.

3. Current Data Quality of GOME level-2 products

3.1 Vertical Column Amount of Ozone

Geophysical validation is a vital tool to assess the quality of Level 2 products and to direct the maturation of Level 1-to-2 GDP retrieval algorithms. GOME total ozone data and related algorithms have been validated from pole to pole (a) through comparisons with ground-based measurements from SAOZ/DOAS UV-visible spectrometers, Brewer and Dobson ultraviolet spectrophotometers, and ultraviolet filter radiometers; and (b) with global data from the TOMS satellite sensor (both V7 and V8) and from modelling/assimilation tools. In-depth validation of the GDP retrieval algorithms has also been carried out using independent DOAS-type algorithms, a novel algorithm based on the direct fitting approach, and the TOMS v7 algorithm.

The DOAS approach adopted in GDP to ultraviolet-visible level 1-to-2 retrievals of total column amounts consists of the spectral fitting of the apparent slant column amount, followed by its conversion into vertical column amount using a calculated Air Mass Factor (AMF). The latter determination is based in part on cloud information inferred from GOME measurements. The spectral fitting of ozone slant columns in the 325 to 335 nm works well. Compared to GDP 2.7, GDP 3.0 included a new determination of effective absorption temperature derived by spectral analysis, better atmospheric databases, and AMFs determined iteratively using a neural network trained on column- and latitude-classified atmospheric profiles and measurement parameters. GDP 3.0 upgrades resulted in a reduction by about 30-50% of the amplitude of the GOME total ozone dependence on the SZA, the latitude, the season, and the ozone column amount. Compared to GDP 3.0, the current version GDP 4.0 includes an improved correction for ozone absorption distortion due to inelastic rotational Raman scattering by air molecules, a new cloud treatment for the retrieval of three auxiliary pieces cloud information, and further improvements to the AMF calculation using on-the-fly radiative transfer modelling The main achievement with GDP 4.0 is the drastic reduction of nearly all remaining dependencies on latitude, season, SZA and ozone column persisting with GDP 3.0.

In general, the average agreement of GDP 4.0 with correlative ozone column measurements is now at the “percent level”, that is, within the precision level of ground-based sensors when the latter are corrected for their own dependencies on the season, solar elevation, temperature etc. At polar latitudes, and at GOME solar zenith angles larger than 80°, preliminary validation indicates that the agreement is slightly worse; however, average differences at low solar elevation usually do not exceed 5%. A remarkable feature of the reprocessed GOME GDP 4.0 data record is that, despite the anticipated degradation of the instrument with time, the total column products do not suffer from any long-term drift of quality. This is the case even in late 2004, when the degradation of the UV ozone channel has reached 42.9%. More qualitatively, GOME gives a consistent picture of the global ozone field with temporal signals and spatial structures similar to those observed by other high-quality sensors.

3.2 Vertical Column Amount of Nitrogen Dioxide

The GOME GDP total nitrogen dioxide product has also been validated from pole to pole, with comparisons to ground-based measurements of the NDSC network of SAOZ/DOAS UV-visible spectrometers and Fourier Transform Infrared spectrometers, and to global data from the HALOE and POAM satellite sensors and tropospheric and stratospheric modelling tools. GDP retrievals have also been compared with GOME NO_2 retrievals performed with independent DOAS-type algorithms.

NO_2 absorption in the usual fitting window (425-450 nm) is optically thin, and retrieval using the two-step DOAS approach is suitable for total column retrieval of this species. The DOAS fit includes amplitudes for interfering absorptions by O_4 and H_2O. GOME total nitrogen dioxide is in reasonable agreement with ground-based and other satellite measurements: within $\pm 5\ 10^{14}$ molec.cm^{-2} in areas of low tropospheric NO_2 and within $\pm 8\ 10^{14}$ molec.cm^{-2} in areas of very low slant column of NO_2. Atmospheric parameters currently in use in the NO_2 AMF calculation introduce a fictitious latitudinal/seasonal variation of a few percent superimposed on the geophysical variations in NO_2. Although it is difficult to make a precise evaluation of the NO_2 total column accuracy (due to various problems such as the photochemical diurnal cycle of NO_2), the overall accuracy is estimated to fall within the 5% to 10% range, provided that the contribution of tropospheric NO_2 to the vertical column remains low. GDP total NO_2 has larger errors under certain circumstances, e.g., in the South Atlantic Anomaly and over polluted areas. In the latter case, current NO_2 AMF values and effective absorption temperatures calculated for pure stratospheric scenarios do not account for variations in the tropospheric burden of NO_2 and are consequently subject to systematic errors. For scenarios of extreme pollution, modelling results suggest that AMF errors can lead to an underestimation of the actual NO_2 vertical column amount by a factor of two.

4. Concluding Remarks

As a consequence of the anticipated degradation of the instrument and concomitant changes of in-flight calibration parameters, a dynamic database has been developed to provide the optimal calibration of level-1 data. This database describes the temporal behaviour of GOME calibration parameters and was validated before operational implementation.

The present errors in the level-1 product have a negligible impact on the quality of the total ozone column density derived by DOAS in the level-1-to-2 processing. The reason is that many errors arising from the changes in calibration parameters cancel because the DOAS algorithm uses reflectances (irradiances divided by the radiances) as the basic measurement input, and intensity calibration errors, which have a polynomial dependence on wavelength, are subsumed in the DOAS polynomial closure term.

Present quality of level-2 data products makes them suitable for a wide variety of geophysical research applications, including ozone trend monitoring and polar process studies. The complete GOME data record from July 1995 onwards has been reprocessed with GDP 4.0 and is available to the public via the ERS Help & Order desk (see Contact Point below in Section 6).

The present level of understanding for GOME data quality is based on a series of validation results presented at GDP upgrade meetings held in November 2004, January and April 2002, January, May and July 1999, January 1998, March 1997, and January, May and June 1996; at a series of GOME science & algorithms workshops; in the existing literature; and on the findings of a GOME validation team responsible for the investigation of data product quality throughout the mission lifetime.

GDP improvement is an ongoing task. This report gives an overview of the current situation as at December 2004, based on a limited set of validation orbits. Further improvements and more validation results based on an extended data set are expected in the future.

5. Documentation

The available ESA documentation for the ERS-2 GOME system comprises:

- GOME WWW site: http://earth.esa.int/esa_doc/doc_gom.html
- GOME Interim Science Report (ESA-SP 1151, 1993)
- GOME Users manual (ESA-SP 1182, 1995)
- Product Specification Document of the GOME Data Processor (ER-PS-DLR-GO-0016, issue 4B, December 15th, 2004)
- GOME Level 0-to-1 Algorithms Description (ER-TN-DLR-GO-0022, issue 5B, April 10th, 2002)
- GOME Level 1-to-2 Algorithms Theoretical Basis Document (ER-TN-DLR-GO-0025, issue 4A, December 15th, 2004)
- Proceedings of GOME Geophysical Validation Campaign Final Results Workshop, ESA-ESRIN, Frascati, 24-26 January 1996 (ESA WPP-108, 1996).
- Proceedings of 3rd ERS Scientific Symposium, Florence, Italy, 17-20 March 1997 (ESA SP-414, Vol. 2, 1997).
- GOME Data Improvement Validation Report (Ed. B. Greco, ESA/ESRIN APP/AEF/17/GB, 1998).
- Proceedings of European Symposium on Atmospheric Measurements from Space, ESA-ESTEC, Noordwijk, The Netherlands, 18-22 January 1999 (ESA WPP-161, 2 Vol., 1999).
- Update Report for GDP 0-to-1 Version 1.5 and GDP 1-to-2 Version 2.4 (ER-TN-DLR-GO-0043, 1999).
- ERS-2 GOME Data Products Delta Characterisation Report 1999 (Ed. J.-C. Lambert and P. Skarlas, IASB, Brussels, Issue 1.0, November 1999).
- ERS-2 GOME GDP 3.0 Implementation and Delta Validation Report, ESA Technical Note ERSE-DTEX-EOAD-TN-02-0006, (Ed. by J.-C. Lambert, IASB, Brussels, Issue 1.0, November 2002)
- ERS-2 GOME GD 4.0 Algorithm Theoretical Basis Document, ESA Technical Note ERSE-DTEX-EOPG-TN-04-0007, 2004.
- Delta validation report for ERS-2 GOME Data Processor upgrade to version 4.0, ESA Technical Note ERSE-CLVL-EOPG-TN-04-0001 (Ed. by J.-C. Lambert, IASB, Brussels, Issue 1.0, December 2004)

In addition a growing scientific literature is available at the GOME WWW site, at the GDP WWW site (http://wdc.dlr.de/sensors/gome/index.html), and at the GOME Validation WWW site (http://www.oma.be/GOME). Links to other relevant GOME sites are provided.

6. Contact point

To order GOME products, or for further information, please contact the ERS Help & Order desk:

EO Help Desk
ESA ESRIN
Via Galileo Galilei, I–00044 Frascati, Italy
Phone: +39 06 94180 777
Fax: +39 06 94180 272
E–mail: eohelp@esa.int
Web Site: http://earth.esa.int

GOME WWW site: http://earth.esa.int/gome